DISSERTATION

AUTOPHAGY MODULATION: ROLE IN ANTI-CANCER THERAPY

Submitted by

Rebecca A. Barnard

Graduate Degree Program in Cell and Molecular Biology

In partial fulfillment of the requirements

For the Degree of Doctor of Philosophy

Colorado State University

Fort Collins, Colorado

Spring 2015

Doctoral Committee:

Advisor: Daniel L. Gustafson

Douglas H. Thamm
Andrew Thorburn
TingTing Yao

ABSTRACT

AUTOPHAGY MODULATION: ROLE IN ANTI-CANCER THERAPY

Autophagy is a conserved lysosomal degradation process characterized by cellular self-digestion. Autophagy results in turnover of the cytoplasm allowing for metabolic maintenance and organelle quality control, particularly during cell stress. These aspects of autophagy can facilitate tumor cell survival and resistance. As such, autophagy inhibition is being explored in clinical trials as a novel approach to chemosensitization. However, there are still a number of unresolved concerns in regards to the use of autophagy inhibition as a therapy.

It is still unclear how autophagy functions in metastasis development. Therefore, we investigated the role of autophagy in metastasis by modulating autophagy in different mouse models and cell based assays that reflect the steps of metastatic development. We found that autophagy was not required for tumor cell colonization within the site of metastasis nor did autophagy alter the metastatic capabilities of the cells. Rather, autophagy appeared to impact the pre-metastatic environment through effects on bone marrow derived cell number which mediate the establishment of the metastatic niche. Stimulating autophagy, before tumor cells disseminated, could speed metastatic development and increase the number of these cells within circulation and eventual sites of metastasis. Correspondingly, inhibiting autophagy could delay metastasis and reduce circulating bone marrow derived cells. These studies suggest that autophagy is most critical in the stages prior to tumor cell arrival at the site of metastasis, by influencing the metastatic microenvironment.

While increased autophagy is often considered to be a common tumor adaptation, it is now apparent that some tumor types are more dependent on autophagy than others. However, it is not well understood which tumors these are. Triple negative, Stat3 activated breast cancers were identified as autophagy dependent by collaborator Dr. Paola Maycotte. We tested the efficacy of autophagy inhibitor chloroquine (CQ) in xenograft models of triple negative and estrogen receptor positive breast cancer. CQ was only efficacious in the triple negative tumors. As some canine osteosarcomas also have constitutive Stat3 activity, we assessed the relationship of Stat3 activity and CQ sensitivity. Unlike in breast cancer, Stat3 phosphorylation did not indicate increased sensitivity to CQ in canine osteosarcoma. However, all the osteosarcoma cell lines responded to treatment. Using microarray analysis we identified potential compensatory pathways that have been previously reported to work in concert with autophagy in other cell types and may serve as useful combinational therapies.

Currently, the only autophagy inhibitor available clinically is CQ or derivative hydroxycholorquine (HCQ). It is still uncertain whether these drugs can actually achieve autophagy inhibition in patients. Dogs serve as a good model for human cancer and there is an unmet need for novel therapies in the treatment of canine lymphoma. Thus we conducted a phase I clinical trial in canine lymphoma patients with the goals of finding a maximum tolerated dose in combination with doxorubicin (DOX) and the relationship of HCQ concentration and autophagy inhibition. We found that this combination can be well tolerated with a 20% reduction in DOX. HCQ can achieve autophagy inhibition in patients, but not consistently. There appears to be a threshold requirement of HCQ needed in order to effectively inhibit autophagy. There was a suggestion of efficacy as response rate was superior to historical data employing DOX alone. Therefore autophagy inhibition warrants further clinical study as an anti-cancer therapy.

ACKNOWLEDGEMENTS

There are many people whose support and guidance have made this work possible. Firstly, I am most grateful to my mentor and advisor, Dr. Daniel Gustafson, for giving me the opportunity to work in his laboratory and providing a pathway towards success in my career as a scientist. It cannot be overstated how much I appreciate his willingness to see my potential and encourage my growth and continuation in science. His knowledge and ability to bring clarity into the all too often clouded path forward with this project was indispensable.

I would also like to thank all the members of my committee, Drs. Douglas Thamm, Andrew Thorburn, and TingTing Yao, for also serving as mentors and providing insight and encouragement along the way. Others whose help was paramount in completing this project include Drs. Paola Maycotte, Daniel Regan, and Luke Wittenburg. I am incredibly appreciative of their enthusiasm and expertise. I would also like to especially thank Dr. Ryan Hansen for his assistance, advice and much needed levity. I also want to acknowledge all the members of the Gustafson lab, ACC researchers and graduate students for their support and friendship as well.

I also want to give thanks to friends and family for their never failing support and encouragement. A special thank you to Dr. Robert McKown for giving me the inspiration to pursue graduate school. To my parents, for ensuring I had every opportunity to succeed and their unwavering support. To my friend Katherine, for her perspective and transcending wisdom. To my animals, for inspiring my work and their unconditional love. Lastly, and most importantly, to my husband Sam. Thank you for never giving up and always following me to where ever life takes us. Thank you all!

TABLE OF CONTENTS

LIST OF TABLES

Chapter 2

Chapter 3

Chapter 4

LIST OF FIGURES

Chapter 2

Chapter 3

Chapter 4

Chapter One

Literature Review and Project Rationale

Autophagy

General Function and Mechanisms

Autophagy is an intracellular process that involves the degradation of the cell's own molecular structures including proteins, organelles, and nucleic acids [1]. Autophagy was first identified by Thomas Ashford and Keith Porter after observing rat hepatic cell lysosomes containing bits and pieces of organelles such as mitochondria and endoplasmic reticulum in various stages of degradation after exposure to the hormone glucagon [2, 3]. Christian de Duve and colleagues, who had also recently discovered the lysosome, confirmed this finding and coined the term "autophagy" at the CIBA Foundation Symposium on Lysosomes in 1963 [3, 4]. In the following decades, the autophagic process was elucidated primarily through genetic studies in *Saccharomyces cerevisiae,* which revealed over thirty autophagy related (ATG) genes.

Autophagy actually refers to multiple processes that involve cellular self-digestion. The three main types of autophagy are termed macroautophagy, chaperone-mediated autophagy, and microautophagy [5]. Macroautophagy, the most commonly studied form, is characterized by distinct double-membraned vesicles called autophagosomes [1]. Cellular components are

sequestered into the autophagosome, where they are trafficked to the lysosome. The autophagosome subsequently fuses with the lysosome to form an autophagolysosome and allows for the contents to be broken down by the lysosomal hydrolases. Macroautophagy is often referred to as the bulk-degradation pathway as it appears to be non-selective in nature [6]. However, organelle-specific subtypes of autophagy have been identified including mitophagy, pexophagy, and ribophagy [7]. Additionally, ubiquitinated protein aggregates can be selectively identified by autophagy specific cargo receptors such as p62/SQSTM1 (sequestosome 1) [8]. Thus, it appears that under certain conditions, macroautophagy may require some discernment in cargo degradation. Chaperone-mediated autophagy, on the other hand, does not require vesicle formation to traffic proteins; rather, hsc73 is responsible for identifying cargo with the KFERQ motif and translocating it directly across the lysosomal membrane via the LAMP2 receptor [5]. Lastly, microautophagy is similar to macroautophagy, but the engulfing membrane originates from the lysosome itself and intermediate vesicles are not required [5]. The focus of this project centers on macroautophagy, and hereafter, macroautophagy will be referred to as autophagy.

Autophagy's main function is considered to be the bulk turnover of the cytoplasm, particularly as a starvation response. Initial observations indicated that autophagy was regulated by amino acid concentration as perfusions of amino acids or plasma into rat livers were successfully able to inhibit autophagy [9]. Thus, autophagy serves to replenish the amino acid pool, allowing the cell to maintain vital functions, such as gluconeogenesis, during nutrient depravation [10]. Yet it has become evident that autophagy is much more than a starvation response. Autophagy has been shown to be induced under a wide range of stress responses including hypoxia, endoplasmic reticulum stress/unfolded protein response, DNA damage, and infection [11]. Importantly, autophagy acts as a quality control mechanism by removing

damaged organelles, such as mitochondria, which may become toxic to the cell, as a result of accumulation of reactive oxygen species [12]. Therefore, autophagy is important for maintaining cellular homeostasis, the loss of which can give rise to a host of pathologies.

The core machinery of autophagy is generally broken down into four main functional groups: 1) Atg1 kinase complex, which is responsible for autophagy initiation; 2) Atg9 cycling complex, which is involved in recruitment to the site of autophagosome formation or phagophore (forming isolation membrane) assembly site (PAS); 3) Phosphoinositide 3-kinase (PtdIns3K) complex, which recruits PtdIns(3)P-binding proteins to the PAS and aids in further expansion of the autophagosome; 4) The ubiquitin like (Ubl) conjugation system, which serves to facilitate cargo encapsulation.

The Atg1 kinase complex is comprised of three main subunits Atg1-Atg13-Atg17 [13]. In mammalian cells, Atg1 exists as a family of proteins called unc-51-like-kinase (ULK1). It associates with mammalian homolog of Atg13 (mAtg13) and focal adhesion kinase family interacting protein of 200 kDa (Fip200, ortholog of yeast Atg17) [13]. mAtg13 and Fip200 are considered to be regulatory subunits as both are subject to phosphorylation events that can alter their affinity and ability to modulate the kinase activity of ULK1 [14]. This complex is often viewed as the initiator and inducer of autophagy as it is directly acted upon by the main autophagy regulator, mammalian target of rapamycin (mTOR) [14]. Once activation of the complex has occurred, little is known about the downstream effects of ULK1 as no substrate has been identified [15]. New evidence suggests that perhaps this complex may function as a scaffold for autophagosome biogenesis. In yeast, the Atg17-Atg31-Atg29 complex dimerizes and assembles with Atg1 and Atg12 [16]. Atg1 was able to sense membrane curvature and bind lipid microsomes suggesting that its role may lie in providing structure for the phagophore [16].

The next step in autophagy is nucleation of the phagophore, which is largely controlled by the Atg9 complex. In mammalian cells, Atg9 exists in the trans-Golgi network. It is a transmembrane protein whose chief function appears to be delivering membrane to the PAS and back. Localization to the PAS is mediated by Atg11, Atg23, and Atg27, whereas return involves Atg1-Atg13, Atg2, and Atg18 [3, 17]. In mammalian cells, vacuole membrane protein 1 (VMP1), which colocalizes with the plasma membrane, also appears to be required for autophagosome formation [13, 18]. It has no known homolog in yeast. Its function seems to be required for the recruitment of the PtdIns3K complex along with $TP_{53}INP_2$ (tumor protein-53-induced nuclear protein-2) [13, 19].

The formation of the autophagosome is also dependent on the PtdIns3K complex. In yeast, there are two, but only Complex I appears to be specific for autophagy [3]. This complex is comprised of Vps34, a class III phosphoinositide 3-kinase, Vps15, required for Vps34 membrane association, and Vps30/Atg6 [3, 20]. Complex I also contains Atg14, which serves to facilitate the interaction between Vps30/Atg6 and Vps34 [20]. This complex is responsible for the generation of phosphatidylinositol (3)- phosphate (PtdIns(3)P). PtdIns(3)P signals recruit additional Atg PtdIns(3)P-binding proteins, such as Atg20, Atg24, Atg18, and Atg21, that are important for correct autophagosome formation but whose specific functions are not clear [20]. Atg14 gives complex I its specificity for autophagy whereas complex II contains Vps38 which targets complex II to the endosome and caboxypeptidase Y sorting pathway [20]. Complex I is also well conserved in mammalian autophagy and contains similar machinery: hVps34, Beclin-1 (homolog of Atg6), p150 (homolog of Vps15), and Atg14 ortholog, Atg14-like protein (Atg14L or Barkor) [13]. A Vps38 ortholog has also been identified as ultraviolet irradiation resistant-associated gene (UVRAG) [13]. Like in yeast, Atg14 seems to direct the complex to the PAS

and facilitate PtdIns(3)P production. UVRAG has multiple regulatory roles in mammals. UVRAG is important for the recruitment of Bax-interacting-factor 1 (Bif-1), which may be involved in autophagosome membrane bending [21]. It may also be important for autophagosome and lysosome fusion through interactions with vesicle tethering complexes [22]. Lastly, UVRAG competes for biding with Atg14L to Beclin-1 (BECN1), as well as interacting with Rubicon which targets the complex to the late endosome and actually reduces Vps34 activity [13].

In both yeast and mammals, the expansion and completion of the autophagosome is dependent on two Ubl conjugation systems. One involves Ubl protein Atg12, which becomes covalently bonded to Atg5. This reaction is catalyzed by Atg7 and Atg10, which are homologous to E1 ubiquitin activating enzyme and E2 ubiquitin conjugating enzyme. Atg5 is subsequently bound to another protein, Atg16 [3]. This multimer is thought to act as a transient coat for the autophagosome as it is localized to the exterior of the autophagosome membrane and is released into the cytosol upon completion [15]. Additionally, it may act as an E3 ubiquitin ligase for the second Ubl system. The second Ubl protein is Atg8 [3, 20]. Atg8 is first cleaved by Atg4 allowing Atg7 to bind and transfer to another E2 like enzyme, Atg3, which facilitates the conjugation of phosphatidlyentahnolamine (PE) to Atg8. This process may also involve the Atg12-Atg5-Atg16 multimer [15]. Atg8-PE is incorporated into the outer surface of the membrane as well as the interior. Surface Atg8-PE is released via Atg4 dependent cleavage where as internal Atg8-PE will be processed within the lysosome [20]. Atg8 is thought to serve several functions including autophagosome expansion and cargo selection. The amount of Atg8 appears to correlate with the size of the autophagosome and a decrease in Atg8 results in smaller vesicles [13, 20]. Atg8 interacts with cargo receptor Atg19 (distant relative of p62/SQSTM1 and

NBR1) and may trigger membrane bending around the cargo to ensure the inclusion of the cargo as well as exclusion of non-cargo [23]. In mammals, there are 4 known homologs of LC3: MAP1LC3, GATE16, GABARAP, and Atg8L which all contain a conserved glycine residue at the C terminus and can be conjugated to PE. LC3 is the most abundant [20]. LC3/Atg8 exhibits the greatest change of all the Atg proteins after autophagy induction [24, 25]. Thus LC3 can be used to monitor changes in autophagy and autophagosome number.

The last stage of autophagy involves the sealing of the autophagosome and its fusion with the lysosome. Once the autophagosome is complete, PtdIns(3)P must be dephosphorylated to allow for the dissociation of the autophagic machinery. This step is carried out by the PtdIns(3)P phosphotase, Ymr1. Loss of Ymr1 results in accumulation of autophagosomes that retain Atg proteins [26]. The completed autophagosome is trafficked to the lysosome via the microtubule system. Autophagosome-lysosome fusion can be hindered by microtubule depolymerizers such as nocodazole and vinblastine, whereas stabilizers, such as taxol, can increase the rate of fusion [27, 28]. Autophagosomes have been observed to travel bi-directionally. Minus end travel is facilitated by dyenein. Dyenein appears to co-localize with LC3 and anti-LC3 antibodies can inhibit autophagosome progression, suggesting a role for LC3 in autophagosome trafficking [29]. The mechanism for plus end movement is still unclear, yet recently, FYCO1, in conjunction with Rab7, has been identified as a potential candidate for the mediator of autophagosome transportation along the plus ends [30].

Once the autophagosome has reached the lysosome, surface bound Atg8 must be released to allow the dissociation of further Atg proteins, particularly Atg14, and participate in the formation of nascent autophagosomes [31]. Atg8 is deconjugated from PE by Atg4, creating a steady state of lipidated/de-lipidated Atg8. Changes in the balance of Atg8 conjugation result in

alteration of autophagosome size and rate of production [31]. However, this has yet to be observed in mammals where different subfamilies of Atg8 have more temporal roles such as the LC3 subfamily, which is involved in phagophore membrane expansion, and the GABARAP subfamily, which participates in membrane closure [31].

The tethering and docking of the autophagosome to the lysosome involves the Rab-SNARE machinery. Lysosomal SNAREs, Vam3/Vam7/Vtl1, facilitate fusion of the membranes by forming a trans-SNARE complex with the vesicle SNAREs, Ytk6/Nyv1, connecting vesicle and lysosome [32, 33]. This interaction is also mediated by the C Vps/HOPS tethering complex, which helps to stabilize the trans-SNARE formation and initiate contact with vesicle and lysosome. C Vps/HOPs acts as the effector complex for Rab7. GTP bound-Rab7 and C Vps/HOPS are able to interact with unpaired SNAREs [34]. The GDP-GTP exchange for Rab7 is carried out by Ccz1-Mon1 complex [24, 35]. Lastly, the autophagosome and lysosome fuse to become the autolysosome. Breakdown of the autophagic membrane is thought to be carried out by Atg15, which has lipase-like activity [36]. This allows the cargo to be released into the lumen of the autophagosome and broken down by lysosomal hydrolases. Some types of cargo are recycled back into the cytosol, such as leucine or tyrosine. Transport is carried out by efflux pump Atg22, thus completing the autophagic cycle [37].

Measuring Activity

Like many cellular processes, measuring autophagy is far from simple. Firstly, there are no absolute criteria defining autophagy nor does autophagy always appear consistent. Additionally, autophagy is a dynamic process. Visualizing autophagy directly and is challenging in real time, as this requires the ability to label and track single molecules. Therefore, most

analyses are merely snapshots in time of the autophagic process and require multiple sampling time points. Despite this, it is important to establish some guidelines for measuring autophagic activity as the demand for autophagy modulating drugs increases and observations of altered autophagy in disease states becomes more apparent.

Autophagy is measured by process competition, that is, autophagosome formation, cargo sequestration, delivery, and turnover back into the cytosol. The measurement of the entirety of this process is referred to as autophagic flux [1]. An estimate of autophagic flux can be analyzed by degradation of autophagy specific cargo or overall protein turnover. There will usually be some degree of basal autophagy that is observable. Other methods that are not as dynamic can be used to show modulation in autophagy. These include autophagosome volume or autophagy biomarker expression. Serum starvation is often used as a positive, autophagy-inducing control for these methods. While one can observe increases or decreases in these indicators, it is not possible to claim a precise "percent autophagy" change. Rather, reporting changes in terms of protein degradation, autophagosome volume, or protein expression is the more appropriate description [38]. These methods, of course, can be problematic and have limitations. Therefore, multiple means of assessing autophagy should be incorporated to give a measure of autophagic flux.

Autophagy was first identified through the use of transmission electron microscopy (TEM) which still remains the gold standard for autophagy analysis [38]. The hallmark of autophagy is the autophagosome. The typical morphology for an autophagosome is a double-membraned lipid bilayer and largely intact cytosol and organelles within the vesicle [39, 40]. Later stage autophagosomes that have fused with the lysosome will have only one membrane and will have organelles in varying stages of degradation. These features are relatively distinctive,

however, lamellar bodies, mitochondria, endoplasmic reticulum, and apoptotic bodies can appear similar to autophagosomes [40]. Immuno-labeling against cytosolic proteins or autophagosome surface marker LC3 with gold particles can help clarify presumed autophagic structures. While counting the number of autophagosomes per cell can be used to quantify autophagy, there is a large degree of variability due to the inconstancy in cell area and autophagosome size. The preferred measure is the percentage of cytoplasm occupied by the autophagosomes [38]. Though TEM is a powerful tool for assessing autophagy, the expertise required for correctly identifying autophagic structures makes it a time consuming and potentially biased assay. Therefore, TEM should never be the sole means of monitoring autophagy [38].

The most widely used marker for autophagy induction is LC3. LC3 is first synthesized as pro-LC3. It is quickly proteolytically cleaved at the C terminus into LC3 I. Upon autophagy induction, LC3 is conjugated to PE and becomes LC3 II. LC3 is the only protein that reliably associates with autophagosomes [38]. In yeast, total LC3 will increase when autophagy is induced, but for mammals, LC3 expression can be more complicated. LC3 I may appear to decrease relative to LC3 II, as LC3 I is consumed in the process or LC3 II can decrease if there is high turnover. LC3 expression is also highly variable across tissue types. In order to get a more accurate reflection of autophagic flux, lysosomal inhibitors, such as CQ or bafilomycin, should be included in the assay [41]. This will prevent turnover of LC3 II and will cause LC3 II to accumulate. This method also allows one to distinguish between induction and late stage blockade. If treatment causes an increase in LC3 II but expression is not substantially enhanced in the presence of a lysosomal inhibitor, this is suggestive of late stage inhibition [41]

Western blot is a useful method of LC3 detection. The LC3 II band will run lower than LC3 I due to the PE conjugation [41]. Thus, either LC3 II expression, or the ratio of LC3 I : LC3

II can be quantified. Another method often used for LC3 detection is immunohistochemistry (IHC). Under basal conditions, LC3 will generally have a diffuse cytosolic staining while induced or late stage autophagy inhibition will cause LC3 to have a more punctate staining [42]. However, LC3 can accumulate in lipid droplets and ubiquitin aggregates [43]. Therefore, it can be difficult to demonstrate that IHC of autophagy related proteins correspond to activity [38]. Fluorescently tagged LC3 has also been employed to measure LC3 expression. Particularly, a tandem GFP-mcherry-LC3 construct can be used to simultaneously analyze induction and flux. GFP is more pH sensitive than mcherry and will be quenched when LC3 is delivered to the lysosome [44]. Flux can then be measured as the ratio of GFP to mcherry by either confocal microscopy or fluorescence activated cell sorting (FACs) [45]. GFP expression alone can also be used to measure total LC3 expression. An additional saponin extraction can be included to deplete cytosolic LC3 and enrich for LC3 II that is incorporated into the autophagosome bilayer [46]. Additionally GFP can allow for single molecule observation in real time when using photoactivatable GFP [47]

Cargo turnover is another means to measure flux. Measurement of specific proteins like p62/SQSTM1 or total protein degradation can be used. SQSTM1 expression is often used as a readout for autophagic activity. SQSTM1 serves as a link between LC3 and polyubiquinated protein aggregates [48]. As a result, SQSTM1 will become incorporated within the autophagosome and ultimately degraded by the lysosome. Inhibition of autophagy will then lead to an increase in SQSTM1 expression whereas elevated autophagic activity will cause decreased SQSTM1 expression [49]. However, SQSTM1 does have other functions in the cell, which include anti-oxidant response, proteasome degradation, and caspase cleavage [50-52]. The multi-functionality of SQSTM1 can complicate interpretation as expression may not be correlative

with LC3 II expression under certain conditions. Therefore, SQSTM1 should not be used in lieu of LC3 turnover, but rather as a complementary measure.

As autophagy is the major source for protein turnover, total protein degradation can be monitored [38]. To follow protein degradation, amino acids should be radioactively labeled and then given time to be incorporated into nascent proteins. Incorporation of labeled proteins is then followed by a lag time before performing the assay. Sufficient time for both label incorporation and waiting is required as long-lived cytosolic protein degradation is most reminiscent of autophagic degradation. Turnover for these proteins is slow, so ample time is needed for labeled amino acids to be incorporated and short-lived proteins to be degraded by the proteasome. As proteins are degraded, the radio-labeled amino acids will be recycled back into the cytosol, allowing soluble radioactivity to be measured [38]. Autophagy is certainly not the sole means of protein degradation, so it is important to use an autophagy inhibitor in tandem to subtract out background activity. This method though may not be suitable for measuring basal autophagy as it can be difficult to detect above background degradation. Inhibiting autophagy can also induce compensatory degradation pathways, which can potentially complicate results [53]. However, the contributions of these other pathways are usually minimal.

While the quantification of autophagy *in vitro* by the aforementioned methods has been well developed, studying autophagy *in vivo* remains a challenge. For one, as autophagy is a dynamic process, serial sampling is required. This can be difficult to achieve in living organisms, particularly for human patients. Autophagy is not only highly variable across species, but also between individuals [38]. Therefore, large sample sizes are needed to account for this variability. Autophagy may also not be uniform across the tissue [38]. Necrotic regions of tumors cannot be used for analysis and activity may differ depending on proximity to blood supply. Therefore,

measurements may depend on how the tissue is sampled. Nevertheless, autophagy can be assessed similarly to *in vitro* methods.

Most of our understanding of autophagic behavior *in vivo* derives from transgenic mice systemically expressing LC3-GFP [54]. Just as in cells, GFP signal can be used to determine LC3 expression within tissues. Mice expressing tissue specific GFP-LC3 have also been generated. Similarly, tumor cell lines have been transfected with the GFP-LC3 or even the tandem GFP-mcherry-LC3 constructs. Measuring flux *in vivo* using the tandem construct has yet to be fully developed though. IHC and western blot can also measure LC3 expression, but IHC does not lend itself well as a dynamic assay [38]. For western blot, the liver serves as the best organ to assess autophagy. Changes in autophagy can be robustly observed in the liver and serial sampling, while difficult, can be achieved by performing partial hepatotectomy [38, 55]. TEM can also be used to measure autophagic volume in tissue, tumor, and blood, but measurements are very dependent on sampling location. Our understanding of autophagy will continue to improve as better *in vivo* methods of monitoring are developed.

Regulation

Autophagy, undoubtedly, must be strictly regulated. Deficiencies in autophagy can lead to a number of disorders including cardiomyophathy, neurodegeneration, and nephropathy as autophagy has been shown to be protective in cases of cardiac ischemia, bacterial invasion of the gut, acute kidney injury, and cerebral ischemia [56-60]. Conversely, if autophagic activity were to become excessive, then over self-consumption would lead to "destruction without construction" and cell death [61]. Thus, in vivo, autophagy and total proteolysis decreases after prolonged periods of stress [62, 63]. However sustained autophagy, rather than leading to cell

death, can actually prevent apoptosis, contributing to dysfunctional cell growth, which may be evidenced in cardiomyocyte hypertrophy, and axonal dystrophy [64, 65]. Why the cell continues to grow and maintain autophagic activity rather than succumb to apoptosis is still unclear.

In yeast, the main stimulus for autophagy induction is nutrient depravation; yet, in higher eukaryotic organisms, autophagy can be induced by a wide variety of stimuli requiring a concerted effort by many pathways and different types of effectors. Initiation of autophagy occurs within minutes of amino acid withdrawal, indicating that there is a pool of primed autophagy machinery available to respond rapidly [66]. Thus, many of the Atg proteins are regulated through post-transcriptional modifications including proteloytic cleavage, acetylation, lipid conjugation, and phosphorylation [14, 67, 68]. However, for prolonged autophagy, a number of transcription factors have been shown to replenish and induce transcription of more Atg proteins [69].

Another layer of regulation recently identified is microRNA (miRNAs) mediated mRNA degradation. miRNAs are small noncoding RNAs approximately 22 nucleotides in length and regulate post-transcriptional gene expression. miRNAs bind to a complementary sequence along the 3'untranslated region (UTR) of a mRNA, targeting the mRNA for degradation [70]. A single miRNA can regulate a large range of cellular processes. Some miRNAs that have been found to control autophagy related protein expression include mir106a, which targets ULK1, mir30a and mir376b which block BECN1, mir204 which controls LC3 expression, mir-885-3p which inhibits Atg13 and Atg9, and mir101, which regulates BECN1, Rab5, and Atg5 [71-75]. miRNA regulation seems to heavily favor the early stages of autophagy, as late stage miRNA targeting has yet to be observed [70]. Additionally, the ability of miRNA to access the 3' UTR may be hindered during stress. The length of the 3' UTR appears to be altered in Atg4 and BECN1

mRNAs that are transcribed during nutrient depravation, reducing miRNA affinity [73, 76]. However, while many studies demonstrate that miRNAs can control autophagy related protein expression, few have demonstrated that these links are relevant in a physiologic setting. Thus, the implications of miRNA regulation of autophagy remains largely unknown [70].

The most well studied and potent inducer of autophagy is nutrient depravation. The mammalian target of rapamycin (mTOR) is the key regulator for starvation induced autophagy [77]. It is the catalytic subunit of the mTORC1 and mTORC2 complexes. These complexes integrate survival related signals such as the presence of amino acids and growth factors. The substrates of mTORC1 include S6 Kinase 1 (S6K1) and eIF-4E binding protein 1 (4E-BP1), which regulate mRNA translation and protein synthesis [77]. These are energy intensive processes, so if survival signals are withdrawn, mTORC1 activity is turned off. If amino acids are present, Rag GTPases become activated and can bind the raptor subunit of mTORC1, relocating the complex to the late endosome or lysosome [78]. There, mTORC1 can interact with another family of GTPases called Rhebs that stimulate the kinase activity of mTORC1. Similarly, growth factor signals also influence the ability of Rheb and mTORC1 to interact [78, 79]. The binding of insulin triggers the PI3K/Akt pathway. Akt phosphorylates the Tuberous Sclerosis Complex (TSC), preventing TSC's ability to activate Rheb's GTPase function. mTORC1 signaling is then inhibited, as GDP-bound Rheb cannot bind to mTORC1 [79]. Once activated, mTORC1 phosphorylates Atg13 and prevents Atg13 from complexing with ULK1 and FIP200 to initiate autophagy [14]. However, if the cell becomes deprived of amino acids, mTORC1 will be turned off, Atg13, ULK1, and FIP200 will be allowed to complex, and autophagy will occur.

Another important nutrient-related autophagy sensor is AMP activated protein kinase (AMPK). A lack of nutrients can quickly lead to a reduction in cellular energy made evident by the increased ratio of AMP:ATP. Higher AMP levels will lead to activation of AMPK [77]. AMPK can both inhibit mTOR and directly promote autophagy. AMPK provides an activating phosphorylation event for TSC and an inhibitory one for raptor [80]. AMPK appears to directly activate ULK1 as well [11]. AMPK also participates in a positive amplification loop with another autophagy inducer called Sirt1 [81]. Sirt1 is part of the Sirtuin family, which are NAD-dependent deacetylases. Sirt1 is responsible for the deacetylation of Atg5, Atg7, LC3 and the autophagy inducing transcription factor forkhead box O3a (FoxO3), increasing their expression [68]. Sirt1 also stimulates LKB1, which can activate AMPK. AMPK can in turn, reduce nicotinamide making it available for NAD^+ production [81].

Transcription factors also play a role in maintaining the starvation-induced autophagy response. The deactivation of Akt due to nutrient withdrawal prevents the inhibitory phosphorylation of FoxO3 and allows for FoxO3 translocation to the nucleus to enhance transcription of autophagy related genes [82]. FoxO3 expression can also be elevated through Sirt1 deacetylation [68]. Additionally, FoxO3 can inhibit mTOR, contributing to the suppression of autophagy inhibitory signals [82]. Another important transcription factor is Stat3, which is induced upon a number of stress stimuli including nutrient depravation. Under baseline conditions, Stat3 is normally found in the cytoplasm. In its non-activated form, Stat3 can actually inhibit autophagy by sequestering a kinase called protein kinase RNA-activated (PKR) that is required for autophagy initiation [83]. However, once Stat3 is activated, it can relocate to the nucleus and promote the transcription of autophagy related genes [69].

The unfolded protein response (UPR), the major stress pathway of the endoplasmic reticulum (ER), can also potently induce autophagy. UPR can arise from stressors such as hypoxia or proteasome blockade. The UPR is triggered by the sequestration of protein chaperone BIP by the accumulation of misfolded proteins [84]. This causes the release of PKR ER-like kinase (PERK) and PKR which phosphorylate eukaryotic initiation factor 2α (eIF2α) and inhibits mRNA translation [84]. The inhibition of eIF2α is also required for the initiation of autophagy, but it is still not clear why [85]. One possibility is that inhibition of eIF2α promotes selective translation including the transcription of ATF4, which regulates LC3 expression [85, 86].

Oxidative stress is another stimulus for autophagy activation. Oxidative stress arises when there is in an imbalance in the cellular level of reactive oxygen species (ROS). Faulty mitochondria or defects in antioxidant enzymes are the main source for increased ROS [87]. Under normal oxygen conditions, a functional mitochondria will generate some ROS during electron transport, however, antioxidant enzymes also exist within the mitochondria to maintain the ROS at a low, steady state level [88]. At basal levels, ROS can serve as signaling molecules in a variety of pathways that include growth and survival promotion. However, high levels can be deleterious to the cell resulting in damage to proteins, lipids, and DNA. Both hyperoxia and hypoxia can increase mitochondrial release of ROS as well as some xenobiotics, which disrupt electron transport and compromise the mitochondrial membrane [87]. Autophagy is then a crucial response to mitigate damage by removing protein aggregates or even the faulty mitochondria itself.

Hypoxia is one condition that can lead to oxidative stress. The key oxygen sensor for the cell is hypoxia inducible factor (HIF), which contains subunits that bind oxygen [89]. When

oxygen concentration drops below a certain threshold, about 5%, the subunits are less likely to have oxygen bound. HIF then becomes stabilized and can act to promote transcription of a number of genes, which include BNIP3 [90]. BNIP3 induces autophagy by disrupting the interaction of BECN1 and Bcl-2 [90]. Bcl-2 sequesters BECN1, preventing BECN1 from forming the nucleation complex [91]. BNIP3's interference frees BECN1 to complex. Hypoxia can also trigger the UPR and activation of AMPK [89]. While it seems paradoxical, hypoxia can also lead to increased ROS. Complex III within the mitochondria may serve as an oxygen sensor for the cell to trigger hypoxic response mechanisms by increasing ROS production [92].

ROS can initiate autophagy by a few different mechanisms. ROS can directly activate autophagy by inhibiting an Atg4 homologue responsible for delipidation of LC3 [93]. Atg4 contains a cysteine that can be oxidized in the presence of ROS. This oxidation event inhibits Atg4 activity allowing for the lipidation of LC3 and continuation of autophagy [93]. ROS can also inhibit mTOR and activate MAP kinases like c-Jun N-terminal kinase 1(JNK1), which disrupts the BECN1/Bcl-2 interaction [11]. ROS activation of autophagy can then lead to degradation of the mitochondria. Deteriorating mitochondria will lose the ability to maintain membrane potential. Additionally, if the cell has taken on too much damage from ROS or other environmental stress, apoptosis may be triggered. One of the first steps in the apoptotic response is permeabilization of the mitochondria [94]. The voltage sensor is PTEN-induced putative kinase 1 (PINK1) located on the outer membrane of the mitochondria [95]. An intact membrane potential will induce proteolytic cleavage of PINK1, which will target PINK1 for proteasome degradation. However, if the membrane potential is compromised, PINK1 is stabilized and will rapidly accumulate on the membrane surface. An E3 ubiquitin ligase called Parkin can then bind to PINK1 and ubiquitinate various mitochondrial proteins, in particular voltage dependent anion

channel 1 (VDAC1) [95]. The cargo adaptor p62/SQSTM1 is capable of binding ubiquitinated proteins and can interact with LC3 to sequester the mitochondria into the autophagosome [95]. The mitochondria will subsequently be degraded, potentially circumventing apoptosis and further cellular damage [96].

One of the detrimental consequences of ROS accumulation is DNA damage. ROS, as their name implies, are highly reactive and can react with DNA causing lesions. DNA lesions can lead to mutagenesis and replicative block. In response, the tumor suppressor p53 is stabilized and translocates to the nucleus. There, p53 can facilitate DNA repair and promote transcription of cell cycle inhibitors, pro-apoptotic proteins, and autophagy inducers, namely AMPK, and mTOR inhibitors DRAM1 and Sestrin2 [69, 97]. In contrast, cytoplasmic p53 can robustly inhibit autophagy by sequestering Fip200 and preventing formation of the ULK1 complex [98]. Therefore cytoplasmic p53 must be depleted in order for autophagy to occur.

Immune related signals from infection or inflammation are another major mechanism for autophagy induction. Cells can detect pathogens through pattern recognition receptors (PRRs) such as the Toll-like receptor family. PRRs recognize specific patterns that are conserved features of pathogens and are termed pathogen associated molecular patterns (PAMPs) [99]. Cellular damage including necrotic cells, environmental stress, and ROS can trigger the immune response in a similar fashion and are called danger associated molecular patterns (DAMPs) [100]. Recognition of PAMPs or DAMPs by PRRs can trigger release of pro-inflammatory cytokines and activation of the immune response coordinator NF-kB. Without immune stimulation, NF-kB is inhibited by IkB [99]. Once the immune cascade is triggered, TAK1 is activated. It in turns activates IKK, which will inhibit IkB and potentiates its degradation [99]. IkB degradation permits NF-kB translocation to the nucleus. There, it can promote transcription

of pro-inflammatory genes along with autophagy related genes such as BECN1 [101]. Autophagy can then be used as a means for pathogen removal. Ubiqutin will be recruited and accumulate around the pathogen. Cargo adaptor p62/SQSTM1 can then facilitate pathogen incorporation into the autophagosome for subsequent degradation [102].

Autophagy is also important for maintaining the inflammatory response. Autophagy can stimulate the production of cytokines while delivering PAMPs to the endosome causing activation of Toll-like receptors located along the endosomal lumen [103]. Activation of these receptors will trigger the production of pro-inflammatory cytokines like Type I interferon. In turn, cytokines will continue to promote autophagic activity by preventing BECN1 sequestration [104]. Autophagy also controls cytokine concentration. Inhibitory cytokines such as IL-17 will be degraded through autophagy where as autophagy promotes inflammatory IFN-α production [104]. The presence or absence of certain cytokines will then influence T-cell and dendritic cell polarization as well as antigen presentation [105, 106]. Additionally, autophagy is required for the secretion of immunomodulatory small molecules like ATP, which is critical for recruitment of dendritic cells [107]. Thus autophagic activity creates a positive amplification loop for the inflammatory response.

Due to the wide range of environmental inducers and functions extending beyond metabolic maintenance, autophagy appears to lie at the crux of cellular health. When autophagy regulation fails, the cell is more susceptible to damage. Without autophagy, the cell is unable to clear compromised mitochondria, protein aggregates, and certain bacteria. Thus, defective autophagy is thought to contribute to a number of disorders including aging, neurodegenerative diseases, heart failure, colitis, and cancer development [12]. A failure to suppress autophagy can also be problematic, as the cell is unable to accommodate the excess of autophagosomes or

initiate apoptosis if the cell has received extensive damage. Therefore, proper regulation of autophagy is integral to cell functionality.

Autophagy in Cancer

Tumor Suppression

Autophagy was initially identified as a mechanism for tumor suppression. Beth Levine and colleagues made the first connection to cancer when they observed mono-allelic deletions of the *beclin-1* locus, 17q21, in breast cancer [108]. They estimated that 50% of breast cancers, 75% of ovarian cancers and 40% of prostate cancers have lost *beclin-1*[109]. In addition, they demonstrated that mice had an increase in spontaneous tumors in a *beclin-1* haplo-insufficient model [110]. Similarly, Atg4 deficient mice showed increased susceptibility to chemically induced fibrosarcomas and Atg7 liver specific deficient mice developed liver adenomas [111, 112]. Breast cancer cells also appeared to lose their tumorigenicity when autophagy was restored [109]. Taken together, this data suggested autophagy was important for preventing tumor development.

With the advent of sequencing, more recent genomic studies have shed light on the frequency of loss of function mutations in autophagy related proteins within cancer patients. It appears that somatic point mutations of BECN1 are actually quite rare. Only 11 of 548 patient samples from a broad range of cancer types contained single nucleotide variants (SNVs) in BECN1 [113]. Eileen White's group also found that there were no mutations or focal losses of BECN1 on its own in breast and ovarian cancers using data from The Cancer Genome Atlas. The 17q21 region also encompasses BRCA1, a well-established tumor suppressor responsible for

DNA repair. Since BECN1 is in such close proximity to BRCA1, it seems that the two are just often lost together [114]. However, mutations in BECN1 binding partners seem to occur frequently, particularly in gastric cancers. Frameshift mutations in UVRAG, which modulates BECN1 activity, is observed in colorectal and gastric cancers exhibiting microsatellite instability [115]. Restoring expression of UVRAG was able to suppress HCT116 colon cancer cell tumorigenicity, suggesting a tumor suppressive role [116]. Yet, UVRAG may not necessarily affect the cell's ability to undergo autophagy in all circumstances [117]. Therefore, UVRAG may function independently of autophagy. Frameshift mutations in core autophagy proteins such as Atg2B, Atg5, and Atg9 have also been observed in gastric and colorectal cancers [118], alhough autophagy functionality has yet to be assessed in such tumors [119]. Thus, it is still unclear if a line between loss of autophagy and tumor development can be firmly established.

Autophagy's role in cellular maintenance appears to be one explanation for its putative tumor suppression. Cardiomyocytes and skeletal muscle with deletions of Atg5 or Atg7 have increased amounts of abnormal mitochondria, ubiquitinated protein aggregates, and inclusion bodies [120, 121]. Hepatocytes deficient in Atg7 also accumulate peroxisomes and β cells have distended ER and Golgi [122, 123]. In Atg5 deficient neurons, diffuse ubiquitin positive proteins are present [124]. Additionally these autophagy deficient cell types exhibited higher levels of ROS. Mouse mammary epithelial cells with a heterozygous deletion of BECN1 also showed increased chromosomal abnormalities including aneuploidy, γ-H2AX foci, and gene amplification under metabolic stress [125, 126]. Anti-oxidant treatment with N-acetyl-cysteine was able to delay aneuploidy, giving further credence to autophagic mitigation of ROS production and DNA damage. Degradation of nuclear components has also been observed in highly mutated mammalian cells. DNA containing histone H1 and γ-H2AX were found inside

autophagosomes and inhibition of autophagy exacerbated nuclear abnormalities [127]. Autophagy, in this case, appears to alleviate some of the key steps in cancer development, particularly genomic instability. With functional autophagy in place, cells will be less susceptible to tumor transformation.

Autophagy may also reduce tumorigenesis through the selective degradation of adaptor p62/SQSTM1. When autophagy is induced, SQSTM1 will be degraded with its cargo, ubiquitinated substrates. The inhibition of autophagy will cause a concomitant increase in SQSTM1. Accumulating SQSTM1 can be problematic as it also serves as a scaffolding protein for a number of different signaling pathways, many of which can be pro-tumorigenic. One such case is stabilization of the transcription factor nuclear factor erythroid 2-related factor (Nrf2). Under basal conditions, the ubiquitin ligase, kelch-like ECH-associated protein-1 (Keap-1), binds Nrf2 causing Nrf2 ubiquitination and degradation [128]. Under oxidizing conditions, Keap-1 will become inactivated and Nrf2 will promote transcription of genes involved in anti-oxidant response and survival. SQSTM1 can also outcompete Keap-1 for binding to Nrf2, allowing constitutive expression of Nrf2 [129]. Mice lacking Atg7 in the liver develop liver adenomas that show increased SQSMT1 inclusion bodies and Nrf2 activity [130]. Similar observations have also been made in 34-37% of non-small cell lung cancers [131]. SQSTM1 also appears to regulate NF-kB. Binding of SQSTM1 to tumor necrosis factor receptor-associated factor 6 (TRAF6) permits TRAF6 to interact with IKK and activates its kinase function [132]. IKK can then inhibit IkB allowing NF-kB to translocate to the nucleus. Therefore autophagy may also serve as a tumor suppressor by keeping SQSMT1 levels low.

Oncogene induced senescence is another barrier against cell transformation. Senescence is the irreversible arrest of the cell cycle. The activation of an oncogene may trigger this process

due to the initial high rate of replication, which may result in DNA damage and build up of ROS [133]. Autophagy appears inextricably linked to this process. A number of studies show that autophagy is elevated in senescent cells and that inhibition of autophagy can delay the onset of senescence [134-136]. Interestingly, senescence related autophagy is not triggered by canonical Ulk1/2 activation, but rather Ulk3. Overexpression of Ulk3 appears sufficient to trigger autophagy dependent senescence [136]. Thus, autophagy may also be used as a last attempt to quell uncontrolled proliferation.

Finally, autophagy can be a mechanism or mediator of cell death. There are many processes during development that require cell attrition for proper formation. It was concluded then that this type of cell death required genetic programming and was referred to as apoptosis [137]. Accidental cell death, likely resulting from stress and requiring little in the way of executionary machinery, unlike apoptosis, was called necrosis. However, cell death lacking the characteristics of apoptotic death was also observed during tissue remodeling such as regression of the Mullerian duct and cavity cell formation of the intestine [138-140]. Generally, cells will exhibit chromosome condensation, shrinkage, DNA degradation and fragmentation, and caspase activation if undergoing apoptotic death. Yet, these dying cells not only lacked these features but also appeared to have remarkably high levels of autophagosomes, the volume of which exceeded the cytoplasm [141]. In HeLa and CHO cells, a pan-caspase inhibitor was not able to prevent cell death. Rather, mitochondria were degraded at such a high rate by autophagy that the cells died shortly thereafter [142]. Inhibition of autophagy was able to partially suppress cell death. Additionally, if autophagy was blocked, but apoptosis allowed to occur, the cells would then revert to an apoptotic death. Thus, the cells could switch between the two mechanisms of death if

one was compromised. In light of this, the terms of cell death were broadened to include autophagy mediated cell death or programmed cell death type II [141].

It appears that neoplastic cells can also succumb to autophagic death. Therapies such as tamoxifen or arsenic trioxide can induce autophagy in MCF-7 and glioma cells, while blockade with 3-MA can prevent cell death [143, 144]. Thus, if cell damage is extensive or metabolic demand high, the consumption of the cell by autophagy could become excessive leading to cell death. However, a recent study by the Kroemer laboratory demonstrated that out of 1,400 compounds, not a single one required autophagy for cell death [145]. Only 59 truly increased autophagic flux and silencing Atg7 did not lead to reduced cytotoxicity. Some new evidence suggests that rather than being the mechanism of death, autophagy is part of a series of events required for programmed necrosis or necroptosis. Previously, it was thought that necrosis was purely accidentally, but now it seems that necrosis can be triggered like apoptosis. The initiation of necroptosis specifically requires the activation of receptor interacting kinase 1 (RIP1) [146]. Some studies demonstrate that activation of RIP1 occurs in tandem with autophagic activity and RIP1 can induce autophagy. Furthermore, necroptosis can be inhibited if autophagy is also inhibited [147, 148]. The new paradigm seems to be shifting toward autophagy promotion of necrotic like cell death instead of autophagy as the actual executioner [149]. Nevertheless, autophagy still appears integral for proper cell death response and proliferation suppression.

Tumor Promotion

Although a large body evidence pointed toward a tumor suppressive role for autophagy, it was not long before other studies revealed the opposite; autophagy may also be tumor promoting. First, the accumulation of autophagosomes was found to be the result of not just

autophagy induction, but also late stage blockade [150]. Particularly, lysomotrophic agents prevented the fusion of the lysosome and autophagosome, preventing the process from going to completion. Furthermore, using lysomotrophic agents could lead to apoptotic cell death during starvation. This finding began to cast doubt on excessive autophagy as a sole means of cell death and that autophagy could actually suppress apoptosis [150]. Additionally cells with defective apoptosis seemed to depend on autophagy for survival and when both apoptosis and autophagy were inhibited during starvation, cells would undergo necrosis [151]. This finding was very relevant in tumor biology as tumors exist within a harsh microenvironment. In fact, autophagy was found to be elevated in regions of hypoxia and limited blood supply [152, 153]. Autophagy thus appears to have a highly contextualized role in cancer development.

Further studies demonstrated that chemotherapy and radiation therapy can induce autophagy. Inhibiting autophagy, either late or early in the process, could sensitize cells and trigger apoptosis [154, 155]. Like previous studies, many oncogenes were found to induce autophagy as well, but for some, autophagy was required for tumorigenesis rather than inducing senescence. In the case of Ras activated tumors, autophagy is necessary to maintain a pool of functional mitochondria and sustain glycolysis [156]. Similarly an MMTV-PyMT mouse model of breast cancer also required autophagy for tumorigenesis [157]. Deletion of Fip200 was able to prevent tumor initiation and decreased glycolysis and cell cycle progression. While these studies seem to stand in direct contrast with previous work, we now know that autophagy's function is context dependent. Autophagy may prevent tumor development initially, but as the tumor has become established or driven by specific, aggressive oncogenes, autophagy may promote continued growth.

To maintain their high rate of proliferation, tumor cells need to correspondingly increase their rate of metabolism. This requires rapid energy generation and synthesis of proteins, nucleotides, and lipids that exceeds normal cellular activity. Some tumors preferentially use glycolytic production of lactate rather than pyruvate even in the presence of oxygen. The observation of tumor aerobic glycolysis has been termed the Warburg effect [158]. Although oxidative respiration is a much more efficient ATP generating process, the byproducts and intermediate substrates generated by glycolysis or glucose itself can be shunted off to pathways for synthesis of macromolecular building blocks such as nucleotides or lipids [159]. For instance, NADPH can be used for glutathione production and glycerol for lipid synthesis. Therefore tumor cells are just as dependent on sources of building material needed for replication as they are energy. Autophagy can then act as another means for providing cellular material. To maximize energy production, tumor cells can take up other carbon sources such as glutamine and even lactate to utilize oxidative respiration as well [160, 161]. Autophagy can then also be used to remove and recycle damaged mitochondria. Many tumors driven by oncogenes such as Ras or Myc create this high metabolic demand and will cause constitutive activation of glucose and glutamine uptake and autophagy [162]. Suppression of autophagy can actually prevent Ras driven tumor formation as autophagy appears to be required to maintain a healthy pool of mitochondria for fatty acid oxidation [156, 163]. By removing damaged or non-critical material, autophagy allows the cell to conserve energy, remove waste, and balance metabolism.

Another important mechanism for tumor progression and survival is suppression of the p53 response. p53 is one of the most important tumor suppressor genes. It is induced by a number of different stress responses, particularly genotoxic stress. p53 is responsible for initiating cell cycle arrest, apoptosis, senescence, DNA damage repair, reduction of glycolysis

and other programs designed to halt proliferation. p53 is estimated to be mutated in 50% of human cancers demonstrating just how critical it is for tumors to manage p53 signaling [164]. Nuclear p53 can activate autophagy. In turn, autophagy can mitigate many of the elements that trigger p53 such as ROS. Thus activation of autophagy creates a negative feedback loop for p53 activation. Autophagy may alleviate cellular damage and subdue p53 activity. p53 wild type tumors do appear to be more dependent on autophagy. In a Kras activated model of pancreatic cancer, autophagy was required for malignant transformation [165]. However, if p53 was removed, autophagy was no longer necessary for tumor development. Autophagy can then be exploited by tumors to overcome the barriers imposed by p53.

If cells are unable to sustain metabolism or have received enough damage to initiate p53, cell death programs become activated. However, the elevated levels of autophagy in tumor cells may raise the threshold for initiation. Cell death during stress ultimately comes down to the cell's ability to maintain ATP [166]. A 50% drop in ATP can trigger necrosis [167]. Restoring ATP can rescue the cell [167]. Autophagy contributes to control of metabolites to allow ATP generation and keep levels in line with the cell's metabolic needs. Thus as long as autophagy can supply ATP and amino acids for gluconeogenesis or ketogenesis adequately, death can be stayed. Additionally the mitophagy function can also keep apoptosis at bay. Permeabilization of the mitochondrial membrane mobilizes apoptosis due to the release of cytochrome c, triggering caspase activation. Mitocondrial permeabilization is generally considered the point of no return [168]. Yet if autophagy is able to remove the mitochondria, apoptosis can be avoided [168]. Autophagy has also been shown to degrade pro-apoptotic proteins like caspase 8 [169]. In turn, caspases can cleave autophagic proteins like Atg3 and BECN1 [170, 171]. The cleaved peptide fragments have been shown to localize to the mitochondria, and promote release of cytochrome

c, at least *in vitro [172]*. Although autophagy is generally considered to suppress apoptosis, many of the same activators like DAPK, JNK, PUMA, NOXA, BIM, and BAD simultaneously drive both pathways forward [173, 174]. Indeed, autophagy is often observed prior to apoptotic death [175]. Low to moderate levels of stress may activate autophagy, delaying the onset of apoptosis, but as stress becomes more severe, autophagy may be inhibited as other pro-apoptotic proteins come on board [166]. Though the tumor cell may die, it can still promote survival responses to other surrounding cells. Dying tumor cells with functional autophagy can release soluble factors like HMGB1 that when taken up by other tumor cells can induce autophagy [176]. Potentially protecting the tumor as a whole. By preserving metabolism and raising the threshold for cell death activation, autophagy can act as a mechanism for tumor survival.

Metastasis

Autophagy's role in the primary tumor appears to be preventative at the outset but may contribute to tumor cell survival once the tumor is established. Autophagy's role in metastatic dissemination and colonization is much less clear. As the majority of cancer deaths ultimately are due to to resistant metastases, identifying autophagy's function in metastasis is critical. Complicating the problem is that the series of events required for metastatic formation, often referred to as the metastatic cascade, may be just as complex if not more so than initial tumorigenesis. The classic model consists of tumor cells disseminating from the primary tumor and utilizing either the lymphatic or circulatory system to reach and colonize lymph nodes or distant organs and develop into solid metastases [177]. During the journey, a cell must adapt and activate different survival programs along the way in order to successfully form metastases.

The initial steps of metastasis require extracellular signals for invasion and migration. As the tumor continues to grow, many regions will become hypoxic and nutrient depleted, leading to necrosis. Necrotic cells can trigger inflammation and the recruitment of a number of different immune cells. Some of these cells, like macrophages, can release signals that promote tumor cell invasion and migration [178]. Autophagy can reduce macrophage infiltration while promoting recruitment of dendritic cells and cytotoxic T cells through the release of ATP and HMGB1 [107, 151, 179]. By promoting the removal of necrotic cells, autophagy can limit macrophage infiltration and diminish migratory signals. Additionally, autophagy can also inhibit cellular motility by degrading internalized integrin receptors, transcription factors like Twist1, which promotes invadopodia formation, and focal adhesion kinases [180-182]. Just as with early tumor development, autophagy may initially inhibit metastasis by suppressing invasion and migration.

Another mechanism epithelial cells may utilize in primary tumor escape is the transient adoption of a mesenchymal phenotype [183]. This switch to a more mesenchymal like nature provides the advantages of decreased tight junctions and polarity, reorganization of the cytoskeleton, and reversion to a more stem cell-like state. Mesenchymal like cells are more motile and better at degrading extracellular matrix to move through basement membranes [184]. This change in phenotype is referred to as epithelial to mesenchymal transition (EMT). EMT may result from the pro-inflammatory cytokines and signals released from infiltrating immune cells. EMT changes are evidenced by a downregulation of epithelial like adhesion molecules such as E-cadherin and cytokeratin, and the dissolution of tight junctions and desmosomes. In turn, mesenchymal markers like N-cadherin and vimentin are upregulated [184]. Matrix metalleoproteinases (MMPs) are activated to enhance extracellular matrix invasion. EMT associated transcription factors include SNAIL, Twist, and zinc finger E box binding (ZEB). In

some models, such as colon and breast cancer, autophagy was shown to degrade Twist and SNAIL, limiting the EMT and reducing cell motility [185, 186]. However, in models of hepatocellular carcinoma, breast cancer, and cholangiocarcimona, autophagy induction correlated with EMT and knockdown of BECN1 was able to suppress EMT. Therefore, autophagy's role in EMT remains unclear and will likely be tumor dependent [187-189].

Once cells have detached from the matrix, autophagy may take on a metastasis supportive role. Non-transformed cells typically die once detached from the extracellular matrix. Contact dependent integrin signaling promotes survival signaling so the loss of attachment as well as well a decrease in nutrients as the cell moves away from nutrient supplies leads to apoptosis [190]. Apoptosis as a result of matrix detachment is called anoikis. Anoikis resistance is a critical step in dissemination, as the cell must survive the lengthy journey from primary tumor, circulation, to finally residing at a distal site. Autophagy induction has been observed in mammary epithelial cells when grown in 3D culture [191]. Similarly, autophagy is required for survival of breast cancer and heptacellular carcinoma cells when grown in suspension [187, 192, 193]. Therefore, autophagy may help cells to become anoikis resistant.

Before tumor cells even arrive, the eventual site of metastasis will undergo changes making it more hospitable to incoming tumor cells. Important events in the establishment of the metastatic microenvironment or niche include remodeling of the extracellular matrix (ECM) and vasculature [194]. The mediators of niche formation are cells recruited from the bone marrow by the tumor. They secrete cytokines and growth factors like SDF-1, and MMPs that assist in changing the constituency of the ECM, particularly, increasing fibronectin, periostin, and tenasin-c [195]. Incorporation of these components can increase the overall stiffness of the ECM, providing better adhesion and supportive scaffolding for tumor cell deposition [195, 196]. The

stroma can also be encouraged to release signals promoting growth and secreting fuel for tumor cells like lactate, glutamine, and ketones. Autophagy has been shown to be elevated in stromal cells within the tumor microenvironment, likely sustaining the production of metabolites [197]. Additionally, bone marrow derived cells can recruit circulating endothelial progenitor cells to build new blood supplies as well as making a more permeable lung vasculature [195]. Autophagy may protect bone marrow derived stem cells from hypoxia and metabolic stress in culture, and thus could have a role in bone marrow derived cell survival [198]. Macrophages can also be recruited to promote an inflammatory, immunosuppressive environment. Autophagy may contribute to immune evasion as models of breast and lung cancer show knockdown of BECN1 or Atg5 coincided with an increase in $CD8^+$ T-cell infiltration and killing, at least in regions of hypoxia [199, 200]. However, in another model of breast cancer, autophagy was required for ATP release, which is essential for recruitment of cytotoxic T-cells and dendritic cells [107]. Thus, the role of autophagy in niche formation is still not clear, but perturbations in autophagy do appear to alter the microenvironment. Whether it has a pro- or anti-metastatic function remains unclear and may be tumor type- and context-dependent.

When a disseminated tumor cell finally reaches the site of metastasis, it likely will not immediately start proliferating but will remain in a state of dormancy. Dormant cells appear similar to senescent cells as they are no longer proliferating and replicating cellular machinery, but the growth arrest is reversible [201]. So rather they are referred to as quiescent cells. A harsh microenvironment or anti-cancer therapy can drive cells into a state of dormancy. This is problematic as these cells may precipitate reoccurrence as may be refractory to chemotherapy since they are not actively cycling. Cells will awaken once conditions become more favorable, particularly when angiogenesis ramps up [202]. Models of breast cancer demonstrate that

disseminated tumor cells will remain dormant and reside in perivascular regions until neovasculature has begun forming. Stable microvasculature may keep cells in a dormant state [203]. Though dormant, cells can secrete factors that contribute to niche formation and immunosuppression. Like senescence, autophagy appears important for maintaining dormancy. The onset of dormancy occurs after the inhibition of growth signaling cascades, particularly PI3K-Akt [204]. Inhibition of this signaling axis allows autophagy to occur. In ovarian cells, the inhibition of autophagy by CQ can interrupt dormancy and growth may once more resume [205]. Autophagy mediated dormancy may be activated by ARH1 (DIRAS3). ARH1 can downregulate epidermal growth factor receptor, which inhibits PI3K signaling. Additionally, ARH1 can promote FOXO3 activity and act as scaffolding for the autophagy initiating complex [206, 207]. Similarly, treatment with imatinib forced murine gastric cancer cells into dormancy and silencing of Atg5 or Atg12 caused cell death [208]. Therefore autophagy may allow cells to remain in a state of dormancy, but aid in keeping expansion in check. Once again, it appears that autophagy likely has opposing roles depending on the stage of metastatic dissemination and growth.

Autophagy in Cancer Therapy

Targeting Autophagy

For many tumor types, autophagy appears to sustain tumor metabolism, enrich the microenviornment, and suppress apoptosis initiation. These tumor-enabling functions implicate autophagy as a mechanism for survival and resistance. Recognition of these observations has raised the question whether inhibiting autophagy can reduce tumor proliferation and make cells more susceptible to other anti-cancer therapies. The next step then, is to determine how to

modulate autophagy. The points along the autophagy pathway that are targeted by current pharmacologic inhibitors include the PtdIns3K complex and autophagosome-fusion event, while autophagy inducers inhibit upstream signaling cascades like mTOR and PI3K.

Although much of the focus in cancer therapy has been focused on autophagy inhibition, many other diseases like neurodegenerative disorders may benefit from stimulating autophagy [209, 210]. Additionally, studies may require demonstration that autophagy stimulation has opposing effects from autophagy inhibition. One of the mot commonly used approaches is inhibition of mTOR by rapamycin or rapalogs [14]. However, rapamycin only targets mTORC1. mTOR also comprises mTORC2 which can reactivate PI3K-Akt signaling, inhibiting autophagy. Newer inhibitors like torin1 and torin2 can inhibit mTORC1 and mTORC2 and are more potent inducers [211]. However, long term inhibition of mTOR also leads to immunosuppression, so safer alternatives are being pursued. The disaccharide trehalose has been found to induce autophagy independent of mTOR inhibition. Trehalose was shown to induce autophagy in neurons and promote clearance of a-synuclein in a model of Huntington's disease [209]. Also, lithium chloride has been found to induce autophagy by inhibiting inositol monophosphatases (IMPase), sustaining PtdIns3 signaling [212]. IMPase inhibitors may be good candidates for autophagy stimulation.

Many of the autophagy inhibitors target the mammalian ortholog of Vps 34, a class III PI3K [213]. Class III PI3K generate only phosphatidylinositol -3-phosphate and are typically involved in vesicle trafficking. As opposed to class I, of which PI3K is a member and can also produce phosphatidylinositol3-bisphosphate or trisphosphate. Inhibition of Vps34 activity will prevent formation of autophagosomes as phosphoinositide signals are required for membrane and nucleation complex recruitment. Inhibitors of Vps34 include 3-methyladenine and

wortmannin. However, 3-methyladenine can actually promote autophagy in nutrient rich conditions as higher concentrations can also inhibit class I PI3K activity [214]. A more specific, small molecule inhibitor called Spautin-1 has also been developed [215]. It preferentially targets BECN1, a subunit of Vps34, by blocking the deubiquitin activity of USP10 and USP13, promoting degradation of BECN1.

Late stage inhibitors typically target the lysosome-autophagosome fusion event, mainly by interfering with lysosome acidification. Vacuolar-type H (+)-ATPases are used for pumping protons across membranes to decrease the lumenal pH. Bafilomycin A1can inhibit these pumps, preventing the necessary acidification for lysosomal function and loss of SNARE function [216]. Similarly weak bases like chloroquine (CQ) and other lumenal alkalizers can increase the pH of the lysosome as well. Acid protease inhibitors like leupeptin and cathepsins block lysosomal hydrolases block the degradation of cargo, preventing cytoplasmic recycling [217].

Currently, the only inhibitor approved by the FDA is CQ and its derivative hydroxycholorqine (HCQ). Developed in 1943 by Hans Andersaag at I.G. Farbenindustrie (part of Bayer), CQ was initially used as an anti-malarial therapy [218]. Similar to its anti-autophagy functions, CQ accumulates in vacuoles preventing heme detoxification in the parasite. CQ and HCQ have also been used for treatment of autoimmune diseases like lupus and rheumatoid arthritis for their immune suppressive capabilities, potentially stemming from their ability to inhibit Toll-like receptors. Beyond these functions and its anti-autopagy activity, CQ can also intercalate DNA and block endocytosis. Thus, interpreting results derived from CQ treatment can be difficult to attribute to autophagy loss of function. In fact, synergism with chemotherapy has been noted, even if cells lack functional autophagy [219]. Similar results were also observed in a melanoma model. CQ was able to normalize vasculature and potentiate delivery of cisplatin

independent of autophagy function [220]. This vasculature normalization appeared to be a result of Notch accumulation due to inhibition of endocytosis. CQ and HCQ are not the most potent autophagy inhibitors and autophagy inhibition is not consistently achieved in patients. Pharmacokinetic studies in animal models and humans indicate that CQ has a long half-life and large volume of distribution [221-223]. Yet, the maximal levels achieved in plasma were only 1.2-5 uM, which are likely not sufficient to inhibit autophagy. However, CQ readily accumulates in lysosomes, so plasma levels may not readily reflect tissue concentrations of CQ. Few studies have determined CQ levels within tumors. Different tumor types may have varying abilities to accumulate CQ with some achieving autophagy inhibition at lower doses of CQ. Development of more potent inhibitors is currently ongoing. Of note, Lys01 and water-soluble form Lys05, which are dimeric forms of CQ, have been shown to be ten times more potent than CQ and may potentially have a better therapeutic index [224]. However, toxicity is observed, particularly in the paneth cells of the intestine, which is similar to the effects observed in people with an Atg16L deletion. The development of better inhibitors will help determine if autophagy inhibition can be a viable therapy.

Pre-Clinical Data

The identification of autophagy as a potentially universal mechanism for tumor survival and resistance has generated a great deal of enthusiasm for autophagy inhibition as a novel approach to chemosensitization. The majority of literature seems to support inhibiting autophagy as a means to potentiate chemotherapy [225]. However, there are still a number of studies where autophagy inhibition failed to enhance or even diminished overall efficacy. Further still, autophagy may elicit opposing effects on a single therapy depending on the cancer model. These results are not surprising, though confusing at times, considering cancer is a complex,

heterogeneous disease. Therefore it will be important to identify the tumor types dependent on autophagy and therapies that genuinely induce cytoprotective autophagy.

First, it is important to distinguish the type of autophagy utilized by the cancer cell. There appear to be four roles autophagy can take on: cytoprotective, cytotoxic, cytostatic, and nonprotective [226]. Cytoprotective autophagy is the most often cited role for autophagy in relation to anti-cancer therapy. If autophagy is cytoprotective, than cells should become more sensitive to a given therapy. However, showing that inhibition of autophagy in the presence of a drug leads to increased apoptosis is not enough to claim a cytoprotective response. Autophagic flux must be enhanced as well. Ideally cells that utilize or treatments that induce cytoprotective autophagy would be candidates for autophagy inhibition therapy. Nonprotective autophagy then refers to autophagy independent survival. Although the cell may have activated autophagy, autophagy functionality does not appear to influence drug efficacy or protect the cell from the assault. This form of autophagy may be characteristic of studies that show a lack or minimal additivity with the combination of autophagy inhibition and therapy [96]. Cytotoxic autophagy meanwhile promotes cell death. To demonstrate this form, autophagy must be induced by the agent and is required for cell death. Although autophagic activity is not likely the mechanism of cell death, autophagy may help to facilitate necrotic or apoptotic cell death. The signaling mechanisms are still unclear but one line of evidence suggests that the autophagosome may serve as a scaffold for activation of caspase-8, which can regulate both apoptosis and necroptosis [227]. Cytostatic autophagy is similar to cytotoxic autophagy in promoting growth inhibition, but instead of autophagy induction contributing to cell death, cells enter growth arrest. This form may be related to autophagy's role in tumor dormancy or senescence. As of now, there is no way to distinguish these forms of autophagy without empirically determining the effects of defective

autophagy on drug sensitivity. It may also be of value to assess the effects of autophagy stimulation. To date, no survival studies have assessed the impact of enhancing autophagy [228]. While the cytoprotective hypothesis would state that increasing autophagy would only make things worse, no study has truly established the relationship. Showing that further increases in autophagy desensitizes cells to therapy may aid in demonstrating a cytoprotective function for autophagy. Continued study should focus on identification of tumor types or therapies that preferentially induce cytoprotective autophagy and will ultimately have the best response to autophagy inhibition therapy.

As the connection of autophagy dysregulation to disease was first identified in breast cancer, autophagy inhibition has been heavily studied in this tumor type. Breast cancer is a heterogeneous disease and is generally categorized into subtypes based on expression of hormone receptors, estrogen (ER) and progesterone (PR), HER2 (ERB2), or lack thereof [229]. Breast cancers that express none of these receptors are classified as triple negative. Therapies such as tamoxifen or trastuzumab can be used to abrogate ER or HER2 signaling. However, no such targeted therapy exists for triple negative breast cancer, which also carries a poor prognosis. Initially, autophagy was seen as a tumor suppressor for breast cancer. In line with that, one of the first combination studies concluded that ER dependent MCF-7 cells succumbed to tamoxifen induced cell death by cytotoxic autophagy [143]. Tamoxifen appeared to greatly enhance autophagic activity and inhibition of autophagy lead to a decrease in tamoxifen sensitivity. However, a number of other studies implicated autophagy as a mechanism of resistance toward tamoxifen therapy [230, 231]. Additionally inhibition of autophagy may promote the switch from necrotic to apoptotic death in tamoxifen treated cells. An even more recent study used a high throughput screen to identify kinases that conferred tamoxifen resistance [232]. The kinase they

identified, HSPB8, also inhibited autophagy. The conclusion from that study was then that increasing autophagy can help overcome resistance. So while it appears clear that tamoxifen induces autophagy, it is not yet evident whether autophagy has a cytoprotective or cytotoxic role in anti-estrogen therapy. Radiation is another common method of treatment for breast cancer. Similar to tamoxifen, a vitamin D analog sensitized MCF-7 and ZR-75 cells to ionizing radiation by inducing cytotoxic autophagy [233, 234]. However, in a syngeneic murine model of breast cancer, autophagy inhibition failed to sensitize cells. As this model system maintains a functional immune system, autophagy's immunomodulatory effects could have had a counterproductive effect on radiation induced death [221]. In HER2+ trastuzumab resistant cells, autophagy also appears to be an important mechanism for acquired resistance. Knockdown of BECN1 could restore trastuzumab sensitivity and low BECN1 expression appears to predict trastuzumab sensitivity as loss of BECN1 is associated with HER2 amplification [235, 236]. Although no targeted therapy exists for triple negative breast cancer, inducing ER stress or inhibiting proteasome degradation may prove to be effective strategies as these cells are highly proliferative and generate a great deal of proteotoxic and genotoxic stress. Not surprisingly then, these cell types have high levels of basal autophagy. Bortezomib (Velcade), a proteasome inhibitor, and nelfinavir and celecoxib, ER stress inducers, appear to synergize with autophagy inhibition [86, 237]. NF-kB, another stress response activator, seems to be another effective target to combine with autophagy inhibition [238]. In a recent study, LC3 expression correlated with a poor prognosis for triple negative cancers only, not hormone dependent or HER2 positive [239]. For breast cancer therapy, autophagy inhibition appears to be effective in triple negative cells, perhaps due to the highly proliferative nature of these cells whereas results are more inconsistent for resistance to anti-estrogen or HER2 therapy.

Autophagy inhibition \ is proving to elicit anti-tumor responses in other cancer types as well. Like breast cancer, autophagy was thought to be a barrier to tumorigenesis in heptacellular carcinoma (HCC) as Atg7 liver specific deletions in mice lead to development of adenomas [122]. Interestingly, mice with systemic mosaic deletions of Atg5 only develop tumors within the liver, most of which are benign, but no other tissue [112]. Thus for HCC, autophagy may still be an important tumor suppressive mechanism. But like most other cancers, once established, autophagy seems to be cytoprotective for HCC. High expression of LC3 correlates to poor prognosis in HCC patients [240]. Additionally, inhibiting autophagy can suppress pulmonary metastasis in an HCC model by restoring anoikis sensitivity and limiting survival during lung colonization [187]. Autophagy may also contribute to sorafenib resistance. Sorafenib is a multikinase inhibitor used as a first line therapy in HCC. Sorafenib resistant HCC cells have elevated levels of autophagy and inhibition by CQ or genetic silencing can potentiate sorafenib efficacy [241, 242]. Yet, similar to taxmoxifen resistant breast cancer cells, increasing autophagy may help to overcome sorafenib resistance. [243] One of the mechanisms for sorafenib resistance is increased Akt signaling. In non-tumorigenic cells, Akt inhibits autophagy through mTOR signaling, but it appears in sorafenib resistant HCC cells, autophagy can co-exist with activated Akt. Akt inhibition can sensitize HCC cells to sorafenib, which drives autophagic flux further. So like the case of tamoxifen resistant cells, autophagy could switch from cytoprotective to cytotoxic in sorafenib resistant HCC cells. Other therapies that have potential utility in combination with CQ include 5-fluoruracil, bortezomib, and cisplatin [244, 245]. While inhibiting autophagy may be an effective strategy for some therapies, it appears that autophagy's role in HCC is complex and inhibition may not always be the most successful option.

Targeting autophagy may be a viable strategy for treating some forms of pancreatic cancer. Pancreatic cancer has one of the lowest survival rates for all cancer types and as of now there exists no particularly effective treatment [246]. Identification of new approaches to chemosensitization are sorely needed. One of the most common mutations is activation of KRAS [246]. Autophagy appears to be one of the necessary mechanisms for tumor initiation of KRAS activated tumors [156]. Low-grade pre-malignant intraepithelial lesions have lower levels of autophagy compared to high-grade lesions and advanced pancreatic ductal adenocarcinoma [247]. CQ and HCQ also have efficacy as single agents, indicating that autophagy inhibition may be particularly effective in pancreatic cancer [247]. In addition, autophagy inhibition enhances sensitivity to gemcitabine, a first line therapy for pancreatic cancer [248]. Yet some recent studies add a degree of complexity to autophagy's role in pancreatic cancer. Rosenfeldt and colleagues substantiated autophagy's importance for KRAS activated tumorigenesis, but only in p53 wild type tumors [165]. If p53 was lost, then autophagy was no longer required. In fact, inhibition of autophagy lead to increased tumor initiation. A subsequent study though demonstrated that while tumors are initiated faster with combined loss of autophagy and p53 in KRAS activated pancreatic cancer, they do not progress into invasive cancer [249]. Furthermore, mouse pancreatic cell lines and patient derived xenografts with differing p53 status all responded to HCQ therapy. Once again, tumor stage may play a role in autophagy dependency, but the evidence does suggest that advanced pancreatic cancer may be particularly reliant on autophagy and as such respond well to autophagy inhibition.

Similar to pancreatic cancer, KRAS mutation is very common in non-small cell lung cancer (NSCLC). Much like pancreatic cancer, autophagy inhibition can prevent the transformation of malignant adenomas, rather leading to the formation of the more benign

oncocytomas [163]. But unlike the former, KRAS activation may not be predictive of autophagy dependence [250]. NSCLC cell lines with activated KRAS are no more sensitive to CQ than wild type KRAS cells. In fact, ectopic expression of KRAS made some more resistant to CQ. p53 status does not appear to play a role either. No correlation was observed between p53 status and CQ sensitivity in NSCLC cell lines. Another common mutation event is constitutive activation of epidermal growth factor receptor (EGFR), which signals through Akt/PI3K and MAPK pathways promoting survival and proliferation [251]. HER2 is in the family of EGFRs and is also commonly amplified in breast cancer. The small molecule inhibitors lapatnib, geftinib, and erlotinib are effective in both breast cancer and NSCLC for disrupting EGFR signaling. Inhibition of EGFR promotes autophagy as activated EGFR can phosphorylate BECN1 and prevent binding to Vps34. In breast cancer, induced autophagy appears to be cytoprotective, and the combination of autophagy and EGFR inhibition is synergistic [252]. Conversely autophagy inhibition decreases efficacy in NSCLC. A tyrosine phosphorylation mutant of BECN1 at the site of EGFR binding enhanced tumorigenesis and reduced response to erlotinib [253]. Although the combination of autophagy inhibition and cytotoxic chemotherapy like cisplatin and 5-fluorouracil seems effective [254, 255]. With NSCLC, autophagy inhibition may not be the most appropriate therapy for all cases.

Other notable solid tumor types responsive to autophagy modulation include melanoma, glioma, colon, and prostate cancer. Autophagy appears to be particularly high in melanoma [256, 257]. A significant subset of patients, 40-60%, carry an activating mutation in BRAF where a glutamic acid has been substituted for valine at codon 600 (BRAF V600E) [258]. Autophagy can suppress early activation of BRAF through oncogene-induced senescence, but like most other cancers, as the disease progresses, autophagy becomes cytoprotective [259]. Vemurafenib is a

highly effective therapy for inhibting BRAF signaling, specifically the V600E mutant [258]. However, patients generally relapse and it appears autophagy may be a means for resistance [260]. Very early studies may have indicated potential biomarkers of high autophagic activity in melanoma patients. Autophagy can regulate secretion of many immune modulators. Melanoma patients exhibiting high levels of autophagy had greater levels of IL1B, CXCL8, LIF, FAM3C, and DKK3 in their serum [261]. In two murine models, low autophagy expressesors had much less of these chemokines compared to their high expressing counterparts. Over-expression of BECN1 could correspondingly increase these levels, potentially suggesting, that at least in the case of melanoma, high autophagic activity could be indicated by these markers. Yet, some results with CQ sensitization may be independent of autophagy as a recent study demonstrates that CQ normalized vasculature and enhanced cisplatin delivery to the tumor regardless of autophagy functionality in a syngeneic model of melanoma [220]. Autophagy expression appears more variable in colon, glioma, and prostate cancers. While over-expression of BECN1 is evident in a subset of some colon cancers, another substantial portion has under-expression. Low levels of BECN1 actually correlate with a poorer prognosis as compared with most other tumor types [262, 263]. In contrast with most other tumors, autophagy is relatively high in normal mucosa [264]. Loss of autophagy in the gut has profound effects such as susceptibility to colitis and an association with Crohn's disease. Therefore, managing autophagy may be more of a burden to overcome for colon cancer. For those that do have functional autophagy, in line with most other studies, autophagy has been found to be a mechanism of resistance to 5-fluorouracil, topotecan, oxalaplatin, and bevacizumab [265-268]. But for irinotecan and topotecan, p53 status may matter [266]. Similarly, high-grade gliomas have lower expression of BECN1 compared to low grade tumors [269]. A decrease in autophagy is also consistent with astrocytic progression

[270]. And yet, autophagy inhibition still appears to synergize with a number of therapies, particularly, the alkylating agent temezolomide [271]. Interestingly, inhibition by early stage inhibitor 3-methyladenine was not able to sensitize cells, only late stage blockade by CQ or Baf A1 could. This also held true in combination with tyrosine kinase inhibitor, imatinib [272]. Perhaps these results more reflect CQ and Baf A1's ability to inhibit endocytosis as well or the autophagosome as a scaffold for apoptosis/necroptosis activators. For prostate cancer, differential autophagic activity may be due to androgen receptor (AR) signaling. Like in breast cancer, prostate cancer may be hormonally driven. AR dependent tumor types suppress autophagy [273]. Inhibition of AR signaling can restore autophagy [274]. This restoration of autophagy may lead to resistance, as inhibition of autophagy can potentiate androgen ablation therapy and restore sensitivity to resistant prostate cancer cells [272, 275]. For these highly aggressive solid tumor types, autophagy inhibition may have some efficacy in a subset. The next challenge then, is to identify those with autophagy dependence, as it is evident that autophagy activation is not a universal phenomenon as previously conceived.

Autophagy inhibition is also having success in hematopoietically-derived tumors, that is the lymphomas, leukemias, and myelomas. In non-transformed cells, autophagy is critical for hematopoietic stem cell maintenance and survival as evidenced by Atg7 deletions [276]. Additionally Atg5, BECN1, and LC3 are important for early lymphocyte development [277, 278]. Mature $CD4^+$ and $CD8^+$ T-cells actually have very low levels of autophagy, but induce it once they have become activated. Atg5 is also critical for B cell survival [279]. Thus, autophagy is already essential for their continued survival. Oncogene activation seems to require even further autophagy activation for tumor transformation. The oncogene c-Myc is either amplified or activated in a majority of hematopoietic cancers. Like in Ras activated cancers, autophagy is

also required for Myc-induced tumorigenesis [280, 281]. Myc appears to cause an increase in UPR and ER stress. Autophagy is able to mitigate these responses and inhibition leads to increased apoptosis. p53 is also commonly lost in Myc activated tumors. Restoration of p53 can restore apoptosis, and inhibition of autophagy can potentiate p53-activated apoptosis [155]. However, some therapies may initiate cell death through apoptosis independent mechanisms such as necroptosis which appear to require autophagy [147]. Thus, in this instance, inhibition of autophagy may not be the best rationale. As with many other cancer types, autophagy inhibition can work syngergistically with bortezomib, ER stress inducers, and histone deacetylases [282-284]. A new approach in multiple myeloma suggests blocking SQSTM1 directly may be effective [285]. Inhibition of SQSTM1 causes a cargo loading failure and can initiate apoptosis. This approach enhanced bortezomib killing. Therefore, hematopoietic tumors may be another autophagy dependent tumor type, however, caution may be needed if certain therapies utilize an apoptotic independent mechanism of cell death. Further investigation should determine if this may be related to the tumor cells ability to undergo functional apoptosis.

Looking at the broad response of autophagy inhibition across tumor types, the main conclusion appears to be that autophagy is not the universal response many predicted it to be. However, there do appear subsets across different cancer types that may be distinctly sensitive to autophagy inhibition. There is some evidence that indicates RAS and MYC activated tumors maintaining wild type p53 are dependent on autophagy and can succumb to apoptosis if treated with an inhibitor, but not for all tumor types. Cytotoxic chemotherapies may overall elicit cytoprotective effects but for targeted therapies, this will be more context dependent. Hormone dependent cancers may not be responsive initially, but once they have become therapy resistant, i.e. no longer dependent on hormone signaling, they become more susceptible to autophagy

inhibition. Triple negative breast cancers, pancreatic cancers, melanoma, and hematopoietic cancers seem to be especially reliant on autophagy. But for many tumor types or therapies, no pattern is really emerging. This ambiguity arises as many studies stand in direct opposition to one another, particularly the story of tamxoifen resistance and EGFR inhibition. A study from the Thorburn laboratory may have one answer as to why cells may not always respond the same [286]. Autophagic activity is not homogenous within a population even under basal conditions. Levels of autophagy are regulated by cell size, cell cycle and spontaneous apoptosis. These differences are transient. The level of activity can predict which cells will live and which will die. They treated cells with death receptor agonists Fas Ligand (FasL) and TRAIL, which can both induce apoptosis. Cells undergoing high autophagic flux had increased sensitivity to FasL but decreased to TRAIL induced apoptosis. The molecular rationale was selective degradation of negative regulator of Fas induced apoptosis, Fap-1 by autophagy. Degradation of Fap-1 allowed Fas induced apoptosis to proceed, whereas Fap-1 is not responsible for regulating TRAIL induced apoptosis. So perhaps a similar mechanism underlies the conflicting results. Though different stimuli can lead to the same result, they may differentially alter autophagic processing or may be sensitive to autophagic levels within the cell. This study underscores that we still have much to learn about autophagy's role in cell death. As autophagy inhibition proceeds into clinical trials, it is imperative that we understand the mechanism of cell death and what biomarkers can predict autophagy dependence if it is to become an effective therapy.

Animal Models of Cancer

For many tumor types, the data in support of autophagy inhibition as a mechanism for chemosensitization appear inconclusive. Much of the problem can be attributed to issues discussed previously such as interpretation of assay output, particularly in an *in vivo* setting,

tumor stage, lack of potent, diverse autophagy inhibitors, and variation of autophagic activity within a population. On top of these difficulties is the choice of animal model. The mouse xenograft model has served cancer research for several decades. In this model, human tumors are either transplanted or subcutaneously injected into the flank of the mouse. The immune system of the mouse has been compromised in order for the tumors to grow. Immune deficiency has been achieved by developing mice lacking a thymus (nude) or T- and B-cells (severe combined immunodeficient [SCID]). As with many cancer therapies, the majority of autophagy related studies have been conducted in immune compromised mice [221]. Since autophagy has immunomodulatory functions, one can appreciate that removal of the immune system can be problematic.

Autophagy is required for the release of ATP as well as HMGB1 upon tumor cell death. ATP and HMGB1 are part of the critical steps for immune related or immunogenic cell death: exposure of calreticulin to the cell surface, release of HMGB1 and ATP. These signals promote recruitment of dendritic and cytotoxic T-cells, which serve to remove the dying tumor cells. A number of therapies elicit immunogenic cell death including anthracyclines, mitoxantrone, and platinum agents [107]. Michaud and colleagues found that autophagy was specifically required for release of ATP, but not HMGB1 or calreticulin [107]. Autophagy deficient murine colon cancer cells, CT-26, or breast cancer cells, MCA205, did not respond to mitoxantrone or oxaliplatin. Inhibiting ATP hydrolysis was able to restore recruitment of T-cells and dendritic cells. Similarly, therapy showed no efficacy in immunodeficient mice and increasing ATP concentrations did not affect growth in autophagy deficient tumors, unlike in the immune competent Balb/c mice. In a follow up study, the group demonstrated that autophagy inhibition could sensitize CT-26 cells to radiation in culture and in immunodeficient mice. However, when

grown in immunocompetent mice, inhibition of autophagy actually reduced radiation efficacy [287]. Autophagy may also control the release of HMGB1 [179]. HMGB1 can induce autophagy in surrounding cells through the rage receptor and also influence the way cells die. Similarly to ATP, HMGB1 can enhance immunogenic cell death and promote necrotic death. When autophagy is high, cells may be more prone to necrotic death due to apoptosis suppression, whereas, autophagy deficient cells would be more apt to undergo apoptosis. Necrotic cell death tends to trigger an inflammatory response where apoptotic cells may not [288]. Autophagy has also been shown to be important for cross-presentation of tumor antigens [289]. Conversely, autophagy may aid in immune evasion. In melanoma, genetic inhibition of autophagy by Atg5 knockdown actually increased calreticulin causing increased infiltration of dendritic and T-cells [290]. Similarly, deletion of Fip200 decreased infiltrating macrophages while promoting cytotoxic T-cell recruitment [157]. These observations, however, were made in untreated cells, so like many other functions of autophagy, the effects will likely be context dependent. Therefore, the dearth of autophagy inhibition studies conducted in immunocompetent animal models makes it difficult to parse out these contextual differences and predict clinical relevancy.

The mouse xenograft model can also be a poor predictor of clinical efficacy. The National Cancer Institute's Developmental Therapeutics Program assessed 39 drugs for which there was xenograft model and Phase II clinical data available [291]. They found that activity in xenograft models did not correspond to clinical activity for tumors of the same histotype, unless that drug was active in at least one-third of xenograft models. The unreliability of the model is largely impacted by the loss of heterogeneity and tissue architecture as cells are grown over time in culture. Compounding this problem, if tumors are grown ectopically, in the flank of the mouse, then they lose the contributions of the microenvironment. It has been demonstrated in a

number of cancer models, that many cell lines grown ectopically will lose the ability to spontaneously metastasize [292]. Furthermore, sensitivity to a compound may also be dependent on tumor location. Colon cancer cells, KLM12L4a were implanted into the flank, cecum, or spleen (to induce liver metastasis). Cells grown ectopically experienced 80% growth reduction with treatments of doxorubicin, whereas cecal cells had only 40% reduction and 10% for liver metastasis [293].

A better model is orthotopic tumor implantation. In this context, the tumor is implanted within the tissue of origins. Orthotopically implanted tumors retain the microenvironment, and are more likely to maintain their invasive and metastatic capabilities. In addition, primary tumors derived directly from the patient can be very good predictors of clinical efficacy [294, 295]. Since primary tumors have not been in culture for long periods, they maintain heterogeneity, architecture, and continue to express relevant markers. Clinically relevant dosing regimens should also be considered. Efficacy is often assessed at the maximum tolerated dose. However, many of these doses are not often achievable in patients [295]. Many promising studies showing CQ sensitization of tumor cells were performed in xenograft models with tumors grown ectopically [221]. Thus, the likelihood of CQ sensitization in the clinic is not clear. More studies should incorporate orthotopic implantation and try to utilize primary tumors with dosing regimens that reflect human equivalent exposures for the best predictive outcome.

Another mouse model alongside the xenograft model is the genetically engineered model (GEM). The earliest models were based on overexpression of viral or cellular oncogenes to promote tumorigenesis [292]. With the advent of genome editing using the cre-lox system, genes can be deleted or added. Either the gene of interest or region of genome is flanked by lox-p sites. When cre-recombinase is expressed, it facilitates homologous recombination at the lox-p sites.

The gene of interest is removed or a target gene can be inserted into the genome. Further refinements have allowed for temporal or tissue specific deletions or expression by developing inducible or promoter controlled cre-recombinase expression. GEMs have provided valuable insight into the early steps of tumorigenesis and address very specific mechanistic questions. For example, The MMTV-PyMT model, in which mice express the mouse mammary tumor virus middle T-antigen gene and develop mammary tumors, was used to demonstrate that autophagy is required for tumor development [157]. GEMs also provide the advantage of spontaneous tumor development and allow the immune system to remain intact. However, they do not appear to be good predictors of clinical efficacy [292, 296]. Though tumors do arise spontaneously, they are artificially driven. Additionally, most GEMs lack systemic spread of disease, so metastasis cannot be assessed [297]. In terms of autophagy, GEMs may not be the best choice for determining efficacy, but they have and continue to provide insights into the role of autophagy in tumorigenesis.

Although the mouse is the commonly used model for cancer, it is certainly not the only animal model. Just as with humans, cancer is the leading cause of death in dogs [298]. A canine model of cancer provides many advantages over the murine model [298, 299]. Cancer develops spontaneously without artificial promotion and in the context of the immune system and proper microenvironment. Dogs also experience recurrence and metastasis. They occupy the same environment as humans and not surprisingly, show similar epidemiologic features. The genome has much greater homology to the human as compared to the mouse. Also, many of the same drivers and mutations in human cancers are present in canine cancer. The loss of PTEN and activation of Ras is evident in canine mammary tumors [300]. Activation of the MAPK and PI3K pathways is present in canine melanoma [301]. Loss of CDKN2B/A and the p16/RB pathway

occurs in canine lymphoma [302]. The large body size of dogs allows for greater tissue and fluid collection as well as serial sampling. The tumor size is more proportional to body size than mice [298]. Lastly, clinical trials can be conducted in canine patients more rapidly due to their shorter lifespan. Therefore, the canine model may serve as an excellent prelude to human clinical trials. Incorporating canine trials into autophagy studies may provide a better indication of autophagy inhibition efficacy. Additionally, the ability to obtain serial samples could aid in establishing the relationship between CQ or HCQ exposure and autophagy inhibition.

Clinical Data

Despite the fact that there is still much that needs to be addressed in regard to autophagy inhibition therapy, clinical trials are underway. The totality of the data does seem to support that autophagy inhibition can enhance cell death, albeit conditionally. This hint of efficacy is enough to drive forward with the addition of HCQ to the standard of care. Though for many of these cancer types, there really exists no effective therapy and survival is very poor. Therefore any increase response can be seen as a success. As of now, the first Phase I trials have been completed. There are currently 53 more trials with HCQ in the use of cancer treatment according to clinicaltrials.gov. Being Phase I trials, little data on clinical efficacy was collected as the main goals of these studies were to determine a maximum tolerated dose and ability of HCQ to inhibit autophagy. These trials were able to show that HCQ can safely be combined with chemotherapy and accumulate within the PBMCs. There is some justification to try and proceed into Phase II trials, but these studies bring to light more challenges that need resolutions for continuing studies.

The first completed Phase I trials with HCQ specifically used for autophagy inhibition are: radiation and adjuvant temozolomide for newly diagnosed glioblastoma multiforme, dose intense temozolomide for advanced solid tumors and melanoma, bortezomib in refractory myeloma, temsirolimus for advanced solid tumors and melanoma, and HDAC inhibitor vorinostat for advanced solid tumors [303-307]. In the majority of these studies, no dose limiting toxicity was observed and the authors recommend 600 mg HCQ twice daily for Phase II studies. In cases where dose limiting toxicity was observed, the combination of radiation and adjuvant temozolomide, and vorinostat, 600 mg once daily was the recommended dose. Dose limiting toxicities included fatigue, gastrointestinal adverse events, neutropenia, thrombocytopenia, and sepsis. Autophagy was measured by accumulation of autophagosomes within PBMCs. For all studies, significant accumulation was observed, overall, but was inconsistent on a patient by patient basis. Tumor measurements were only taken in the temsirolimus study. In that study, accumulation of autophagosomes was only observed in the 600 mg twice daily or 1200 mg total cohort. In line with this, the radiation and temozolomide study reported that most patients did not achieve autophagy inhibition, but could not dose escalate anymore due to toxicity. In the dose intense temozolomide study, they noted that rather than a linear relationship, a threshold level of HCQ was required to elicit autophagy inhibition. Taken together, this data suggests that 1200 mg daily is required to achieve inhibition, but this may not be possible in all patients depending on the therapy combination. However, this was just for PBMCs, and as only one study assessed the tumor levels, the relevance of these findings is uncertain for actual tumor measurements. These findings also highlight that HCQ is not a very potent autophagy inhibitor and new drugs with a better therapeutic index will be required to make autophagy inhibition therapy a viable strategy.

For the temozolomide and radiation trial, efficacy data were collected. There was no significant improvement in survival with the addition of HCQ, which the authors believe is due to the fact that they could not achieve autophagy inhibition in most patients. In the other studies, modest responses were reported, with the best response being partial response in 13.6% in the dose intense temozolomide study and 14% in the bortezomib study. Stable disease for a period was noted in 27% of the dose intense temozolomide study, 45% in bortezomib, and 74% in temsirolimus. Perhaps more in depth study as to why some patients responded, such as mutation status or successful autophagy inhibition, may help guide treatment decisions in future trials.

Project Rationale

There is compelling evidence for the inhibition of autophagy as a novel approach to chemosensitization. As a result, the enthusiasm pushing clinical trials forward is not likely to subside any time soon. It behooves us then to resolve the questions and challenges still preventing us from making a more definitive claim on whether autophagy inhibition will be a successful therapy. Therefore, the large overarching goal of this project was to address some of these remaining questions to determine if autophagy inhibition can be an effective anti-cancer therapy.

The role of autophagy has largely been studied in the setting of primary tumor development and progression. Yet the majority of patients succumb to metastatic disease. From the few studies that have investigated autophagy in a metastatic setting, the results are largely conflicting. In **Chapter 2 (Autophagy influences the establishment of the metastatic microenvironment),** we tested the effect of modulating autophagy along different points of the

metastatic cascade using cell based assays and mouse models that attempt to mimic these various time points. We employed multiple methods of inhibition, both pharmacologic and genetic knockdown, to better discern whether observed results were due to autophagy or off-target, independent effects. We also tested autophagy stimulation using the sugar trehalose. Cell lines used were murine breast cancer, melanoma, and osteosarcoma. These particular cell lines were chosen as they could allow us to use syngeneic, orthotopic models, keeping in context the immune system and microenvironment. Autophagy inhibition was first tested *in vitro* to determine if it could reduce cellular proliferation in these cell types. Following those experiments, we used an experimental metastasis mouse model to ascertain autophagy's role in lung colonization and survival. We also developed a surgical resection model and tested autophagy modulation as an adjuvant or neoadjuvant therapy. From these studies we determined that autophagy did not affect metastatic burden or survival, but could hinder or promote cell arrival to the lungs. The addition of chemotherapy, cisplatin, did not increase survival either, but rather was antagonistic. Measuring immune cell populations in the lung by flow cytometry suggested this may be an immune related response. Assessing the metastatic characteristics of the cells by invasion, migration, and anchorage independence assays showed that autophagy was not affecting the metastatic capabilities of the cells. We then assessed the amount of bone marrow derived cells, mediators of pre-metastatic niche formation, present within the lung and circulation before the arrival of tumor cells. We found that more of this cell type was present in autophagy stimulated mice and less in the blood of autophagy inhibited mice. In summation, we observed that autophagy may be influencing the metastatic microenvironment before and even after the cells arrive. This impact on the environment seemed to alter metastatic development more so than any direct cellular characteristics. We then conclude that autophagy inhibition may

best be used as a neoadjuvant therapy or in metastasis prevention; however, it will not be successful as a single agent. Yet, a great deal of caution should be used in deciding chemotherapy combinations.

Although autophagy is thought of as a universal response to tumor stress, it has become apparent that dependence on autophagy is not equal across tumor types. While KRAS, MYC or p53 wild type tumors were thought to be biomarkers for autophagy dependence, this relationship only exists in some tumors. Therefore, other markers of autophagy dependence are needed. Preliminary work by collaborator Dr. Paola Maycotte identified triple negative breast cancer cells as especially dependent on autophagy using an autophagy focused shRNA library. She also observed that autophagy was dispensable in hormone dependent or luminal breast cancers. In **Chapter 3 (*In silico* approaches identify autophagy dependent cell types and pathways),** we treated one autophagy dependent and one autophagy independent human breast tumor with CQ in orthotopic, mouse xenograft models. We found that the autophagy dependent tumor was responsive to CQ treatment, as tumor growth was slowed. No effect was observed on the autophagy independent tumor's growth. Dr. Maycotte had also observed that the autophagy dependent breast cancers had constitutively activated Stat3, where their independent counterparts did not. She demonstrated that Stat3 could regulate autophagy, and Stat3 inhibition could minimize cell death attributed to autophagy knockdown. As a subset of canine osteosarcoma also has constitutive activation of Stat3, we sought to determine if Stat3 activity correlated to autophagy inhibition in canine osteosarcoma. Using western blot analysis we determined Stat3 expression in six different canine osteosarcoma cell lines and assessed CQ sensitivity by proliferation assays. We found that Stat3 activation did not correlate to CQ sensitivity, but neither did sensitivity to a Stat3 inhibitor. We concluded that the canine osteosarcomas may not

be reliant on Stat3 despite its being constitutively activated. Thus the predictive value of Stat3 activity may be tumor type dependent. We also used microarray analysis to identify pathways altered upon autophagy inhibition in the six canine osteosarcomas and six human breast cancers, three dependent on autophagy and three not. Pathway analysis returned similar upregulated pathways in the two different tumor types. Of note, proteasome degradation, histone deacetylation, ER stress, and cholesterol synthesis were upregulated. As targeting cholesterol synthesis was a novel approach for killing canine osteosarcoma cells, we tested the combination of lovastatin and CQ. We found that this combination was actually not successful. However, the other pathways we identified have been linked to autophagy in other cancer types and could still prove to be effective targets in breast cancer and osteosarcoma.

In vivo assessment of autophagy is very challenging due to the dynamic nature of the pathway. A canine model of cancer would allow for greater ease of serial sampling than what can usually be obtained within human clinics and the physiologic data would be more relevant than murine data. Additionally, there is a great, unmet need for novel therapies in the treatment of canine cancer. Lymphoma is one of the most prevalent canine cancers and is a good model for human lymphoma. Single agent doxorubicin is often used in lieu of CHOP therapy due to cost and treatment duration. However, response rate is lower. We show that the combination of doxorubicin and CQ is additive in canine lymphoma cell lines. In **Chapter 4** (**Phase I clinical trial and pharmacodynamic evaluation of combination hydroxychloroquine and doxorubicin treatment in pet dogs treated for spontaneously occurring lymphoma),** we conducted a Phase I clinical trial of the combination HCQ and doxorubicin for the treatment of lymphoma. The goals of the trial were to determine a maximum tolerated dose of HCQ in combination with doxorubicin, the concentration of HCQ within the plasma and tumor, and if

autophagy inhibition was achieved within the tumor. HCQ was administered 72h prior to doxorubicin administration with the aim of sensitizing cells. PBMCs, lymph node aspirates, tumor biopsies, and plasma were collected pre and 3 days post HCQ treatment. Autophagy modulation was assessed by LC3 expression as determined by western blot or flow cytometry. Electron microscopy was also used to quantify the number of autophagosomes within PBMCs. HCQ on its own was well tolerated, but dose limiting toxicity, Grade 5 sepsis occurred at 12.5 mg/kg HCQ and 30 mg/m^2 doxorubcin. No indications of autophagy inhibition were observed until 12.5 mg/kg HCQ. Therefore, doxorubicin was reduced by 20% to 25 mg/m^2. The combination of 12.5 mg/kg and 25 mg/m^2 doxorubicin was well tolerated and used for the duration of the study. HCQ accumulated in the tumor almost threefold over that in plasma. There was not a correlation between plasma and tumor levels. Overall, there was an increase in LC3 II expression and autophagosome number, but not on a patient to patient basis. LC3 II expression did not correlate between plasma and tumor. Taken with the HCQ concentration data, it appears that blood may not be a good surrogate for tumor measurements. There was a trend for LC3 II expression and tumor HCQ levels, but rather than a true linear relationship, it appears that more of a threshold level of HCQ is required to achieve autophagy inhibition. 100% of patients responded, with best response being complete remission. The progression free interval was 4.7 months, which is comparable to historical single agent doxorubicin. With superior response rates and comparable progression free interval to single agent doxorubicin, the combination of HCQ and doxorubicin does hint at potential added benefit. It still remains to be seen if this effect is due to autophagy inhibition, as a number of patients did not appear to have evidence of altered autophagy. With the development of better inhibitors or more sensitive assays, we may be able to better answer this question in the future.

References

1. Klionsky, D.J., et al., *A comprehensive glossary of autophagy-related molecules and processes (2nd edition).* Autophagy, 2011. **7**(11): p. 1273-94.

2. Ashford, T.P. and K.R. Porter, *Cytoplasmic components in hepatic cell lysosomes.* J Cell Biol, 1962. **12**: p. 198-202.

3. Feng, Y., et al., *The machinery of macroautophagy.* Cell Res, 2014. **24**(1): p. 24-41.

4. Deter, R.L., P. Baudhuin, and C. De Duve, *Participation of lysosomes in cellular autophagy induced in rat liver by glucagon.* J Cell Biol, 1967. **35**(2): p. C11-6.

5. Cuervo, A.M., *Autophagy: many paths to the same end.* Mol Cell Biochem, 2004. **263**(1-2): p. 55-72.

6. Dengjel, J., A.R. Kristensen, and J.S. Andersen, *Ordered bulk degradation via autophagy.* Autophagy, 2008. **4**(8): p. 1057-9.

7. Suzuki, K., *Selective autophagy in budding yeast.* Cell Death Differ, 2013. **20**(1): p. 43-8.

8. Shaid, S., et al., *Ubiquitination and selective autophagy.* Cell Death Differ, 2013. **20**(1): p. 21-30.

9. Mortimore, G.E. and A.R. Poso, *Intracellular protein catabolism and its control during nutrient deprivation and supply.* Annu Rev Nutr, 1987. **7**: p. 539-64.

10. Mizushima, N. and D.J. Klionsky, *Protein turnover via autophagy: implications for metabolism.* Annu Rev Nutr, 2007. **27**: p. 19-40.

11. Kroemer, G., G. Marino, and B. Levine, *Autophagy and the integrated stress response.* Mol Cell, 2010. **40**(2): p. 280-93.

12. Murrow, L. and J. Debnath, *Autophagy as a stress-response and quality-control mechanism: implications for cell injury and human disease.* Annu Rev Pathol, 2013. **8**: p. 105-37.

13. Yang, Z. and D.J. Klionsky, *Mammalian autophagy: core molecular machinery and signaling regulation.* Curr Opin Cell Biol, 2010. **22**(2): p. 124-31.

14. Jung, C.H., et al., *ULK-Atg13-FIP200 complexes mediate mTOR signaling to the autophagy machinery.* Mol Biol Cell, 2009. **20**(7): p. 1992-2003.

15. Klionsky, D.J., *The molecular machinery of autophagy: unanswered questions.* J Cell Sci, 2005. **118**(Pt 1): p. 7-18.

16. Ragusa, M.J., R.E. Stanley, and J.H. Hurley, *Architecture of the Atg17 complex as a scaffold for autophagosome biogenesis.* Cell, 2012. **151**(7): p. 1501-12.

17. He, C., et al., *Self-interaction is critical for Atg9 transport and function at the phagophore assembly site during autophagy.* Mol Biol Cell, 2008. **19**(12): p. 5506-16.

18. Ropolo, A., et al., *The pancreatitis-induced vacuole membrane protein 1 triggers autophagy in mammalian cells.* J Biol Chem, 2007. **282**(51): p. 37124-33.

19. Nowak, J., et al., *The TP53INP2 protein is required for autophagy in mammalian cells.* Mol Biol Cell, 2009. **20**(3): p. 870-81.

20. Yang, Z. and D.J. Klionsky, *An overview of the molecular mechanism of autophagy.* Curr Top Microbiol Immunol, 2009. **335**: p. 1-32.

21. Takahashi, Y., C.L. Meyerkord, and H.G. Wang, *Bif-1/endophilin B1: a candidate for crescent driving force in autophagy.* Cell Death Differ, 2009. **16**(7): p. 947-55.

22. Liang, C., et al., *Beclin1-binding UVRAG targets the class C Vps complex to coordinate autophagosome maturation and endocytic trafficking.* Nat Cell Biol, 2008. **10**(7): p. 776-87.

23. Sawa-Makarska, J., et al., *Cargo binding to Atg19 unmasks additional Atg8 binding sites to mediate membrane-cargo apposition during selective autophagy.* Nat Cell Biol, 2014. **16**(5): p. 425-433.

24. Reggiori, F. and D.J. Klionsky, *Autophagic processes in yeast: mechanism, machinery and regulation.* Genetics, 2013. **194**(2): p. 341-61.

25. Kirisako, T., et al., *Formation process of autophagosome is traced with Apg8/Aut7p in yeast.* J Cell Biol, 1999. **147**(2): p. 435-46.

26. Cebollero, E., et al., *Phosphatidylinositol-3-phosphate clearance plays a key role in autophagosome completion.* Curr Biol, 2012. **22**(17): p. 1545-53.

27. Aplin, A., et al., *Cytoskeletal elements are required for the formation and maturation of autophagic vacuoles.* J Cell Physiol, 1992. **152**(3): p. 458-66.

28. Fass, E., et al., *Microtubules support production of starvation-induced autophagosomes but not their targeting and fusion with lysosomes.* J Biol Chem, 2006. **281**(47): p. 36303-16.

29. Kimura, S., T. Noda, and T. Yoshimori, *Dynein-dependent movement of autophagosomes mediates efficient encounters with lysosomes.* Cell Struct Funct, 2008. **33**(1): p. 109-22.

30. Pankiv, S., et al., *FYCO1 is a Rab7 effector that binds to LC3 and PI3P to mediate microtubule plus end-directed vesicle transport.* J Cell Biol, 2010. **188**(2): p. 253-69.

31. Nair, U., et al., *A role for Atg8-PE deconjugation in autophagosome biogenesis.* Autophagy, 2012. **8**(5): p. 780-93.

32. Tong, J., X. Yan, and L. Yu, *The late stage of autophagy: cellular events and molecular regulation.* Protein Cell, 2010. **1**(10): p. 907-15.

33. Nair, U., et al., *SNARE proteins are required for macroautophagy.* Cell, 2011. **146**(2): p. 290-302.

34. Grosshans, B.L., D. Ortiz, and P. Novick, *Rabs and their effectors: achieving specificity in membrane traffic.* Proc Natl Acad Sci U S A, 2006. **103**(32): p. 11821-7.

35. Wang, C.W., et al., *The Ccz1-Mon1 protein complex is required for the late step of multiple vacuole delivery pathways.* J Biol Chem, 2002. **277**(49): p. 47917-27.

36. Epple, U.D., et al., *Aut5/Cvt17p, a putative lipase essential for disintegration of autophagic bodies inside the vacuole.* J Bacteriol, 2001. **183**(20): p. 5942-55.

37. Yang, Z., et al., *Atg22 recycles amino acids to link the degradative and recycling functions of autophagy.* Mol Biol Cell, 2006. **17**(12): p. 5094-104.

38. Klionsky, D.J., et al., *Guidelines for the use and interpretation of assays for monitoring autophagy.* Autophagy, 2012. **8**(4): p. 445-544.

39. Yla-Anttila, P., et al., *Monitoring autophagy by electron microscopy in Mammalian cells.* Methods Enzymol, 2009. **452**: p. 143-64.

40. Eskelinen, E.L., *To be or not to be? Examples of incorrect identification of autophagic compartments in conventional transmission electron microscopy of mammalian cells.* Autophagy, 2008. **4**(2): p. 257-60.

41. Mizushima, N. and T. Yoshimori, *How to interpret LC3 immunoblotting.* Autophagy, 2007. **3**(6): p. 542-5.

42. Holt, S.V., et al., *The development of an immunohistochemical method to detect the autophagy-associated protein LC3-II in human tumor xenografts.* Toxicol Pathol, 2011. **39**(3): p. 516-23.

43. Martinet, W., et al., *Detection of autophagy in tissue by standard immunohistochemistry: possibilities and limitations.* Autophagy, 2006. **2**(1): p. 55-7.

44. Kimura, S., T. Noda, and T. Yoshimori, *Dissection of the autophagosome maturation process by a novel reporter protein, tandem fluorescent-tagged LC3.* Autophagy, 2007. **3**(5): p. 452-60.

45. Gump, J.M. and A. Thorburn, *Sorting cells for basal and induced autophagic flux by quantitative ratiometric flow cytometry.* Autophagy, 2014. **10**(7): p. 1327-34.

46. Eng, K.E., et al., *A novel quantitative flow cytometry-based assay for autophagy.* Autophagy, 2010. **6**(5): p. 634-41.

47. Patterson, G.H. and J. Lippincott-Schwartz, *Selective photolabeling of proteins using photoactivatable GFP.* Methods, 2004. **32**(4): p. 445-50.

48. Bjorkoy, G., et al., *p62/SQSTM1 forms protein aggregates degraded by autophagy and has a protective effect on huntingtin-induced cell death.* J Cell Biol, 2005. **171**(4): p. 603-14.

49. Bjorkoy, G., et al., *Monitoring autophagic degradation of p62/SQSTM1.* Methods Enzymol, 2009. **452**: p. 181-97.

50. Komatsu, M., et al., *The selective autophagy substrate p62 activates the stress responsive transcription factor Nrf2 through inactivation of Keap1.* Nat Cell Biol, 2010. **12**(3): p. 213-23.

51. Bardag-Gorce, F., et al., *Modifications in P62 occur due to proteasome inhibition in alcoholic liver disease.* Life Sci, 2005. **77**(20): p. 2594-602.

52. Norman, J.M., G.M. Cohen, and E.T. Bampton, *The in vitro cleavage of the hAtg proteins by cell death proteases.* Autophagy, 2010. **6**(8): p. 1042-56.

53. Ding, W.X., et al., *Linking of autophagy to ubiquitin-proteasome system is important for the regulation of endoplasmic reticulum stress and cell viability.* Am J Pathol, 2007. **171**(2): p. 513-24.

54. Mizushima, N., et al., *In vivo analysis of autophagy in response to nutrient starvation using transgenic mice expressing a fluorescent autophagosome marker.* Mol Biol Cell, 2004. **15**(3): p. 1101-11.

55. Ni, H.M., et al., *Dissecting the dynamic turnover of GFP-LC3 in the autolysosome.* Autophagy, 2011. **7**(2): p. 188-204.

56. Yan, L., et al., *Autophagy in chronically ischemic myocardium.* Proc Natl Acad Sci U S A, 2005. **102**(39): p. 13807-12.

57. Cabrera, S., et al., *ATG4B/autophagin-1 regulates intestinal homeostasis and protects mice from experimental colitis.* Autophagy, 2013. **9**(8): p. 1188-200.

58. Conway, K.L., et al., *Atg16l1 is required for autophagy in intestinal epithelial cells and protection of mice from Salmonella infection.* Gastroenterology, 2013. **145**(6): p. 1347-57.

59. Jiang, M., et al., *Autophagy in proximal tubules protects against acute kidney injury.* Kidney Int, 2012. **82**(12): p. 1271-83.

60. Wang, P., et al., *Induction of autophagy contributes to the neuroprotection of nicotinamide phosphoribosyltransferase in cerebral ischemia.* Autophagy, 2012. **8**(1): p. 77-87.

61. Mizushima, N., *Autophagy: process and function.* Genes Dev, 2007. **21**(22): p. 2861-73.

62. Mortimore, G.E., N.J. Hutson, and C.A. Surmacz, *Quantitative correlation between proteolysis and macro- and microautophagy in mouse hepatocytes during starvation and refeeding.* Proc Natl Acad Sci U S A, 1983. **80**(8): p. 2179-83.

63. de Waal, E.J., et al., *Quantitative changes in the lysosomal vacuolar system of rat hepatocytes during short-term starvation. A morphometric analysis with special reference to macro- and microautophagy.* Cell Tissue Res, 1986. **243**(3): p. 641-8.

64. Rifki, O.F. and J.A. Hill, *Cardiac autophagy: good with the bad.* J Cardiovasc Pharmacol, 2012. **60**(3): p. 248-52.

65. Cherra, S.J., 3rd and C.T. Chu, *Autophagy in neuroprotection and neurodegeneration: A question of balance.* Future Neurol, 2008. **3**(3): p. 309-323.

66. Rigbolt, K.T., et al., *Characterization of early autophagy signaling by quantitative phosphoproteomics.* Autophagy, 2014. **10**(2): p. 356-71.

67. Ichimura, Y., et al., *A ubiquitin-like system mediates protein lipidation.* Nature, 2000. **408**(6811): p. 488-92.

68. Lee, I.H., et al., *A role for the NAD-dependent deacetylase Sirt1 in the regulation of autophagy.* Proc Natl Acad Sci U S A, 2008. **105**(9): p. 3374-9.

69. Pietrocola, F., et al., *Regulation of autophagy by stress-responsive transcription factors.* Semin Cancer Biol, 2013. **23**(5): p. 310-22.

70. Frankel, L.B. and A.H. Lund, *MicroRNA regulation of autophagy.* Carcinogenesis, 2012. **33**(11): p. 2018-25.

71. Huang, Y., A.Y. Chuang, and E.A. Ratovitski, *Phospho-DeltaNp63alpha/miR-885-3p axis in tumor cell life and cell death upon cisplatin exposure.* Cell Cycle, 2011. **10**(22): p. 3938-47.

72. Zhu, H., et al., *Regulation of autophagy by a beclin 1-targeted microRNA, miR-30a, in cancer cells.* Autophagy, 2009. **5**(6): p. 816-23.

73. Korkmaz, G., et al., *miR-376b controls starvation and mTOR inhibition-related autophagy by targeting ATG4C and BECN1.* Autophagy, 2012. **8**(2): p. 165-76.

74. Frankel, L.B., et al., *microRNA-101 is a potent inhibitor of autophagy.* Embo j, 2011. **30**(22): p. 4628-41.

75. Xiao, J., et al., *MiR-204 regulates cardiomyocyte autophagy induced by ischemia-reperfusion through LC3-II.* J Biomed Sci, 2011. **18**: p. 35.

76. Di Giammartino, D.C., K. Nishida, and J.L. Manley, *Mechanisms and consequences of alternative polyadenylation.* Mol Cell, 2011. **43**(6): p. 853-66.

77. Zoncu, R., A. Efeyan, and D.M. Sabatini, *mTOR: from growth signal integration to cancer, diabetes and ageing.* Nat Rev Mol Cell Biol, 2011. **12**(1): p. 21-35.

78. Sancak, Y., et al., *The Rag GTPases bind raptor and mediate amino acid signaling to mTORC1.* Science, 2008. **320**(5882): p. 1496-501.

79. Saucedo, L.J., et al., *Rheb promotes cell growth as a component of the insulin/TOR signalling network.* Nat Cell Biol, 2003. **5**(6): p. 566-71.

80. Gwinn, D.M., et al., *AMPK phosphorylation of raptor mediates a metabolic checkpoint.* Mol Cell, 2008. **30**(2): p. 214-26.

81. Ruderman, N.B., et al., *AMPK and SIRT1: a long-standing partnership?* Am J Physiol Endocrinol Metab, 2010. **298**(4): p. E751-60.

82. Mammucari, C., et al., *FoxO3 controls autophagy in skeletal muscle in vivo.* Cell Metab, 2007. **6**(6): p. 458-71.

83. Shen, S., et al., *Cytoplasmic STAT3 represses autophagy by inhibiting PKR activity.* Mol Cell, 2012. **48**(5): p. 667-80.

84. Ron, D. and P. Walter, *Signal integration in the endoplasmic reticulum unfolded protein response.* Nat Rev Mol Cell Biol, 2007. **8**(7): p. 519-29.

85. Rouschop, K.M., et al., *The unfolded protein response protects human tumor cells during hypoxia through regulation of the autophagy genes MAP1LC3B and ATG5.* J Clin Invest, 2010. **120**(1): p. 127-41.

86. Milani, M., et al., *The role of ATF4 stabilization and autophagy in resistance of breast cancer cells treated with Bortezomib.* Cancer Res, 2009. **69**(10): p. 4415-23.

87. Cadenas, E. and K.J. Davies, *Mitochondrial free radical generation, oxidative stress, and aging.* Free Radic Biol Med, 2000. **29**(3-4): p. 222-30.

88. Turrens, J.F., *Mitochondrial formation of reactive oxygen species.* J Physiol, 2003. **552**(Pt 2): p. 335-44.

89. Liu, L., et al., *Hypoxic reactive oxygen species regulate the integrated stress response and cell survival.* J Biol Chem, 2008. **283**(45): p. 31153-62.

90. Bellot, G., et al., *Hypoxia-induced autophagy is mediated through hypoxia-inducible factor induction of BNIP3 and BNIP3L via their BH3 domains.* Mol Cell Biol, 2009. **29**(10): p. 2570-81.

91. Liang, X.H., et al., *Protection against fatal Sindbis virus encephalitis by beclin, a novel Bcl-2-interacting protein.* J Virol, 1998. **72**(11): p. 8586-96.

92. Guzy, R.D. and P.T. Schumacker, *Oxygen sensing by mitochondria at complex III: the paradox of increased reactive oxygen species during hypoxia.* Exp Physiol, 2006. **91**(5): p. 807-19.

93. Scherz-Shouval, R., et al., *Reactive oxygen species are essential for autophagy and specifically regulate the activity of Atg4.* Embo j, 2007. **26**(7): p. 1749-60.

94. Thorburn, J., et al., *Autophagy controls the kinetics and extent of mitochondrial apoptosis by regulating PUMA levels.* Cell Rep, 2014. **7**(1): p. 45-52.

95. Geisler, S., et al., *PINK1/Parkin-mediated mitophagy is dependent on VDAC1 and p62/SQSTM1.* Nat Cell Biol, 2010. **12**(2): p. 119-31.

96. Gewirtz, D.A., *Cytoprotective and nonprotective autophagy in cancer therapy.* Autophagy, 2013. **9**(9): p. 1263-5.

97. Achanta, G. and P. Huang, *Role of p53 in sensing oxidative DNA damage in response to reactive oxygen species-generating agents.* Cancer Res, 2004. **64**(17): p. 6233-9.

98. Morselli, E., et al., *p53 inhibits autophagy by interacting with the human ortholog of yeast Atg17, RB1CC1/FIP200.* Cell Cycle, 2011. **10**(16): p. 2763-9.

99. Sumpter, R., Jr. and B. Levine, *Autophagy and innate immunity: triggering, targeting and tuning.* Semin Cell Dev Biol, 2010. **21**(7): p. 699-711.

100. Matzinger, P., *The danger model: a renewed sense of self.* Science, 2002. **296**(5566): p. 301-5.

101. Copetti, T., et al., *p65/RelA modulates BECN1 transcription and autophagy.* Mol Cell Biol, 2009. **29**(10): p. 2594-608.

102. Zheng, Y.T., et al., *The adaptor protein p62/SQSTM1 targets invading bacteria to the autophagy pathway.* J Immunol, 2009. **183**(9): p. 5909-16.

103. Lee, H.K., et al., *Autophagy-dependent viral recognition by plasmacytoid dendritic cells.* Science, 2007. **315**(5817): p. 1398-401.

104. Deretic, V., T. Saitoh, and S. Akira, *Autophagy in infection, inflammation and immunity.* Nat Rev Immunol, 2013. **13**(10): p. 722-37.

105. Lee, H.K., et al., *In vivo requirement for Atg5 in antigen presentation by dendritic cells.* Immunity, 2010. **32**(2): p. 227-39.

106. Castillo, E.F., et al., *Autophagy protects against active tuberculosis by suppressing bacterial burden and inflammation.* Proc Natl Acad Sci U S A, 2012. **109**(46): p. E3168-76.

107. Michaud, M., et al., *Autophagy-dependent anticancer immune responses induced by chemotherapeutic agents in mice.* Science, 2011. **334**(6062): p. 1573-7.

108. Aita, V.M., et al., *Cloning and genomic organization of beclin 1, a candidate tumor suppressor gene on chromosome 17q21.* Genomics, 1999. **59**(1): p. 59-65.

109. Liang, X.H., et al., *Induction of autophagy and inhibition of tumorigenesis by beclin 1.* Nature, 1999. **402**(6762): p. 672-6.

110. Qu, X., et al., *Promotion of tumorigenesis by heterozygous disruption of the beclin 1 autophagy gene.* J Clin Invest, 2003. **112**(12): p. 1809-20.

111. Marino, G., et al., *Tissue-specific autophagy alterations and increased tumorigenesis in mice deficient in Atg4C/autophagin-3.* J Biol Chem, 2007. **282**(25): p. 18573-83.

112. Takamura, A., et al., *Autophagy-deficient mice develop multiple liver tumors.* Genes Dev, 2011. **25**(8): p. 795-800.

113. Lee, J.W., et al., *Somatic mutations of BECN1, an autophagy-related gene, in human cancers.* Apmis, 2007. **115**(6): p. 750-6.

114. Laddha, S.V., et al., *Mutational landscape of the essential autophagy gene BECN1 in human cancers.* Mol Cancer Res, 2014. **12**(4): p. 485-90.

115. Kim, M.S., et al., *Frameshift mutation of UVRAG, an autophagy-related gene, in gastric carcinomas with microsatellite instability.* Hum Pathol, 2008. **39**(7): p. 1059-63.

116. Liang, C., et al., *Autophagic and tumour suppressor activity of a novel Beclin1-binding protein UVRAG.* Nat Cell Biol, 2006. **8**(7): p. 688-99.

117. Knaevelsrud, H., et al., *UVRAG mutations associated with microsatellite unstable colon cancer do not affect autophagy.* Autophagy, 2010. **6**(7): p. 863-70.

118. Kang, M.R., et al., *Frameshift mutations of autophagy-related genes ATG2B, ATG5, ATG9B and ATG12 in gastric and colorectal cancers with microsatellite instability.* J Pathol, 2009. **217**(5): p. 702-6.

119. Lebovitz, C.B., S.B. Bortnik, and S.M. Gorski, *Here, there be dragons: charting autophagy-related alterations in human tumors.* Clin Cancer Res, 2012. **18**(5): p. 1214-26.

120. Raben, N., et al., *Suppression of autophagy in skeletal muscle uncovers the accumulation of ubiquitinated proteins and their potential role in muscle damage in Pompe disease.* Hum Mol Genet, 2008. **17**(24): p. 3897-908.

121. Nakai, A., et al., *The role of autophagy in cardiomyocytes in the basal state and in response to hemodynamic stress.* Nat Med, 2007. **13**(5): p. 619-24.

122. Komatsu, M., et al., *Impairment of starvation-induced and constitutive autophagy in Atg7-deficient mice.* J Cell Biol, 2005. **169**(3): p. 425-34.

123. Jung, H.S., et al., *Loss of autophagy diminishes pancreatic beta cell mass and function with resultant hyperglycemia.* Cell Metab, 2008. **8**(4): p. 318-24.

124. Hara, T., et al., *Suppression of basal autophagy in neural cells causes neurodegenerative disease in mice.* Nature, 2006. **441**(7095): p. 885-9.

125. Mathew, R., et al., *Autophagy suppresses tumor progression by limiting chromosomal instability.* Genes Dev, 2007. **21**(11): p. 1367-81.

126. Karantza-Wadsworth, V., et al., *Autophagy mitigates metabolic stress and genome damage in mammary tumorigenesis.* Genes Dev, 2007. **21**(13): p. 1621-35.

127. Park, Y.E., et al., *Autophagic degradation of nuclear components in mammalian cells.* Autophagy, 2009. **5**(6): p. 795-804.

128. Itoh, K., et al., *Keap1 represses nuclear activation of antioxidant responsive elements by Nrf2 through binding to the amino-terminal Neh2 domain.* Genes Dev, 1999. **13**(1): p. 76-86.

129. Copple, I.M., et al., *Physical and functional interaction of sequestosome 1 with Keap1 regulates the Keap1-Nrf2 cell defense pathway.* J Biol Chem, 2010. **285**(22): p. 16782-8.

130. Inami, Y., et al., *Persistent activation of Nrf2 through p62 in hepatocellular carcinoma cells.* J Cell Biol, 2011. **193**(2): p. 275-84.

131. Inoue, D., et al., *Accumulation of p62/SQSTM1 is associated with poor prognosis in patients with lung adenocarcinoma.* Cancer Sci, 2012. **103**(4): p. 760-6.

132. Wooten, M.W., et al., *The p62 scaffold regulates nerve growth factor-induced NF-kappaB activation by influencing TRAF6 polyubiquitination.* J Biol Chem, 2005. **280**(42): p. 35625-9.

133. Grasso, D. and M.I. Vaccaro, *Macroautophagy and the oncogene-induced senescence.* Front Endocrinol (Lausanne), 2014. **5**: p. 157.

134. Singh, K., et al., *Autophagy-dependent senescence in response to DNA damage and chronic apoptotic stress.* Autophagy, 2012. **8**(2): p. 236-51.

135. Patschan, S., et al., *Lipid mediators of autophagy in stress-induced premature senescence of endothelial cells.* Am J Physiol Heart Circ Physiol, 2008. **294**(3): p. H1119-29.

136. Young, A.R., et al., *Autophagy mediates the mitotic senescence transition.* Genes Dev, 2009. **23**(7): p. 798-803.

137. Kerr, J.F., A.H. Wyllie, and A.R. Currie, *Apoptosis: a basic biological phenomenon with wide-ranging implications in tissue kinetics.* Br J Cancer, 1972. **26**(4): p. 239-57.

138. Bursch, W., *The autophagosomal-lysosomal compartment in programmed cell death.* Cell Death Differ, 2001. **8**(6): p. 569-81.

139. Gozuacik, D. and A. Kimchi, *Autophagy as a cell death and tumor suppressor mechanism.* Oncogene, 2004. **23**(16): p. 2891-906.

140. Schweichel, J.U. and H.J. Merker, *The morphology of various types of cell death in prenatal tissues.* Teratology, 1973. **7**(3): p. 253-66.

141. Clarke, P.G., *Developmental cell death: morphological diversity and multiple mechanisms.* Anat Embryol (Berl), 1990. **181**(3): p. 195-213.

142. Xue, L., G.C. Fletcher, and A.M. Tolkovsky, *Mitochondria are selectively eliminated from eukaryotic cells after blockade of caspases during apoptosis.* Curr Biol, 2001. **11**(5): p. 361-5.

143. Bursch, W., et al., *Active cell death induced by the anti-estrogens tamoxifen and ICI 164 384 in human mammary carcinoma cells (MCF-7) in culture: the role of autophagy.* Carcinogenesis, 1996. **17**(8): p. 1595-607.

144. Kanzawa, T., et al., *Induction of autophagic cell death in malignant glioma cells by arsenic trioxide.* Cancer Res, 2003. **63**(9): p. 2103-8.

145. Shen, S., et al., *Association and dissociation of autophagy, apoptosis and necrosis by systematic chemical study.* Oncogene, 2011. **30**(45): p. 4544-56.

146. Galluzzi, L. and G. Kroemer, *Necroptosis: a specialized pathway of programmed necrosis.* Cell, 2008. **135**(7): p. 1161-3.

147. Bonapace, L., et al., *Induction of autophagy-dependent necroptosis is required for childhood acute lymphoblastic leukemia cells to overcome glucocorticoid resistance.* J Clin Invest, 2010. **120**(4): p. 1310-23.

148. Khan, M.J., et al., *Inhibition of autophagy rescues palmitic acid-induced necroptosis of endothelial cells.* J Biol Chem, 2012. **287**(25): p. 21110-20.

149. Kroemer, G. and B. Levine, *Autophagic cell death: the story of a misnomer.* Nat Rev Mol Cell Biol, 2008. **9**(12): p. 1004-10.

150. Boya, P., et al., *Inhibition of macroautophagy triggers apoptosis.* Mol Cell Biol, 2005. **25**(3): p. 1025-40.

151. Degenhardt, K., et al., *Autophagy promotes tumor cell survival and restricts necrosis, inflammation, and tumorigenesis.* Cancer Cell, 2006. **10**(1): p. 51-64.

152. Hu, Y.L., et al., *Hypoxia-induced autophagy promotes tumor cell survival and adaptation to antiangiogenic treatment in glioblastoma.* Cancer Res, 2012. **72**(7): p. 1773-83.

153. Schaaf, M.B., et al., *The autophagy associated gene, ULK1, promotes tolerance to chronic and acute hypoxia.* Radiother Oncol, 2013. **108**(3): p. 529-34.

154. Abedin, M.J., et al., *Autophagy delays apoptotic death in breast cancer cells following DNA damage.* Cell Death Differ, 2007. **14**(3): p. 500-10.

155. Amaravadi, R.K., et al., *Autophagy inhibition enhances therapy-induced apoptosis in a Myc-induced model of lymphoma.* J Clin Invest, 2007. **117**(2): p. 326-36.

156. Guo, J.Y., et al., *Activated Ras requires autophagy to maintain oxidative metabolism and tumorigenesis.* Genes Dev, 2011. **25**(5): p. 460-70.

157. Wei, H., et al., *Suppression of autophagy by FIP200 deletion inhibits mammary tumorigenesis.* Genes Dev, 2011. **25**(14): p. 1510-27.

158. Warburg, O., *On the origin of cancer cells.* Science, 1956. **123**(3191): p. 309-14.

159. Vander Heiden, M.G., L.C. Cantley, and C.B. Thompson, *Understanding the Warburg effect: the metabolic requirements of cell proliferation.* Science, 2009. **324**(5930): p. 1029-33.

160. Sonveaux, P., et al., *Targeting lactate-fueled respiration selectively kills hypoxic tumor cells in mice.* J Clin Invest, 2008. **118**(12): p. 3930-42.

161. Son, J., et al., *Glutamine supports pancreatic cancer growth through a KRAS-regulated metabolic pathway.* Nature, 2013. **496**(7443): p. 101-5.

162. White, E., *Exploiting the bad eating habits of Ras-driven cancers.* Genes Dev, 2013. **27**(19): p. 2065-71.

163. Guo, J.Y., et al., *Autophagy suppresses progression of K-ras-induced lung tumors to oncocytomas and maintains lipid homeostasis.* Genes Dev, 2013. **27**(13): p. 1447-61.

164. Soussi, T. and K.G. Wiman, *Shaping genetic alterations in human cancer: the p53 mutation paradigm.* Cancer Cell, 2007. **12**(4): p. 303-12.

165. Rosenfeldt, M.T., et al., *p53 status determines the role of autophagy in pancreatic tumour development.* Nature, 2013. **504**(7479): p. 296-300.

166. Loos, B., et al., *The variability of autophagy and cell death susceptibility: Unanswered questions.* Autophagy, 2013. **9**(9): p. 1270-85.

167. Lemasters, J.J., et al., *The mitochondrial permeability transition in cell death: a common mechanism in necrosis, apoptosis and autophagy.* Biochim Biophys Acta, 1998. **1366**(1-2): p. 177-96.

168. Loos, B., et al., *At the core of survival: autophagy delays the onset of both apoptotic and necrotic cell death in a model of ischemic cell injury.* Exp Cell Res, 2011. **317**(10): p. 1437-53.

169. Hou, W., et al., *Autophagic degradation of active caspase-8: a crosstalk mechanism between autophagy and apoptosis.* Autophagy, 2010. **6**(7): p. 891-900.

170. Oral, O., et al., *Cleavage of Atg3 protein by caspase-8 regulates autophagy during receptor-activated cell death.* Apoptosis, 2012. **17**(8): p. 810-20.

171. Luo, S. and D.C. Rubinsztein, *Apoptosis blocks Beclin 1-dependent autophagosome synthesis: an effect rescued by Bcl-xL.* Cell Death Differ, 2010. **17**(2): p. 268-77.

172. Wirawan, E., et al., *Caspase-mediated cleavage of Beclin-1 inactivates Beclin-1-induced autophagy and enhances apoptosis by promoting the release of proapoptotic factors from mitochondria.* Cell Death Dis, 2010. **1**: p. e18.

173. Maiuri, M.C., et al., *BH3-only proteins and BH3 mimetics induce autophagy by competitively disrupting the interaction between Beclin 1 and Bcl-2/Bcl-X(L).* Autophagy, 2007. **3**(4): p. 374-6.

174. Zalckvar, E., et al., *DAP-kinase-mediated phosphorylation on the BH3 domain of beclin 1 promotes dissociation of beclin 1 from Bcl-XL and induction of autophagy.* EMBO Rep, 2009. **10**(3): p. 285-92.

175. Marino, G., et al., *Self-consumption: the interplay of autophagy and apoptosis.* Nat Rev Mol Cell Biol, 2014. **15**(2): p. 81-94.

176. Tang, D., et al., *Endogenous HMGB1 regulates autophagy.* J Cell Biol, 2010. **190**(5): p. 881-92.

177. Pantel, K. and R.H. Brakenhoff, *Dissecting the metastatic cascade.* Nat Rev Cancer, 2004. **4**(6): p. 448-56.

178. Tlsty, T.D. and L.M. Coussens, *Tumor stroma and regulation of cancer development.* Annu Rev Pathol, 2006. **1**: p. 119-50.

179. Thorburn, J., et al., *Autophagy regulates selective HMGB1 release in tumor cells that are destined to die.* Cell Death Differ, 2009. **16**(1): p. 175-83.

180. Qiang, L., et al., *Regulation of cell proliferation and migration by p62 through stabilization of Twist1.* Proc Natl Acad Sci U S A, 2014. **111**(25): p. 9241-6.

181. Caino, M.C., et al., *Metabolic stress regulates cytoskeletal dynamics and metastasis of cancer cells.* J Clin Invest, 2013. **123**(7): p. 2907-20.

182. Tuloup-Minguez, V., et al., *Autophagy modulates cell migration and beta1 integrin membrane recycling.* Cell Cycle, 2013. **12**(20): p. 3317-28.

183. Hay, E.D., *An overview of epithelio-mesenchymal transformation.* Acta Anat (Basel), 1995. **154**(1): p. 8-20.

184. Lamouille, S., J. Xu, and R. Derynck, *Molecular mechanisms of epithelial-mesenchymal transition.* Nat Rev Mol Cell Biol, 2014. **15**(3): p. 178-96.

185. Lv, Q., F. Hua, and Z.W. Hu, *DEDD, a novel tumor repressor, reverses epithelial-mesenchymal transition by activating selective autophagy.* Autophagy, 2012. **8**(11): p. 1675-6.

186. Qiang, L. and Y.Y. He, *Autophagy deficiency stabilizes TWIST1 to promote epithelial-mesenchymal transition.* Autophagy, 2014. **10**(10): p. 1864-5.

187. Peng, Y.F., et al., *Autophagy inhibition suppresses pulmonary metastasis of HCC in mice via impairing anoikis resistance and colonization of HCC cells.* Autophagy, 2013. **9**(12): p. 2056-68.

188. Akalay, I., et al., *EMT impairs breast carcinoma cell susceptibility to CTL-mediated lysis through autophagy induction.* Autophagy, 2013. **9**(7): p. 1104-6.

189. Nitta, T., et al., *Autophagy may promote carcinoma cell invasion and correlate with poor prognosis in cholangiocarcinoma.* Int J Clin Exp Pathol, 2014. **7**(8): p. 4913-21.

190. Guadamillas, M.C., A. Cerezo, and M.A. Del Pozo, *Overcoming anoikis--pathways to anchorage-independent growth in cancer.* J Cell Sci, 2011. **124**(Pt 19): p. 3189-97.

191. Debnath, J., et al., *The role of apoptosis in creating and maintaining luminal space within normal and oncogene-expressing mammary acini.* Cell, 2002. **111**(1): p. 29-40.

192. Fung, C., et al., *Induction of autophagy during extracellular matrix detachment promotes cell survival.* Mol Biol Cell, 2008. **19**(3): p. 797-806.

193. Avivar-Valderas, A., et al., *Regulation of autophagy during ECM detachment is linked to a selective inhibition of mTORC1 by PERK.* Oncogene, 2013. **32**(41): p. 4932-40.

194. Sleeman, J.P., *The metastatic niche and stromal progression.* Cancer Metastasis Rev, 2012. **31**(3-4): p. 429-40.

195. Kaplan, R.N., et al., *VEGFR1-positive haematopoietic bone marrow progenitors initiate the pre-metastatic niche.* Nature, 2005. **438**(7069): p. 820-7.

196. Levental, K.R., et al., *Matrix crosslinking forces tumor progression by enhancing integrin signaling.* Cell, 2009. **139**(5): p. 891-906.

197. Martinez-Outschoorn, U.E., et al., *Stromal-epithelial metabolic coupling in cancer: integrating autophagy and metabolism in the tumor microenvironment.* Int J Biochem Cell Biol, 2011. **43**(7): p. 1045-51.

198. Herberg, S., et al., *Stromal cell-derived factor-1beta mediates cell survival through enhancing autophagy in bone marrow-derived mesenchymal stem cells.* PLoS One, 2013. **8**(3): p. e58207.

199. Noman, M.Z., et al., *Blocking hypoxia-induced autophagy in tumors restores cytotoxic T-cell activity and promotes regression.* Cancer Res, 2011. **71**(18): p. 5976-86.

200. Garg, A.D., et al., *ROS-induced autophagy in cancer cells assists in evasion from determinants of immunogenic cell death.* Autophagy, 2013. **9**(9): p. 1292-307.

201. Sosa, M.S., P. Bragado, and J.A. Aguirre-Ghiso, *Mechanisms of disseminated cancer cell dormancy: an awakening field.* Nat Rev Cancer, 2014. **14**(9): p. 611-22.

202. Almog, N., et al., *Transcriptional switch of dormant tumors to fast-growing angiogenic phenotype.* Cancer Res, 2009. **69**(3): p. 836-44.

203. Ghajar, C.M., et al., *The perivascular niche regulates breast tumour dormancy.* Nat Cell Biol, 2013. **15**(7): p. 807-17.

204. Jo, H., et al., *Cancer cell-derived clusterin modulates the phosphatidylinositol 3'-kinase-Akt pathway through attenuation of insulin-like growth factor 1 during serum deprivation.* Mol Cell Biol, 2008. **28**(13): p. 4285-99.

205. Lu, Z., et al., *The tumor suppressor gene ARHI regulates autophagy and tumor dormancy in human ovarian cancer cells.* J Clin Invest, 2008. **118**(12): p. 3917-29.

206. Lu, Z., et al., *DIRAS3 regulates the autophagosome initiation complex in dormant ovarian cancer cells.* Autophagy, 2014. **10**(6): p. 1071-92.

207. Lu, Z., et al., *ARHI (DIRAS3) induces autophagy in ovarian cancer cells by downregulating the epidermal growth factor receptor, inhibiting PI3K and Ras/MAP signaling and activating the FOXo3a-mediated induction of Rab7.* Cell Death Differ, 2014. **21**(8): p. 1275-89.

208. Gupta, A., et al., *Autophagy inhibition and antimalarials promote cell death in gastrointestinal stromal tumor (GIST).* Proc Natl Acad Sci U S A, 2010. **107**(32): p. 14333-8.

209. Sarkar, S., et al., *Trehalose, a novel mTOR-independent autophagy enhancer, accelerates the clearance of mutant huntingtin and alpha-synuclein.* J Biol Chem, 2007. **282**(8): p. 5641-52.

210. Aguib, Y., et al., *Autophagy induction by trehalose counteracts cellular prion infection.* Autophagy, 2009. **5**(3): p. 361-9.

211. Thoreen, C.C., et al., *An ATP-competitive mammalian target of rapamycin inhibitor reveals rapamycin-resistant functions of mTORC1.* J Biol Chem, 2009. **284**(12): p. 8023-32.

212. Sarkar, S., et al., *Lithium induces autophagy by inhibiting inositol monophosphatase.* J Cell Biol, 2005. **170**(7): p. 1101-11.

213. Miller, S., et al., *Shaping development of autophagy inhibitors with the structure of the lipid kinase Vps34.* Science, 2010. **327**(5973): p. 1638-42.

214. Wu, Y.T., et al., *Dual role of 3-methyladenine in modulation of autophagy via different temporal patterns of inhibition on class I and III phosphoinositide 3-kinase.* J Biol Chem, 2010. **285**(14): p. 10850-61.

215. Liu, J., et al., *Beclin1 controls the levels of p53 by regulating the deubiquitination activity of USP10 and USP13.* Cell, 2011. **147**(1): p. 223-34.

216. Yoshimori, T., et al., *Bafilomycin A1, a specific inhibitor of vacuolar-type H(+)-ATPase, inhibits acidification and protein degradation in lysosomes of cultured cells.* J Biol Chem, 1991. **266**(26): p. 17707-12.

217. Moriyasu, Y. and Y. Inoue, *Use of protease inhibitors for detecting autophagy in plants.* Methods Enzymol, 2008. **451**: p. 557-80.

218. Solomon, V.R. and H. Lee, *Chloroquine and its analogs: a new promise of an old drug for effective and safe cancer therapies.* Eur J Pharmacol, 2009. **625**(1-3): p. 220-33.

219. Maycotte, P., et al., *Chloroquine sensitizes breast cancer cells to chemotherapy independent of autophagy.* Autophagy, 2012. **8**(2): p. 200-12.

220. Maes, H., et al., *Tumor vessel normalization by chloroquine independent of autophagy.* Cancer Cell, 2014. **26**(2): p. 190-206.

221. Bristol, M.L., et al., *Autophagy inhibition for chemosensitization and radiosensitization in cancer: do the preclinical data support this therapeutic strategy?* J Pharmacol Exp Ther, 2013. **344**(3): p. 544-52.

222. Mzayek, F., et al., *Randomized dose-ranging controlled trial of AQ-13, a candidate antimalarial, and chloroquine in healthy volunteers.* PLoS Clin Trials, 2007. **2**(1): p. e6.

223. Moore, B.R., et al., *Pharmacokinetics, pharmacodynamics, and allometric scaling of chloroquine in a murine malaria model.* Antimicrob Agents Chemother, 2011. **55**(8): p. 3899-907.

224. McAfee, Q., et al., *Autophagy inhibitor Lys05 has single-agent antitumor activity and reproduces the phenotype of a genetic autophagy deficiency.* Proc Natl Acad Sci U S A, 2012. **109**(21): p. 8253-8.

225. Thorburn, A., D.H. Thamm, and D.L. Gustafson, *Autophagy and cancer therapy.* Mol Pharmacol, 2014. **85**(6): p. 830-8.

226. Gewirtz, D.A., *The four faces of autophagy: implications for cancer therapy.* Cancer Res, 2014. **74**(3): p. 647-51.

227. Young, M.M., et al., *Autophagosomal membrane serves as platform for intracellular death-inducing signaling complex (iDISC)-mediated caspase-8 activation and apoptosis.* J Biol Chem, 2012. **287**(15): p. 12455-68.

228. Gewirtz, D.A., *When cytoprotective autophagy isn't... and even when it is.* Autophagy, 2014. **10**(3): p. 391-2.

229. *Comprehensive molecular portraits of human breast tumours.* Nature, 2012. **490**(7418): p. 61-70.

230. Qadir, M.A., et al., *Macroautophagy inhibition sensitizes tamoxifen-resistant breast cancer cells and enhances mitochondrial depolarization.* Breast Cancer Res Treat, 2008. **112**(3): p. 389-403.

231. Samaddar, J.S., et al., *A role for macroautophagy in protection against 4-hydroxytamoxifen-induced cell death and the development of antiestrogen resistance.* Mol Cancer Ther, 2008. **7**(9): p. 2977-87.

232. Gonzalez-Malerva, L., et al., *High-throughput ectopic expression screen for tamoxifen resistance identifies an atypical kinase that blocks autophagy.* Proc Natl Acad Sci U S A, 2011. **108**(5): p. 2058-63.

233. Wilson, E.N., et al., *A switch between cytoprotective and cytotoxic autophagy in the radiosensitization of breast tumor cells by chloroquine and vitamin D.* Horm Cancer, 2011. **2**(5): p. 272-85.

234. Bristol, M.L., et al., *Dual functions of autophagy in the response of breast tumor cells to radiation: cytoprotective autophagy with radiation alone and cytotoxic autophagy in radiosensitization by vitamin D 3.* Autophagy, 2012. **8**(5): p. 739-53.

235. Vazquez-Martin, A., C. Oliveras-Ferraros, and J.A. Menendez, *Autophagy facilitates the development of breast cancer resistance to the anti-HER2 monoclonal antibody trastuzumab.* PLoS One, 2009. **4**(7): p. e6251.

236. Negri, T., et al., *Chromosome band 17q21 in breast cancer: significant association between beclin 1 loss and HER2/NEU amplification.* Genes Chromosomes Cancer, 2010. **49**(10): p. 901-9.

237. Thomas, S., et al., *Preferential killing of triple-negative breast cancer cells in vitro and in vivo when pharmacological aggravators of endoplasmic reticulum stress are combined with autophagy inhibitors.* Cancer Lett, 2012. **325**(1): p. 63-71.

238. Kanematsu, S., et al., *Autophagy inhibition enhances sulforaphane-induced apoptosis in human breast cancer cells.* Anticancer Res, 2010. **30**(9): p. 3381-90.

239. Lefort, S., et al., *Inhibition of autophagy as a new means of improving chemotherapy efficiency in high-LC3B triple-negative breast cancers.* Autophagy, 2014: p. 0.

240. Wu, D.H., et al., *Autophagic LC3B overexpression correlates with malignant progression and predicts a poor prognosis in hepatocellular carcinoma.* Tumour Biol, 2014.

241. Shimizu, S., et al., *Inhibition of autophagy potentiates the antitumor effect of the multikinase inhibitor sorafenib in hepatocellular carcinoma.* Int J Cancer, 2012. **131**(3): p. 548-57.

242. Fischer, T.D., et al., *Role of autophagy in differential sensitivity of hepatocarcinoma cells to sorafenib.* World J Hepatol, 2014. **6**(10): p. 752-8.

243. Zhai, B., et al., *Inhibition of Akt reverses the acquired resistance to sorafenib by switching protective autophagy to autophagic cell death in hepatocellular carcinoma.* Mol Cancer Ther, 2014. **13**(6): p. 1589-98.

244. Guo, X.L., et al., *Targeting autophagy potentiates chemotherapy-induced apoptosis and proliferation inhibition in hepatocarcinoma cells.* Cancer Lett, 2012. **320**(2): p. 171-9.

245. Hui, B., et al., *Proteasome inhibitor interacts synergistically with autophagy inhibitor to suppress proliferation and induce apoptosis in hepatocellular carcinoma.* Cancer, 2012. **118**(22): p. 5560-71.

246. Ryan, D.P., T.S. Hong, and N. Bardeesy, *Pancreatic adenocarcinoma.* N Engl J Med, 2014. **371**(11): p. 1039-49.

247. Yang, S., et al., *Pancreatic cancers require autophagy for tumor growth.* Genes Dev, 2011. **25**(7): p. 717-29.

248. Hashimoto, D., et al., *Autophagy is needed for the growth of pancreatic adenocarcinoma and has a cytoprotective effect against anticancer drugs.* Eur J Cancer, 2014. **50**(7): p. 1382-90.

249. Yang, A., et al., *Autophagy is critical for pancreatic tumor growth and progression in tumors with p53 alterations.* Cancer Discov, 2014. **4**(8): p. 905-13.

250. Morgan, M.J., et al., *Regulation of autophagy and chloroquine sensitivity by oncogenic RAS in vitro is context-dependent.* Autophagy, 2014. **10**(10): p. 1814-26.

251. Gazdar, A.F., *Epidermal growth factor receptor inhibition in lung cancer: the evolving role of individualized therapy.* Cancer Metastasis Rev, 2010. **29**(1): p. 37-48.

252. Han, J., et al., *Interaction between Her2 and Beclin-1 proteins underlies a new mechanism of reciprocal regulation.* J Biol Chem, 2013. **288**(28): p. 20315-25.

253. Wei, Y., et al., *EGFR-mediated Beclin 1 phosphorylation in autophagy suppression, tumor progression, and tumor chemoresistance.* Cell, 2013. **154**(6): p. 1269-84.

254. Kaminskyy, V.O., et al., *Suppression of basal autophagy reduces lung cancer cell proliferation and enhances caspase-dependent and -independent apoptosis by stimulating ROS formation.* Autophagy, 2012. **8**(7): p. 1032-44.

255. Pan, X., et al., *Autophagy inhibition promotes 5-fluorouraci-induced apoptosis by stimulating ROS formation in human non-small cell lung cancer A549 cells.* PLoS One, 2013. **8**(2): p. e56679.

256. Lazova, R., V. Klump, and J. Pawelek, *Autophagy in cutaneous malignant melanoma.* J Cutan Pathol, 2010. **37**(2): p. 256-68.

257. Ma, X.H., et al., *Measurements of tumor cell autophagy predict invasiveness, resistance to chemotherapy, and survival in melanoma.* Clin Cancer Res, 2011. **17**(10): p. 3478-89.

258. Chapman, P.B., et al., *Improved survival with vemurafenib in melanoma with BRAF V600E mutation.* N Engl J Med, 2011. **364**(26): p. 2507-16.

259. Maddodi, N., et al., *Induction of autophagy and inhibition of melanoma growth in vitro and in vivo by hyperactivation of oncogenic BRAF.* J Invest Dermatol, 2010. **130**(6): p. 1657-67.

260. Ma, X.H., et al., *Targeting ER stress-induced autophagy overcomes BRAF inhibitor resistance in melanoma.* J Clin Invest, 2014. **124**(3): p. 1406-17.

261. Kraya, A.A., et al., *Identification of secreted proteins that reflect autophagy dynamics within tumor cells.* Autophagy, 2014: p. 0.

262. Koukourakis, M.I., et al., *Beclin 1 over- and underexpression in colorectal cancer: distinct patterns relate to prognosis and tumour hypoxia.* Br J Cancer, 2010. **103**(8): p. 1209-14.

263. Yang, Z., et al., *High expression of Beclin-1 predicts favorable prognosis for patients with colorectal cancer.* Clin Res Hepatol Gastroenterol, 2014.

264. Groulx, J.F., et al., *Autophagy is active in normal colon mucosa.* Autophagy, 2012. **8**(6): p. 893-902.

265. Sasaki, K., et al., *Chloroquine potentiates the anti-cancer effect of 5-fluorouracil on colon cancer cells.* BMC Cancer, 2010. **10**: p. 370.

266. Li, D.D., et al., *The inhibition of autophagy sensitises colon cancer cells with wild-type p53 but not mutant p53 to topotecan treatment.* PLoS One, 2012. **7**(9): p. e45058.

267. Chen, M.C., et al., *Resistance to irinotecan (CPT-11) activates epidermal growth factor receptor/nuclear factor kappa B and increases cellular metastasis and autophagy in LoVo colon cancer cells.* Cancer Lett, 2014. **349**(1): p. 51-60.

268. Selvakumaran, M., et al., *Autophagy inhibition sensitizes colon cancer cells to antiangiogenic and cytotoxic therapy.* Clin Cancer Res, 2013. **19**(11): p. 2995-3007.

269. Pirtoli, L., et al., *The prognostic role of Beclin 1 protein expression in high-grade gliomas.* Autophagy, 2009. **5**(7): p. 930-6.

270. Huang, X., et al., *Reduced expression of LC3B-II and Beclin 1 in glioblastoma multiforme indicates a down-regulated autophagic capacity that relates to the progression of astrocytic tumors.* J Clin Neurosci, 2010. **17**(12): p. 1515-9.

271. Kanzawa, T., et al., *Role of autophagy in temozolomide-induced cytotoxicity for malignant glioma cells.* Cell Death Differ, 2004. **11**(4): p. 448-57.

272. Shingu, T., et al., *Inhibition of autophagy at a late stage enhances imatinib-induced cytotoxicity in human malignant glioma cells.* Int J Cancer, 2009. **124**(5): p. 1060-71.

273. Bennett, H.L., et al., *Androgens modulate autophagy and cell death via regulation of the endoplasmic reticulum chaperone glucose-regulated protein 78/BiP in prostate cancer cells.* Cell Death Dis, 2010. **1**: p. e72.

274. Bennett, H.L., et al., *Does androgen-ablation therapy (AAT) associated autophagy have a pro-survival effect in LNCaP human prostate cancer cells?* BJU Int, 2013. **111**(4): p. 672-82.

275. Nguyen, H.G., et al., *Targeting autophagy overcomes Enzalutamide resistance in castration-resistant prostate cancer cells and improves therapeutic response in a xenograft model.* Oncogene, 2014. **33**(36): p. 4521-30.

276. Mortensen, M., et al., *The autophagy protein Atg7 is essential for hematopoietic stem cell maintenance.* J Exp Med, 2011. **208**(3): p. 455-67.

277. Pua, H.H., et al., *A critical role for the autophagy gene Atg5 in T cell survival and proliferation.* J Exp Med, 2007. **204**(1): p. 25-31.

278. Pua, H.H. and Y.W. He, *Maintaining T lymphocyte homeostasis: another duty of autophagy.* Autophagy, 2007. **3**(3): p. 266-7.

279. Miller, B.C., et al., *The autophagy gene ATG5 plays an essential role in B lymphocyte development.* Autophagy, 2008. **4**(3): p. 309-14.

280. Dey, S., F. Tameire, and C. Koumenis, *PERK-ing up autophagy during MYC-induced tumorigenesis.* Autophagy, 2013. **9**(4): p. 612-4.

281. Hart, L.S., et al., *ER stress-mediated autophagy promotes Myc-dependent transformation and tumor growth.* J Clin Invest, 2012. **122**(12): p. 4621-34.

282. Granato, M., et al., *JNK and macroautophagy activation by bortezomib has a pro-survival effect in primary effusion lymphoma cells.* PLoS One, 2013. **8**(9): p. e75965.

283. Mahoney, E., et al., *Identification of endoplasmic reticulum stress-inducing agents by antagonizing autophagy: a new potential strategy for identification of anti-cancer therapeutics in B-cell malignancies.* Leuk Lymphoma, 2013. **54**(12): p. 2685-92.

284. Gammoh, N., et al., *Role of autophagy in histone deacetylase inhibitor-induced apoptotic and nonapoptotic cell death.* Proc Natl Acad Sci U S A, 2012. **109**(17): p. 6561-5.

285. Chen, S., et al., *Targeting SQSTM1/p62 induces cargo loading failure and converts autophagy to apoptosis via NBK/Bik.* Mol Cell Biol, 2014. **34**(18): p. 3435-49.

286. Gump, J.M., et al., *Autophagy variation within a cell population determines cell fate through selective degradation of Fap-1.* Nat Cell Biol, 2014. **16**(1): p. 47-54.

287. Ko, A., et al., *Autophagy inhibition radiosensitizes in vitro, yet reduces radioresponses in vivo due to deficient immunogenic signalling.* Cell Death Differ, 2014. **21**(1): p. 92-9.

288. Rock, K.L. and H. Kono, *The inflammatory response to cell death.* Annu Rev Pathol, 2008. **3**: p. 99-126.

289. Uhl, M., et al., *Autophagy within the antigen donor cell facilitates efficient antigen cross-priming of virus-specific CD8+ T cells.* Cell Death Differ, 2009. **16**(7): p. 991-1005.

290. Maes, H., et al., *Autophagy: shaping the tumor microenvironment and therapeutic response.* Trends Mol Med, 2013. **19**(7): p. 428-46.

291. Johnson, J.I., et al., *Relationships between drug activity in NCI preclinical in vitro and in vivo models and early clinical trials.* Br J Cancer, 2001. **84**(10): p. 1424-31.

292. Talmadge, J.E., et al., *Murine models to evaluate novel and conventional therapeutic strategies for cancer.* Am J Pathol, 2007. **170**(3): p. 793-804.

293. Wilmanns, C., et al., *Modulation of Doxorubicin sensitivity and level of p-glycoprotein expression in human colon-carcinoma cells by ectopic and orthotopic environments in nude-mice.* Int J Oncol, 1993. **3**(3): p. 413-22.

294. Killion, J.J., R. Radinsky, and I.J. Fidler, *Orthotopic models are necessary to predict therapy of transplantable tumors in mice.* Cancer Metastasis Rev, 1998. **17**(3): p. 279-84.

295. Peterson, J.K. and P.J. Houghton, *Integrating pharmacology and in vivo cancer models in preclinical and clinical drug development.* Eur J Cancer, 2004. **40**(6): p. 837-44.

296. Bearss, D.J., et al., *Genetic determinants of response to chemotherapy in transgenic mouse mammary and salivary tumors.* Oncogene, 2000. **19**(8): p. 1114-22.

297. Sharpless, N.E. and R.A. Depinho, *The mighty mouse: genetically engineered mouse models in cancer drug development.* Nat Rev Drug Discov, 2006. **5**(9): p. 741-54.

298. Hansen, K. and C. Khanna, *Spontaneous and genetically engineered animal models; use in preclinical cancer drug development.* Eur J Cancer, 2004. **40**(6): p. 858-80.

299. Pinho, S.S., et al., *Canine tumors: a spontaneous animal model of human carcinogenesis.* Transl Res, 2012. **159**(3): p. 165-72.

300. Uva, P., et al., *Comparative expression pathway analysis of human and canine mammary tumors.* BMC Genomics, 2009. **10**: p. 135.

301. Fowles, J.S., C.L. Denton, and D.L. Gustafson, *Comparative analysis of MAPK and PI3K/AKT pathway activation and inhibition in human and canine melanoma.* Vet Comp Oncol, 2013.

302. Fosmire, S.P., et al., *Inactivation of the p16 cyclin-dependent kinase inhibitor in high-grade canine non-Hodgkin's T-cell lymphoma.* Vet Pathol, 2007. **44**(4): p. 467-78.

303. Rosenfeld, M.R., et al., *A phase I/II trial of hydroxychloroquine in conjunction with radiation therapy and concurrent and adjuvant temozolomide in patients with newly diagnosed glioblastoma multiforme.* Autophagy, 2014. **10**(8): p. 1359-68.

304. Rangwala, R., et al., *Phase I trial of hydroxychloroquine with dose-intense temozolomide in patients with advanced solid tumors and melanoma.* Autophagy, 2014. **10**(8): p. 1369-79.

305. Vogl, D.T., et al., *Combined autophagy and proteasome inhibition: a phase 1 trial of hydroxychloroquine and bortezomib in patients with relapsed/refractory myeloma.* Autophagy, 2014. **10**(8): p. 1380-90.

306. Rangwala, R., et al., *Combined MTOR and autophagy inhibition: phase I trial of hydroxychloroquine and temsirolimus in patients with advanced solid tumors and melanoma.* Autophagy, 2014. **10**(8): p. 1391-402.

307. Mahalingam, D., et al., *Combined autophagy and HDAC inhibition: a phase I safety, tolerability, pharmacokinetic, and pharmacodynamic analysis of hydroxychloroquine in combination with the HDAC inhibitor vorinostat in patients with advanced solid tumors.* Autophagy, 2014. **10**(8): p. 1403-14.

Chapter Two

Autophagy influences the establishment of the metastatic microenvironment

Summary

The autophagy pathway has been recognized as a mechanism of survival and therapy resistance in cancer. Yet the extent of autophagy's function in metastatic progression is still uncertain. Therefore, we tested the effect of autophagy modulation in different mouse models and cell based assays that reflect different points along the metastatic cascade. Both pharmacologic and genetic inhibition of autophagy was able to reduce cellular proliferation in murine breast cancer, melanoma, and osteosarcoma cell lines. However, neither treatment with chloroquine (CQ) or Beclin-1 (BECN-1) knockdown was able to delay metastasis development in experimentally induced metastasis models. Both methods were able to significantly increase the time until metastases formed if given before cells had arrived in the lung in an orthotopic model of breast cancer. Autophagy stimulation by trehalose was able to accelerate metastasis. There was no alteration in the metastatic capability of the cells as determined by anchorage independent growth, invasion, and migration assays. Rather, autophagy modulation impacted the number of bone marrow derived cells (BMDCs), which mediate the establishment of the pre-metastatic niche. Cisplatin was also administered in combination with CQ and BECN-1 knockdown. No enhancement was observed and the combination with CQ was actually antagonistic. We found

that this may be due to changes in the infiltrating immune cell populations, particularly increased neutrophils in the CQ and combination treated mice. Autophagy appears to be most critical at the pre-metastatic stage by potentially priming the micorenvironment through increasing BMDC number. Autophagy continues to influence the makeup of the metastatic microenvironment even after tumor cells have arrived, but this role is much less clear. It may, however, impact chemotherapy efficacy, and caution should be used when developing autophagy inhibition combination strategies.

Introduction

Macroautophagy (hereafter called autophagy) is a lysosomal degradation process characterized by self-consumption of cytoplasmic material, including organelles and proteins. One of the defining features of this process is the formation of distinctive double-membraned vesicles, called autophagosomes. These autophagosomes traffic the intended cargo to the lysosome [1]. Autophagy was initially identified as a response to nutrient withdrawal, particularly to the removal of amino acids [2]. However, many stress stimuli, such as hypoxia, inflammation, and DNA damage, have been found to induce autophagy [3]. Additionally, autophagy appears to be necessary for basic cell maintenance as deficiencies in the process may be attributed to cancer, neurodegeneration, cardiomyopathy, and many other disorders [4].

Autophagy has a complex and often contradictory role in cancer development. On one hand, mice deficient in autophagy show accumulation of aberrant organelles and misfolded proteins potentially leading to elevated levels of reactive oxygen species, inflammation, and genomic instability. Thus, autophagy acts as a quality control mechanism [5-7]. In addition, mice

with a heterozygous disruption of the critical autophagy gene *beclin-1* have a greater susceptibility to tumor formation [7]. Increased development of chemically-induced fibrosarcomas has also been demonstrated in *Atg4* deficient mice [6]. On the other hand, elevated levels of autophagy have also been observed in many other tumor types and have been correlated to a more metastatic and aggressive phenotype [8-10]. Additionally, certain cancer stem cell populations are reliant on autophagy [11, 12]. Inhibiting autophagy *in vitro* can increase tumor cell death and sensitize cells to some chemotherapy drugs [13-15]. A great deal of cross-talk also exists between the autophagy and apoptosis networks. Autophagy can be cytoprotective as it removes toxic oxygen radicals or damaged proteins that can trigger apoptosis [16, 17]. Taken together, autophagy appears to be acting as a mechanism of chemoresistance or survival. Functional autophagy may be important for preventing tumor formation by maintaining genomic stability and mitigating cellular damage. However, once a tumor has been established, autophagy may allow the cells to withstand the harsh tumor microenvironment or stress induced by anti-cancer therapies. Hence, the idea of sensitizing cells to chemotherapy or radiation by inhibiting autophagy has spurred a number of clinical trials [18-23].

Metastasis remains the major cause of death from cancer, and although our understanding of autophagy in primary tumor development is increasing, the role of autophagy in metastasis progression is still poorly understood [24]. One of the first steps in the metastatic cascade is the ability of cells to invade and escape the primary tumor. A recent study demonstrated that activation of autophagy complex ULK-1/Fip200 was instrumental in inhibiting cell motility. Cells were less invasive when autophagy was inhibited, particularly under metabolic stress [25]. In addition, autophagy has been shown to be integral in β1-integrin receptor internalization and degradation [26]. However, once cells have detached from the extracellular matrix (ECM),

autophagy may be crucial for survival [27, 28]. Normally cells undergo apoptosis if they detach from the ECM, also known as anoikis, as there is a sudden loss of growth factors, downregulation of survival pathways due to loss of integrin interaction, and metabolic and oxidative stress [29]. Autophagy is induced in breast cancer epithelial cells when they have become detached and is necessary for their continued survival [27, 28, 30]. Autophagy may then allow for resistance to anoikis. Yet, in a model of hepatocellular carcinoma, autophagy inhibition did not alter invasion, migration, or anchorage independent growth [31, 32]. Rather, autophagy was only necessary in early metastatic colonization of the lung and autophagy levels appeared higher in earlier stage metastatic lesions. Therefore, there still remains a great deal of uncertainty surrounding the role of autophagy in metastasis.

While there have been studies examining the effect of autophagy inhibition on metastasis in an *in vivo* setting, most have been performed in immune deficient mouse models [31, 33-36]. The functionality of the immune system can influence the efficacy of autophagy inhibition and anti-cancer therapies [37, 38]. Therefore, it is important to consider the effect of autophagy in an immune competent model. Since it is still unclear what role autophagy plays in metastatic progression and few models have examined autophagy in an immune competent model, we investigated the effect of autophagy modulation on multiple steps in the metastatic cascade utilizing multiple cancer models both *in vitro* and *in vivo*. Additionally, we examined autophagy modulation in clinically relevant surgical adjuvant and neoadjuvant syngeneic mouse models.

Material and Methods

Cell Lines and Cell Culture

The 4T1-luc cell line and B16-F10 lines were generously provided by Dr. S. Dow at CSU. The 4T1-luc line was transfected with the RSV-pGL4.17 plasmid containing the firefly luciferase gene along with a neomycin selection cassette. The plasmid was constructed by subcloning a HindIII fragment with the Rous Sarcoma Virus (RSV) 5' LTR promoter into the pGL4.17 plasmid (Promega Corporation, Madison, WI). The DLM8 line was provided by Dr. D. Thamm at CSU. All cell lines were maintained in DMEM (Cellgro, Herndon, VA) with 10% fetal bovine serum (FBS) (Cellgro, Herndon, VA), 5% penicillin+streptomycin (Hyclone Laboratories Inc, Logan, UT), and 1 mM sodium pyruvate (Cellgro, Herndon, VA) at 37°C and 5% CO_2.

Becn-1 and Atg7 Knockdown

Lentiviral particles containing a pKLO vector with Becn-1 or Atg7 mouse short hairpin RNA (shRNA) made in HEK293FT cells. 4T1-luc, B16-F10, and DLM8 cells were transduced with the lentiviruses containing the pKLO Becn-1 shRNA, Atg7, or a non-silencing shRNA using 8 μg/mL polybrene (Sigma, St. Louis, MO). 2 μg /mL Puromycin (Calbiochem, San Diego, CA) was used for 1 week to select for successfully transduced cells. Cells were then maintained in medium containing 1 μg /mL puromycin. To confirm Becn-1 or Atg7 knockdown and autophagy inhibition by LC3 II decrease, cells were treated with EBSS (Hyclone Laboratories, Logan, UT) with /without 10 μM CQ (Sigma, St. Louis, MO) or 5 nM bafilomycin A1 (Baf A1, Sigma, St. Louis, MO) for 2 h.

Western Blot Analysis

After treatment, cells were lysed with a lysis buffer (0.01% Triton X-100, 150 mM NaCl, 10 mM Tris pH 7.5, 0.2 mM Na-Orthovanadate, 34.8 μg/mL PMSF, and 1x Protease Inhibitor Cocktail, [Roche, Indianapolis, IN]). For protein extraction from tissue, samples were collected fresh, covered in lysis buffer, and flash frozen in liquid nitrogen. Samples were then homogenized and sonicated. The lysate was centrifuged at 14,000 rpm for 5 min at 4°C and supernatant collected.

Protein was quantitated using a bicinchoninic acid (BCA) protein assay (Pierce, Rockford, IL). 40 μg of protein was used in SDS-PAGE and transferred onto PVDF membranes (Millipore, Billerica, MA). Blots were blocked in 2.5% milk in Tris-buffered saline-Tween 20 for one hour at room temperature. Blots were probed with anti-LC3 (NB100-2220 Novus Biologicals, Littleton, CO) at 1:1000, anti-Beclin-1 (NB 110-87318, Novus Biologicals, Littleton, CO) at 1:2000, anti-Atg7 (NB110-74811, Novus Biologicals, Littleton, CO) at 1:500, anti-actin at 1:5000 (A5441 Sigma, St. Louis, MO), or anti-tubulin at 1:5000 (T-5168 Sigma, St. Louis, MO) antibodies and incubated overnight at 4°C. Blots were incubated for one hour at room temperature with either anti-rabbit (31460, Pierce, Rockford, IL) or anti-mouse (31430 Pierce, Rockford, IL) secondary antibodies conjugated to HRP at 1:5000. Blots were developed using West Dura (Pierce, Rockford, IL) and imaged in a ChemiDoc XRS$^+$ (Bio Rad, Hercules, CA) using Image Labs version 3.0 software for analysis. Densitometry was measured using ImageJ64 and target protein was normalized to actin or tubulin.

RT-qPCR

To quantitate Becn-1 or Atg7 knockdown, qPCR was used to compare mRNA expression. RNA was isolated using the RNeasy kit (Qiagen) per manufacturer's instructions with on-column DNase I digestion (Qiagen). The concentration and purity of the RNA was measured using a Nanodrop 1000 (Thermoscientific) with ND-1000 version 3.8.1 software. 1 μg of RNA was used to synthesize cDNA using a QuantiTect kit (Qiagen) following the included protocol. The reaction took place in a MJ Mini Personal Thermal Cycler (Bio Rad). A single cycle of 30 min at 42°C and 3 min at 95°C was used. Negative controls containing no reverse transcriptase were run simultaneously. Primers were designed using Primer-BLAST (NCBI). The forward primer for Becn-1 was: CCAGCCTCTGAAACTGGACA and the reverse primer was GCCTGGGCTCTGGTAACTAA. The forward primer for Atg7 was: atgccaggacaccctgtgaa and the reverse primer was: aaggtatcaaaccccaaggca. Hsp90ab1 (Hsp90) and Tata Binding Protein (Tbp) were not significantly changed across all cell types and were used as reference genes. Forward primer for Hsp90: CCCACCACCCTGCTCTGTACTACT and reverse primer: GCCTGAAAGGCAAAGGTCTCCACC. Forward primer for Tbp: GGACCAGAACAACAGCCTTC and reverse primer: CCGTAAGGCATCATTGGACT. A concentration of 100 nM for the forward primer and 300 nM was used in the reaction. Master mix containing SYBR Green dye was used (iQ SYBR Green Super Mix, Bio Rad). A total reaction volume of 25 μL and 100 ng of cDNA was used. Increase of fluorescence to measure amplification was performed by the Mx3000p (Stratagene) and analyzed using the Mx3000p version 2.0 software. 1 cycle of 95°C for 10 min followed by 40 cycles of 95°C for 30 sec and 60°C for 1 min was used. A dissociation curve cycle was also added to confirm that single product was being amplified. Amplification efficiencies were determined using a standard curve

of serially diluted cDNA samples with an efficiency of 97.8% for Becn-1, 92.4% for Atg7, 92.7% for Tbp, and 103.2% for Hsp90. All samples were run in triplicate. Samples were compared by subtracting the geometric mean of Ct values for Hsp90 and Tbp from Becn-1 and Atg7 to give the ΔCt. The ΔCt was then transformed into $2^{(-_{\Delta}Ct)}$, as suggested in Pfaffl [39].

Proliferation Assays

For adherent assays, cells were seeded into a 96 well tissue culture plate in quadruplicates. A concentration of 1,000 cells per well was used for the 4T1 and B16-F10 cells and 2,000 cells per well for the DLM8. Cells were allowed to attach for 24h then dosed with 10 μM CQ (Sigma, St. Louis, MO), 5 nM Baf A1 (Sigma, St. Louis, MO), 100 mM trehalose (Alfa Aesar, Ward Hill, MA), cisplatin (Pfizer, New York City, NY) IC_{50} or vehicle for 72h. Cisplatin IC_{50} (Dm) was determined as described in Chou and Talalay [40]. Knockdown or non-silencing control lines were grown for 72h. For anchorage independent growth assays, cells were seeded into 96 well tissue culture plates (BD Falcon) coated with PolyHEMA (Sigma, St. Louis, MO) at a concentration of 2,000 cells per well for 4T1 and B16-F10 or 4,000 cells per well for DLM8. Cells were immediately incubated with 10 μM CQ (Sigma, St. Louis, MO), 5 nM Baf A1 (Sigma, St. Louis, MO), 100 mM trehalose (Alfa Aeasar, Ward Hill, MA), cisplatin (Pfizer, New York City, NY) IC_{50} or vehicle and incubated for 48h. For knockdown or non-silencing controls, cells were grown for 48h. Cells were treated with 10% Alamar Blue (200 μg/mL rezazurin salt in PBS) and incubated for 2h. Plates were read at 530/590 nm excitation/emission in a Synergy HT plate reader (BioTEK, Winooski, VT). All experiments were repeated in triplicate.

Invasion and Migration Assays

Invasion and migration assays (BD Biosciences, Bedford, MA; cat# 351163 and 354167) were performed according to manufacturer's instructions. Briefly, cells were seeded at 12,500 per well in serum free DMEM media with 10μM CQ (Sigma, St. Louis, MO), 5 nM Baf A1 (Sigma, St. Louis, MO), 100 mM trehalose (Alfa Aesar, Ward Hill, MA), or vehicle in triplicate. DMEM with 10% FBS was used as a chemoattractant. Cells were incubated for 20h and then stained with 4 ug/mL Calcein dye (Invitrogen, Carlsbad, CA) for 1 hour. Plates were read at 494/517 nm excitation/emission in a Syngergy HT (BioTEK, Winooski, VT) plate reader.

Bliss Analysis

Dose curves for cisplatin (Pfizer, New York City, NY) were generated in order to determine the IC_{50} (Dm) as described in Chou and Talalay [40]. Growth inhibition for each cell line was then determined using the various methods of autophagy inhibition in combination with cisplatin at the IC_{50}. Since single doses were used, the Bliss model of independence was used to determine if the combination was antagonistic, additive, or syngergistic. The additive effect for a drug is E_{xy} as predicted by the individual effect (fraction of affected cells) of each drug E_x and E_y. Thus E_{xy} is defined as $E_{xy} = (E_x + E_y) – (E_xE_y)$ for $0 < E < 1$. The ratio of the actual observed effect compared to the predicted effect was calculated. This value was used to determine combination efficacy, with < 0.8 as antagonistic, 0.8 – 1.2 as additive, and > 1.2 as synergistic.

Animals

All animal studies were performed in accordance with the Colorado State University's Animal Care and Use Committee. 6-8 week old female Balb/c and C57Bl/6J mice were purchased from the National Cancer Institute (Frederick, MD) or The Jackson Laboratory (Bar

Harbor, ME). The number of mice per cohort was determined using a power analysis with a variability of 30%, power of 0.8 and ability to detect a 50% difference in means. For experimental metastasis studies, mice were pretreated for 72 hours with either 60 mg/kg CQ diphosphate salt (Sigma, St. Louis, MO) or 0.9% saline given by intraperitoneal (ip) injection. This dosing regimen was demonstrated to be effective in Maycotte et al, 2014 [41]. Mice continued to receive CQ or vehicle daily until the end of the study. 300,000 4T1-luc or B16-F10 cells in serum free DMEM media were injected into the tail vein of mice. Additional mice, not receiving CQ, were challenged with either 4T1-luc cells pretreated with 10 μM CQ for 2 hours or 4T1-luc Becn-1 knockdown cells. For detection of 4T1 luciferase positive metastases, mice were injected with 50 μL of 30 mg/mL luciferin (Gold Bio, St. Louis, MO) i.p. 5 minutes before being anesthetized with isoflurane. Mice were imaged thrice weekly using the IVIS-100 Imaging System (Perkin-Elmer, Waltham, MA) with a 1 min exposure and medium sensitivity setting. Once metastases were visible, mice were sacrificed. Mice challenged with B16-F10 cells were weighed daily and sacrificed after 10% weight loss. Mice were sacrificed by cardiac stick exsanguination under isoflurane anesthesia. Lungs were harvested for subsequent flow cytometry and immunofluorescence microscopy analysis.

For surgical adjuvant studies, 1 x 10^6 4T1-luc cells in 100ul serum free DMEM, were implanted subcutaneously into the 4th mammary fat pad. Tumor volume was measured with digital calipers using the formula short diameter^2 x long diameter x 0.5. Once tumors reached 100 mm^3, they were removed and mice began treatment 24 h after, receiving either 60 mg/kg CQ, i.p. daily, a human equivalent exposure of cisplatin at 3 mg/kg, i.p. q14 days, a combination of both, or vehicle. Mice were imaged thrice weekly until the appearance of luciferase positive metastases.

For neoadjuvant studies, 4T1-luc, 4T1-luc Becn-1 knockdown, or 4T1-luc NS cells were implanted and treatment began 24h after, similarly to the surgical adjuvant studies. For autophagy stimulation, 2% trehalose or 2% sucrose was dissolved in drinking water and given *ad libitum*. After tumors reached 100 mm^3, they were removed and mice were imaged thrice weekly until luciferase positive metastases were visible, for survival studies, or 15 days after starting treatment.

Flow Cytometry

Upon study completion, mice were exsanguinated by cardiac stick under isoflourane anesthesia. Whole blood was collected into EDTA-treated microtainer tubes (BD Biosciences, Bedford, MA) and diluted 1:1 in PBS. Peripheral blood leukocytes were isolated by lysing red cells using ACK solution (150 mM NH_4Cl, 10 mM $KHCO_3$ and 0.1 mM Na_2EDTA). After blood collection, the lungs were first perfused with 6 mL PBS via cardiac puncture and then removed. The right lung lobe was immediately placed on ice in HBSS + 5% fetal bovine serum until further processing. Lung tissues were minced in 6-well culture plates using a razor blade, followed by digestion in 3 mL of 2x collagenase D (Roche, Indianapolis, IN) diluted in HBSS + 0.1% FBS/EDTA for 30 minutes at 37°C. Following digestion, tissues were triturated using an 18-ga needle and 3 mL syringe, and filtered through 70 μm cell strainers (x2) (BD Biosciences, Bedford, MA). Lastly, red cells were lysed using ACK solution and remaining cells re-suspended in FACS buffer (PBS with 2% fetal bovine serum and 0.05% sodium azide) for immunostaining.

To minimize non-specific binding, normal mouse serum (Jackson Immunoresearch, West Grove, PA) and un-labeled anti-mouse CD16/32 (eBiosciences San Diego, CA) were applied to cells before immunostaining. Cells were then incubated with directly labeled rat anti-mouse

monoclonal antibodies (eBiosciences San Diego, CA, unless otherwise noted) directed against mouse CD11b (clone M1/70), mouse Ly6C (clone AL-21), mouse Ly6G (clone 1A8), mouse MHC II (clone M5/114.15.2), mouse CD86 (clone GL1), mouse CD117 (clone 2B8), mouse CD133 (clone 13A4), mouse F4/80 (clone MCA497; AbD Serotec, Raleigh, NC) mouse CD11c (clone N418), mouse CCR2 (clone 475301; R&D Systems, Minneapolis, MN), mouse VEGFR-1 (clone 141522; R&D systems, Minneapolis, MN), mouse VLA-4 (clone R1-2) in 96-well round-bottom plates for 30 min at room temperature (RT). Cells were washed and incubated with streptavidin conjugates when necessary. Flow cytometry was conducted using a Dako/CyanADP flow cytometer with Summit software (Little Rock, AR). Analysis was done with FlowJo software (Ashland, OR

Immunofluorescence

Left lung lobes were embedded in O.C.T. compound (Electron Microscopy Sciences, Hatfield, PA), frozen at 150 C°. O.C.T. and cryo-sectioned at 5 µm. Slides were fixed in ice-cold acetone for 10 min and air-dried. Prior to immunostaining, nonspecific binding was blocked by pre-incubation of sections with 5% donkey serum (Jackson Immunoresearch, West Grove, PA) in 1% BSA for 30 min at RT. Primary antibody labeling (1:100 anti-LC3, NB100-2220; Novus Biologicals, Littleton CO) was performed at RT for 1 hr in incubation buffer (1% BSA). After removal of the primary antibody, tissues were washed with PBS-T, followed by addition of goat anti-rabbit IgG conjuvated to Cy5 for 30 min at RT (Molecular Probes, Eugene, OR) Lastly, tissues were counter stained with DAPI cover-slipped, and visualized using an Olympus BX41 microscope and DP70 microscope digital camera. Figures were assembled using Adobe Photoshop (CS5).

Statistics

All statistical analysis was performed in Prism version 5.0a. Percent inhibition was determined by dividing the corrected relative fluorescence of the treated or knockdown cells over the corrected relative fluorescence of the controls. Significance of percent inhibition was determined by 1 sample T-test using 100% as a theoretical mean. For time to metastasis, a Log Rank and Gehan-Breslow-Wilcoxon analysis was used to compare survival curves. A one-tailed student's T-test, assuming LC3 II increases after CQ treatment and BECN1 decreases after shRNA knockdown, was used to compare mean relative density of LC3-II or Becn-1 in mouse tumor samples analyzed by Western Blot. Student's T-test was also used to compare mean percentage of cells expressing the specified surface marker in different treatment groups as determined by flow cytometric analysis. A one-way ANOVA with Bonferoni post test was used for mean comparison of drug treatment and culture type. For invasion and migration assays, the mean relative fluorescence of the negative control was subtracted from the relative fluorescence of each replicate. A one-way ANOVA with Bonferoni post test was used for mean comparison of treatment. A p value of less than 0.05 was considered significant. All error bars represent standard deviation.

Results

Pharmacologic and Genetic Inhibition of Autophagy

Autophagy was inhibited pharmacologically using CQ and Baf A1. CQ is a 4-aminoquinolone that blocks autophagy by increasing lysosomal pH, due to CQ's properties as a

weak base, and preventing fusion of the autophagosome [42]. CQ has been in use for decades as anti-malarial therapy and its derivative, hydroxychloroquine is currently being investigated in clinical trials to enhance efficacy of anti-cancer therapeutics [43]. Though CQ is one of the most commonly used means of inhibiting autophagy, it has other non-autophagic effects and observed sensitivity to CQ could be independent of autophagy [44]. Thus, we chose another pharmacologic inhibitor of autophagy, Baf A1, which is another lysomotrophic agent that blocks autophagy similarly to CQ. Doses of 10 μM CQ and 5 nM Baf A1 were sufficient to inhibit autophagy in 4T1 mammary carcinoma, B16-F10 melanoma, and DLM8 osteosarcoma, murine cell lines (Fig. 2.1) and have worked previously in other cell lines [45]. Higher doses of both drugs can be used to achieve more complete inhibition of autophagy, yet these saturating doses approach the IC_{50} and the autophagy-independent effects of the drugs may obfuscate the autophagy-dependent effects.

Genetic knockdown of autophagy, targeting Beclin-1/Atg6 (Becn-1) and Atg7 was also performed. Knockdown of these genes has been previously shown to inhibit autophagy [46, 47]. By using multiple means of blocking autophagy, any observed effects can more likely be attributed to autophagy inhibition. To create the Becn-1 and Atg7 knockdown cells, a Becn-1, Atg7, or non-silencing shRNA was delivered by lentivirus. After lentiviral transduction, Becn-1 or Atg7 was significantly reduced as determined by western blot and qRT-PCR analysis (Fig 2.2).

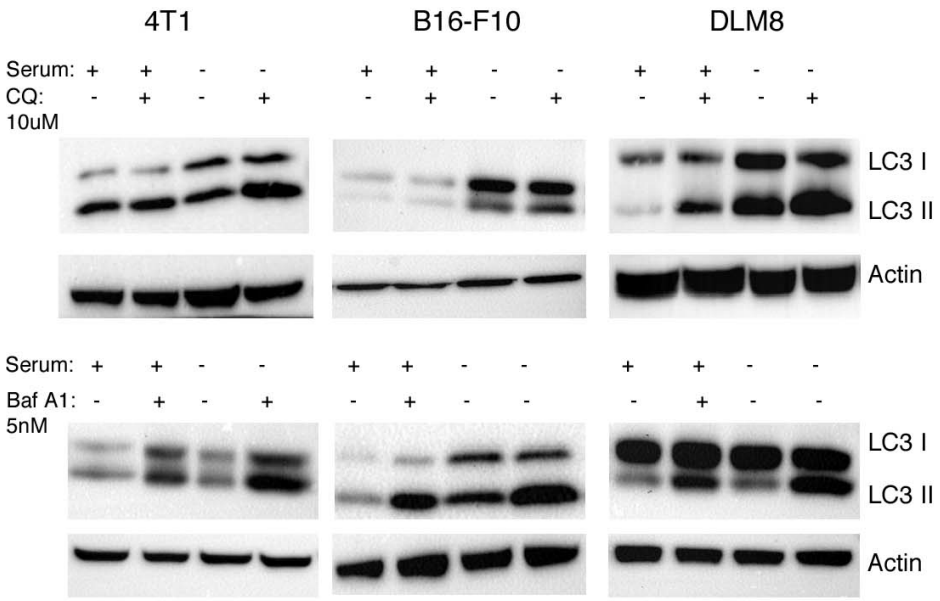

Figure 2.1 Pharmacologic inhibition of autophagy. 4T1, B16-F10, and DLM8 cells were treated with +/- EBSS serum free media for 2h as a positive control for autophagy induction. Media was also supplemented with +/- 10 μM CQ or 5 nM Baf A1 to block autophagy and prevent turnover of LC3 II.

To ensure autophagy was successfully inhibited after shRNA knockdown, cells were grown without serum for 2 hours. Autophagy is induced upon the removal of serum and thus serum starvation serves as a positive control [48]. The mammalian homologue of Atg8, LC3, serves as a marker for autophagy. LC3 is cleaved and conjugated to phosphatidylethanolamine, termed LC3 II, upon autophagy induction. In addition, it is incorporated onto the surface of autophagosomes, and correlates to the number of autophagosomes present. Therefore, increases in LC3 II are indicative of increased autophagy levels [48]. However, LC3 II is degraded in the lysosome as well, so to accurately measure autophagic flux and prevent LC3 II degradation, CQ or Baf A1 were also included in the assay. When cells were treated with serum free media, LC3 II expression was markedly decreased in the Becn-1 and Atg7 knockdowns compared to the non-

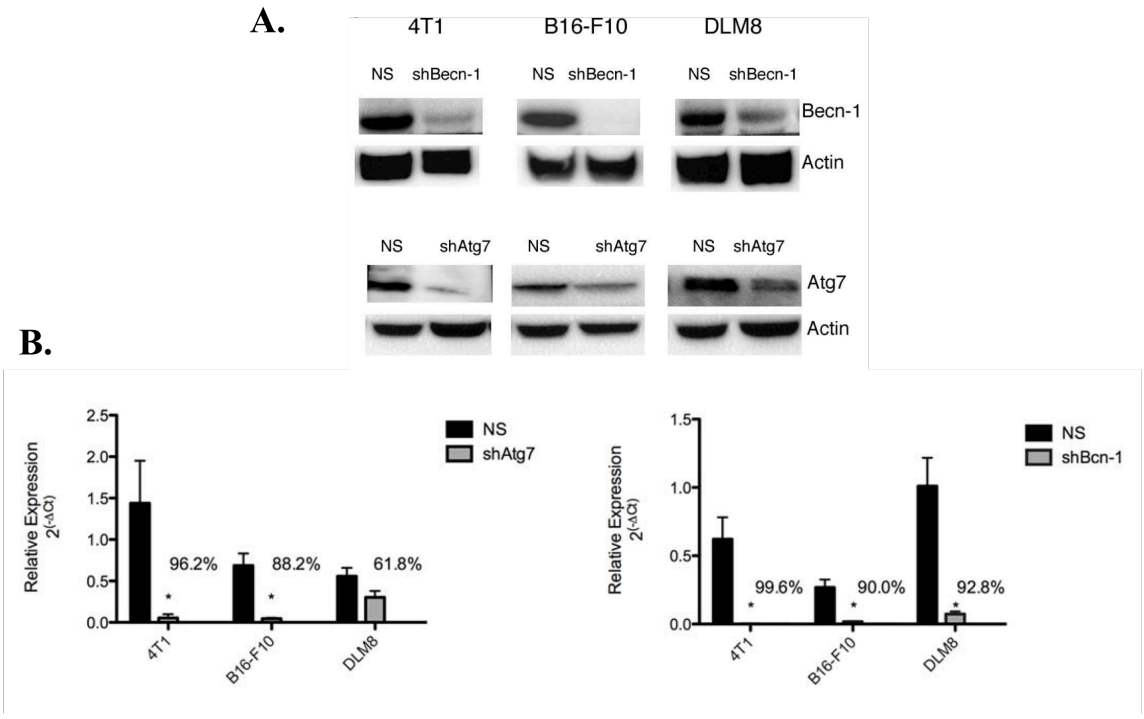

Figure 2.2 Expression of Becn-1 and Atg7 after lentiviral delivery of shRNA. (A) 4T1, B16-F10, and DLM8 cells were transduced with a lentivirus containing either a BECN-1, Atg7 or non-silencing shRNA (NS). Both proteins are reduced compared to the NS control. RT-qPCR was used to determine the level of **(B)** Atg7 or Becn-1 mRNA expression, normalized to Hsp90 and Tbp. Expression was significantly reduced in cells that received the shRNA against Becn-1 or Atg7 compared to the non-silencing control.

silencing controls (2.3) indicating knockdown of either gene was sufficient to reduce autophagy induction.

Autophagy inhibition slows growth in vitro but not in experimentally induced metastases.

We tested the effect of autophagy inhibition using the aforementioned methods on the proliferation of 4T1, B16-F10, and DLM8 cells. These cell types were selected as they represent different types of cancer, can be used in syngeneic mouse models, and are highly metastatic [49-51]. In all cell types, all methods of autophagy inhibition were able to significantly reduce proliferation (Fig. 2.4).

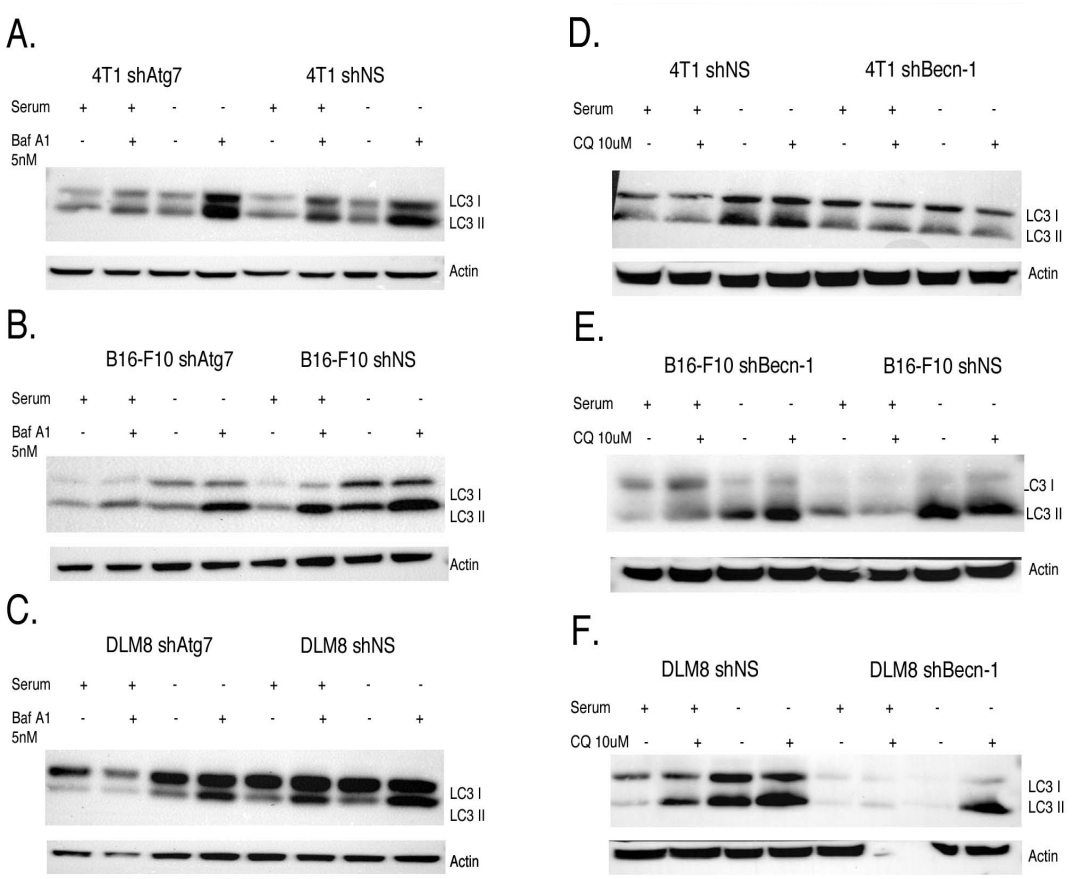

Figure 2.3 Autophagy inhibition after knockdown of Becn-1 and Atg7. After knockdown of Becn-1 and Atg7 by lentiviral delivered shRNA, **(A)** 4T1-shAtg7, **(B**) B16-F10-shAtg7, **(C)** DLM8-shAtg7, **(D)** 4T1-shBecn-1, **(E)** B16-F10-shBecn-1, and **(F)** DLM8-shAtg7 cells were serum starved and treated with +/- CQ or Baf A1. Serum starvation was not able to induce LC3-II expression as robustly in the shRNA treated cells compared to the NS control.

Next, we tested whether similar results could be recapitulated in experimental metastases. Mice were first pre-treated with 60 mg/kg CQ for 72h so autophagy would already be inhibited, systemically.

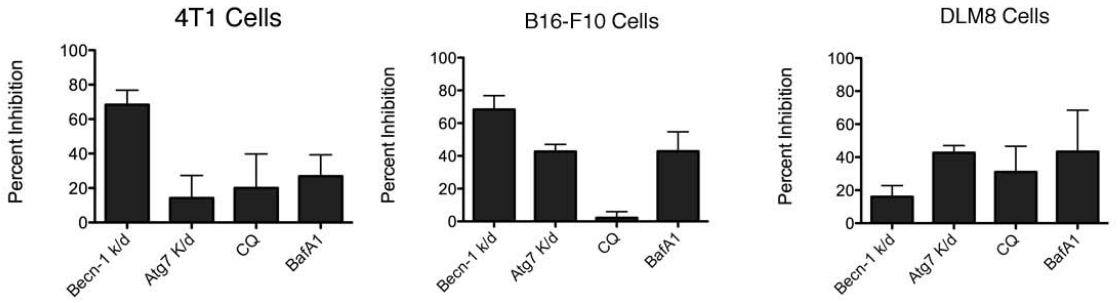

Figure 2.4 Autophagy inhibition decreases cell proliferation. 4T1, B16-F10, and DLM8 cell proliferation with or without functional autophagy was assessed by Alamar Blue assay. Cells were treated for 72 h +/- 10 μM CQ or 5 nM Baf A1. Becn-1 and Atg7 knockdown cells were grown for 72h. Graphs represent the mean and standard deviation of the percentage of growth inhibition compared to control cells. All methods of inhibition significantly inhibited growth.

After pre-treatment, Balb/c or C57Bl/6J mice were challenged with 4T1-luc or B16-F10 cells delivered intravenously into the tail vein. Mice continued to receive treatment and were monitored for the development of luciferase positive 4T1 metastases or 10% weight loss in the B16-F10 challenged mice. CQ was not able to delay the development of 4T1 metastases, nor significantly prolong survival in the B16-F10 challenged mice (Fig. 2.5).

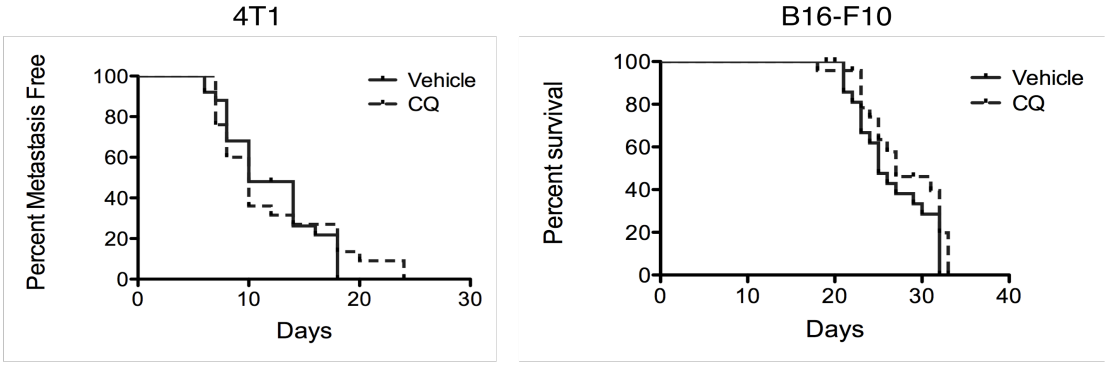

Figure 2.5 CQ treatment does not delay experimentally induced metastases. Kaplan-Meier event free survival of 4T1 and B16-F10 challenged mice. Mice were first pretreated with CQ and then challenged with either 4T1 or B16-F10 cells injected via the tail vein, n=25. Mice continued to receive treatment until the development of luciferase positive metastases or 10% weight loss.

To ensure CQ was effectively inhibiting autophagy, expression of LC3-II was measured in the liver, which responds to both CQ and autophagy modulating effects [45]. LC3-II was increased in CQ treated mice indicating pharmacodynamic efficacy (Fig 2.6). In addition, LC3 positive punctate were visible in the tumor-burdened lungs of mice treated with CQ (Fig 2.6).

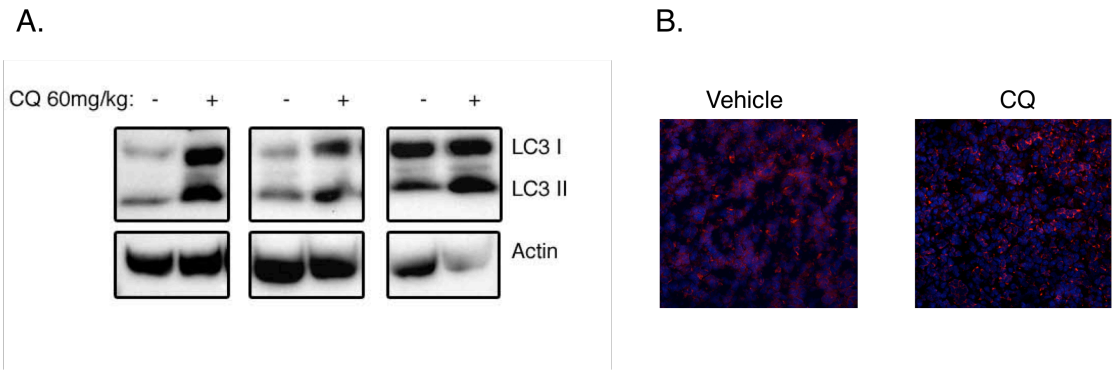

Figure 2.6 CQ inhibits autophagy *in vivo*. (A) Western blot analysis of liver samples from treated mice. Mice were treated with 60mg/kg, daily, IP CQ or vehicle for 72h, n=3. LC3 I/II increases after administration of CQ. **(B)** Representative images of LC3 (Red) expression in the lungs of CQ or vehicle treated mice

To determine if tumor cells with impaired autophagy, rather than the murine host, would have an altered ability to colonize the lung, mice were also challenged with 4T1-luc Becn-1 knockdown cells or 4T1-luc cells that had been treated with 10 μM CQ, 2 h prior to injection. Again, neither Becn-1 knockdown nor CQ pretreatment of the cells had an effect on the time to metastasis development (Fig 2.7).

Autophagy inhibition has an additive effect in combination with cisplatin in vitro, but is antagonistic in a neoadjuvant setting.

It is not likely that autophagy inhibition will ever be used as a single agent therapy, but will be combined with one if not multiple different anti-cancer therapies in the clinic. Therefore we

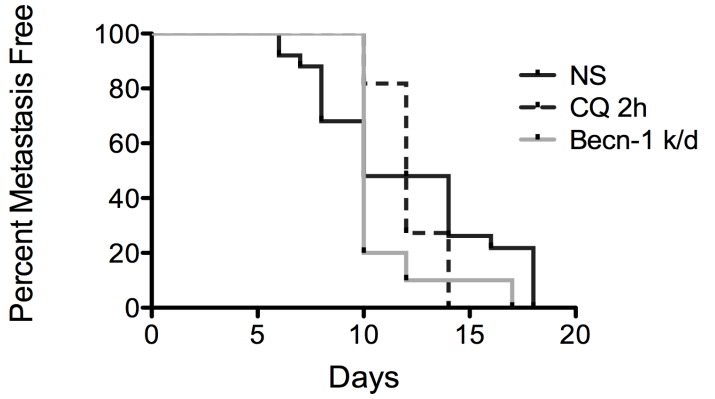

Figure 2.7 Autophagy deficient cells can still colonize the lung. Mice received either 4T1-luc Becn-1 knockdown cells, cells treated with 10 μM CQ 2 h prior, or NS control cells, then followed until the development of luciferase positive metastases.

tested the combination of autophagy and cisplatin, which is a clinically relevant therapeutic for all three types of cancer [52-54]. The combination of cisplatin, at the IC_{50}, and autophagy inhibition, had at least an additive effect on growth inhibition compared to either treatment alone, according to the Bliss independence model of syngergy (Fig. 2.8 and Tables 2.1-2.3).

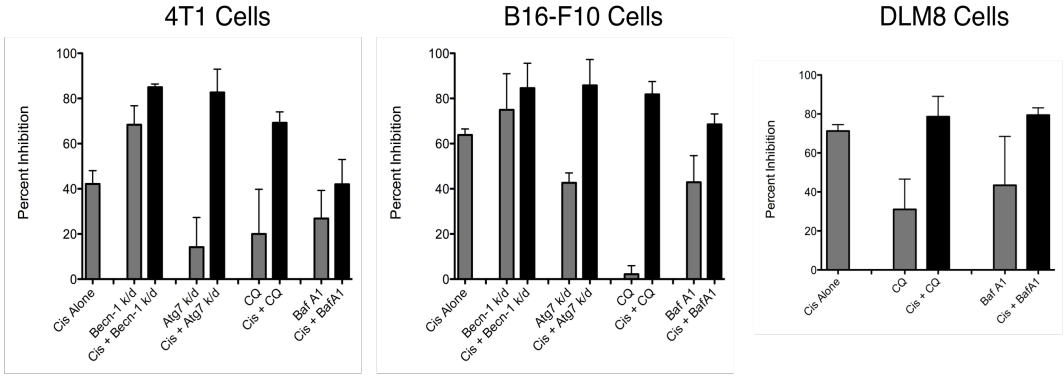

Figure 2.8 The combination of cisplatin and autophagy inhibition is additive in culture. 4T1, B16-F10, and DLM8 cell proliferation with or without functional autophagy in combination with cisplatin was assessed by Alamar Blue assay. Cells were treated for 72 h +/- 10 μM CQ or 5 nM Baf A1. Becn-1 and Atg7 knockdown cells were grown for 72 h. Graphs represent the mean and standard deviation of the percentage of growth inhibition compared to control cells.

Table 2.1 Bliss Analysis for 4T1 cells

4T1				
Cis Alone	Becn-1 Alone	Combo	Bliss Value	Ratio
0.42	0.42	0.85	0.66	1.28
Cis Alone	Atg7 Alone	Combo	Bliss Value	Ratio
0.42	0.55	0.83	0.74	1.12
Cis Alone	CQ Alone	Combo	Bliss Value	Ratio
0.42	0.15	0.70	0.51	1.35
Cis Alone	Baf A1 Alone	Combo	Bliss Value	Ratio
0.42	0.04	0.42	0.44	0.95

Values represent treatment effect expressed as fraction of affected cells. A ratio of < 0.8 = antagonistic, 0.8 – 1.2 = additive, and > 1.2 = synergistic

Table 2.2 Bliss Analysis for DLM8 cells.

DLM8				
Cis Alone	CQ Alone	Combo	Bliss Value	Ratio
0.71	0.48	0.79	0.70	1.12
Cis Alone	Baf A1 Alone	Combo	Bliss Value	Ratio
0.71	0.50	0.79	0.74	1.07

Values represent treatment effect expressed as fraction of affected cells. A ratio of < 0.8 = antagonistic, 0.8 – 1.2 = additive, and > 1.2 = synergistic

Table 2.3 Bliss Analysis for B16-F10 cells.

B16-F10				
Cis Alone	Becn-1 Alone	Combo	Bliss Value	Ratio
0.64	0.67	0.85	0.88	0.96
Cis Alone	Atg7 Alone	Combo	Bliss Value	Ratio
0.64	0.51	0.86	0.83	1.05
Cis Alone	CQ Alone	Combo	Bliss Value	Ratio
0.64	0.22	0.82	0.72	1.13
Cis Alone	Baf A1 Alone	Combo	Bliss Value	Ratio
0.64	0.24	0.69	0.73	0.94

Values represent treatment effect expressed as fraction of affected cells. A ratio of < 0.8 = antagonistic, 0.8 – 1.2 = additive, and > 1.2 = synergistic

To observe the effect of autophagy inhibition in a more realistic metastatic setting, CQ was given as either surgical adjuvant or neoadjuvant therapy in mice challenged with 4T1-luc cells implanted, orthotopically, into the mammary fat pad. Cisplatin was also given at the human equivalent exposure either in combination or as a single agent therapy. For the surgical adjuvant model, mice received treatment 24 h after resection of tumors that had reached 100 mm^3. Mice were then imaged thrice weekly until the development of luciferase positive metastases. As with the experimental metastasis model, CQ had no significant effect on median time to metastasis development (Fig 2.9). However, neither did cisplatin nor the combination. Cisplatin was able to elicit more necrosis within the primary tumor compared to vehicle, so the dose was not completely ineffective (Table 2.4). If mice were given neoadjuvant therapy, treatment beginning 24h after cell implantation and subsequent tumor resection at 100 mm^3, both CQ and cisplatin

were able to significantly delay metastatic development as compared to vehicle (Fig 2.9). The neoadjuvant study was repeated with similar results.

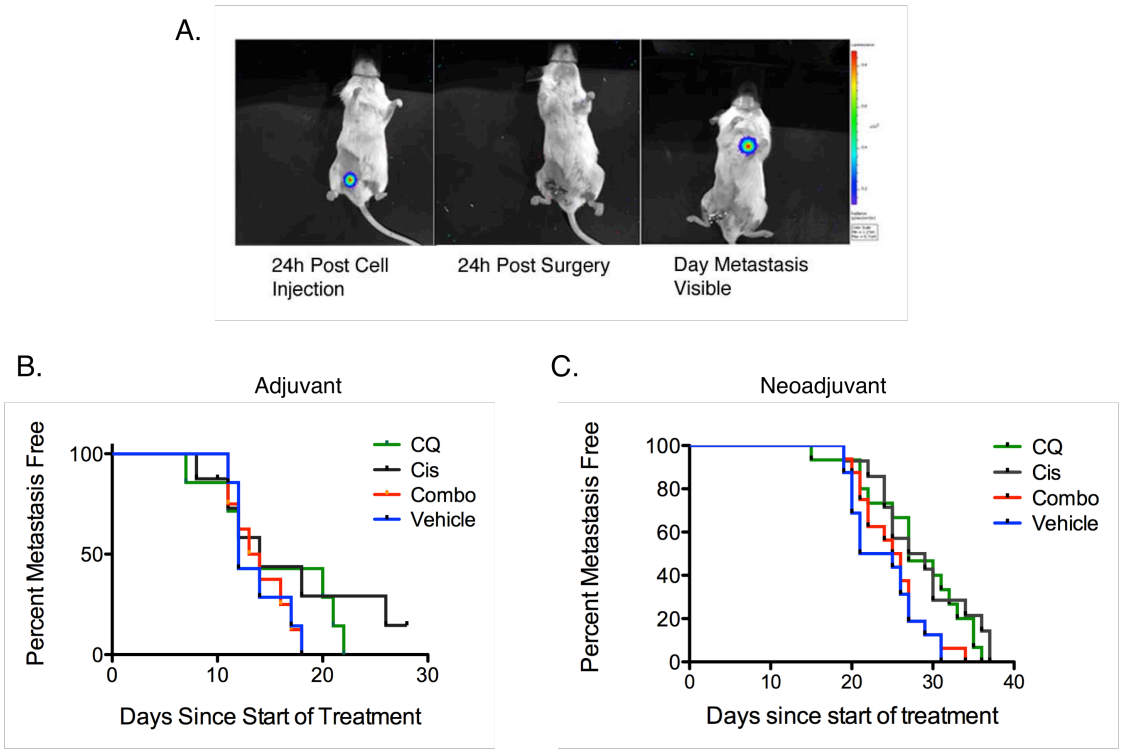

Figure 2.9. CQ as a neoadjuvant therapy is able to delay metastasis, but is antagonistic when given in combination with cisplatin. (A) Representative serial images of a mouse 24 h after cell implant, 24 h after surgery, and the day metastases were visible. 4T1-luc cells were implanted into the mammary fat pad of Balb/c mice. 60 mg/kg, daily, IP CQ, 3 mg/kg, IP q14d cisplatin, a combination of the two, or vehicle was given either 24h after cell implant, neoadjuvant therapy, or 24 h after resection of 100-200 mm^3 tumors, surgical adjuvant therapy. **(B)** Time to metastasis development using adjuvant therapy. No significant difference in treatment was observed. **(C)** Time to metastasis development using neoadjuvant therapy. Curve represents combined two studies. There was a significant delay in metastatic development for both single agent CQ and cisplatin since start of treatment and after tumor removal. However, the combination therapy had an antagonistic trend.

Interestingly, the combination was not significantly different than the vehicle, and was significantly antagonistic to both CQ and cisplatin ($p = 0.0351$ and $p = 0.0399$), with mice doing more poorly than either CQ or cisplatin alone (CQ median time = 27 days, cisplatin median time = 28.5 days, combination = 25 days). To determine if this effect was due to systemic or tumor

Table 2.4. Percentange of necrosis on resected primary tumors following treatment

Treatment	% Necrosis			
	<5	5 to 10	10 to 20	>20
CQ (n=6)	3 (50.0%)	0	1 (16.7%)	2 (33.3%)
Combo (n=9)	4 (44.4%)	3 (33.3%)	1 (11.1%)	1 (11.1%)
Cisplatin (n=6)	1 (16.7%)	4 (66.7%)	0	1 (16.7%)
Vehicle (n=8)	5 (62.8%)	2 (25.0%)	1 (12.5%)	0

autophagy inhibition, mice were also challenged with 4T1-luc Becn-1 knockdown or NS cells and cisplatin was given neoadjuvantly. In this setting, autophagy inhibition by Becn-1 knockdown, again, significantly slowed metastatic development compared to vehicle ($p = 0.0297$, median time = 22.5 days v 19 days) (Fig 2.10). While the Becn-1 knockdown and cisplatin combination was not as markedly antagonistic (median time = 26 days v 24.5 days) it still did not have an additive effect as the *in vitro* results suggested.

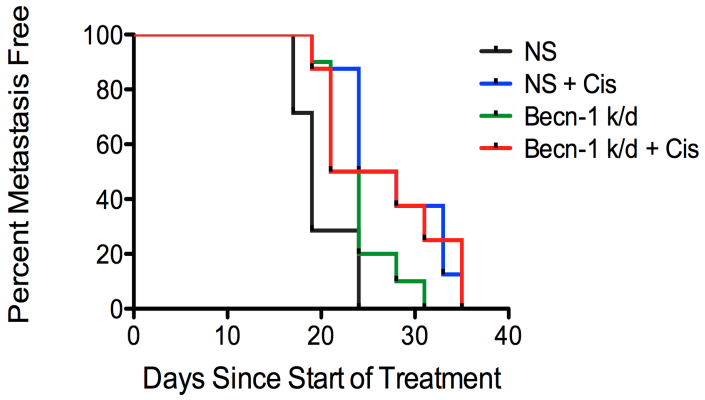

Figure 2.10 Becn-1 knockdown also delays metastasis and is not additive in combination with cisplatin. Time to metastatic development using neoadjvuant cisplatin therapy on 4T1-luc-shBecn-1 challenged mice. Becn-1 knockdown, cisplatin alone, and the combination all significantly delayed metastases, but the combination did not enhance cisplatin efficacy.

Since autophagy is known to play a role in key immune responses such as monocyte differentiation, cross-presentation of tumor antigens, and ATP-release, we surmised that the antagonism or lack of additivity with cisplatin and autophagy inhibition may be attributed to autophagy related immunomodulatory functions [37, 55, 56]. Immune cell populations were assessed in the lungs of neoadjuvantly treated mice after the development of metastases. There was a significant increase in the number of "infiltrating" neutrophils ($CD11b^+/Ly6g^+$) present in the lungs of both CQ and combination treated mice compared to vehicle or cisplatin (CQ vs vehicle $p = 0.033$, combination vs vehicle $p = 0.0092$, CQ vs cisplatin $p = 0.038$, and combination vs cisplatin $p = 0.048$) (Fig 2.11). While not statistically significant, we also found a corresponding decrease in T-cells, particularly $CD8^+$ cells. Infiltrating neutrophils can have modulating effects on the microenvironment including promotion of invasion and angiogenesis and immune suppression through the release of arginase-1 [57]. Therefore, the shift in immune cell populations could impact cisplatin efficacy.

Autophagy stimulation hastens metastatic development due to the potentiation of the pre-metastatic niche.

Since mice fared worse when cisplatin was combined with autophagy inhibition, we investigated if the reverse, autophagy stimulation, would affect cisplatin efficacy. Additionally, enhanced autophagy has yet to be truly tested in a survival model. Trehalose has been shown to be an effective inducer of autophagy and 2% trehalose dissolved in drinking water has been used in studies investigating the neurological effects of autophagy stimulation.[58-60] Similar to the other neoadjuvant models, 4T1-luc cells were orthotopically implanted, and treatment began 24 h after, either 2% sucrose or 2% trehalose with or without cisplatin. LC3 expression was significantly increased in the tumors resected from trehalose treated mice compared to the

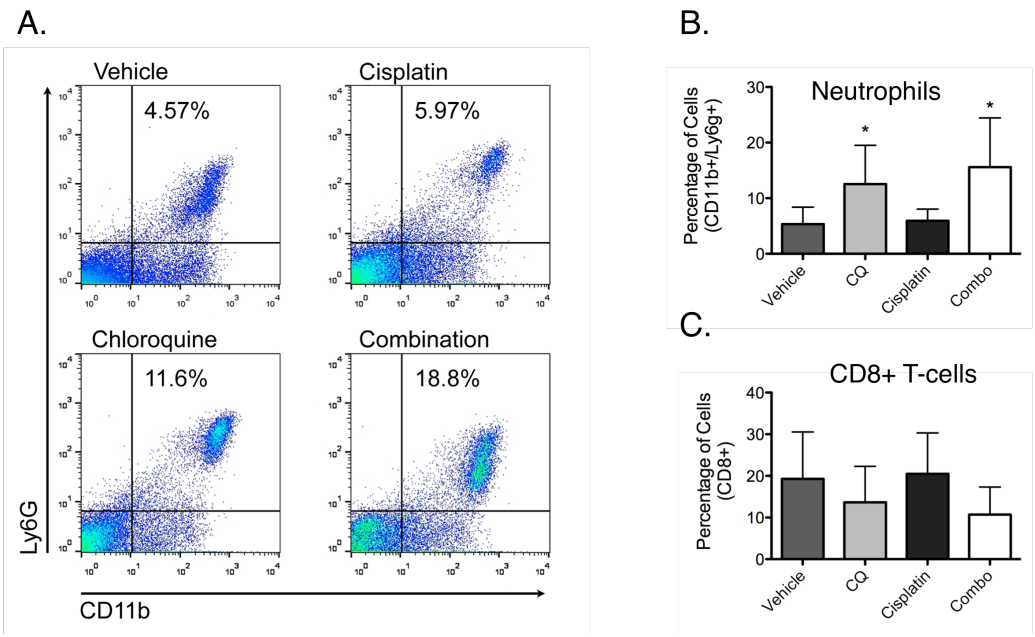

Figure 2.11 Autophagy alters neutrophil infiltration. (A) Representative flow plots and **(B)** corresponding graph of infiltrating neutrophils in lungs of treated mice. There is a significant increase in CQ and combination treated mice. **(C)** Though not significant, there is a trend of decreased CD8+ cells in CQ and combination treated mice.

sucrose, indicating stimulation of autophagy (Fig 2.12). Trehalose treatment, alone, significantly shortened the time to metastatic development compared to sucrose treated mice ($p = 0.0146$) (Fig 5B). The addition of trehalose neither enhanced nor hindered cisplatin efficacy (Fig 2.12).

To determine if trehalose altered the metastatic characteristics of the cells, anchorage independent growth, invasion, and migration assays were used. For anchorage independent assays, cells were either grown in standard 96 well plates or ones treated with PolyHEMA to prevent attachment. Trehalose did not enhance proliferation of detached cells nor did autophagy inhibition significantly augment growth inhibition (Fig 2.13). The few exceptions were CQ treatment in B16-F10 cells, which caused greater inhibition in suspended cells while

Baf A1 induced inhibition was actually greater in adherent cells. This was also true for CQ treated adherent 4T1 cells. Neither autophagy inhibition nor stimulation altered migration or invasion significantly (data not shown).

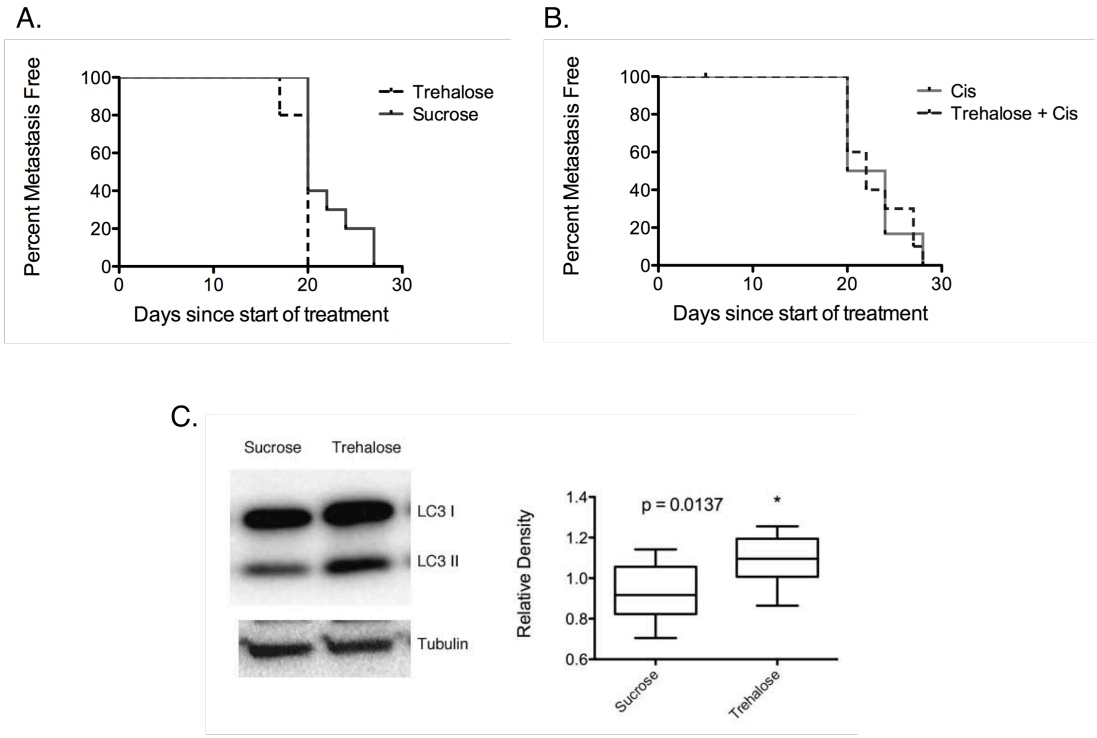

Figure 2.12 Stimulating autophagy by trehalose decreases time to metastasic development. (A) 4T1-luc cells were implanted into the mammary fat pad of Balb/c mice. After a 24h period, mice were then given 2% trehalose or sucrose dissolved in water and received either 3 mg/kg, q14 d i.p. cisplatin or vehicle. Tumors were resected at 100mm^3. Mice were monitored thrice weekly for the development of luciferase positive metastases. **(B)** Trehalose neither hindered or enhanced cisplatin efficacy. **(C)** Western blot analysis for LC3 II expression in trehalose treated tumors. LC3 II is significantly increased in trehalose treated tumors.

Since autophagy appeared to be more necessary for lung colonization than other points in the metastatic cascade in a model of hepatacellular carcinoma, we investigated if certain cell populations lung in the lung had been altered by changes in autophagy [31, 32]. It has been demonstrated that before tumor cells enter the lung, it is primed with bone marrow derived cells (BMDCs) expressing VEGFR1 and VLA-4 (integrin $\alpha_4\beta_1$), which promote vascularization, cell

migration, and breakdown of basement membranes [61].

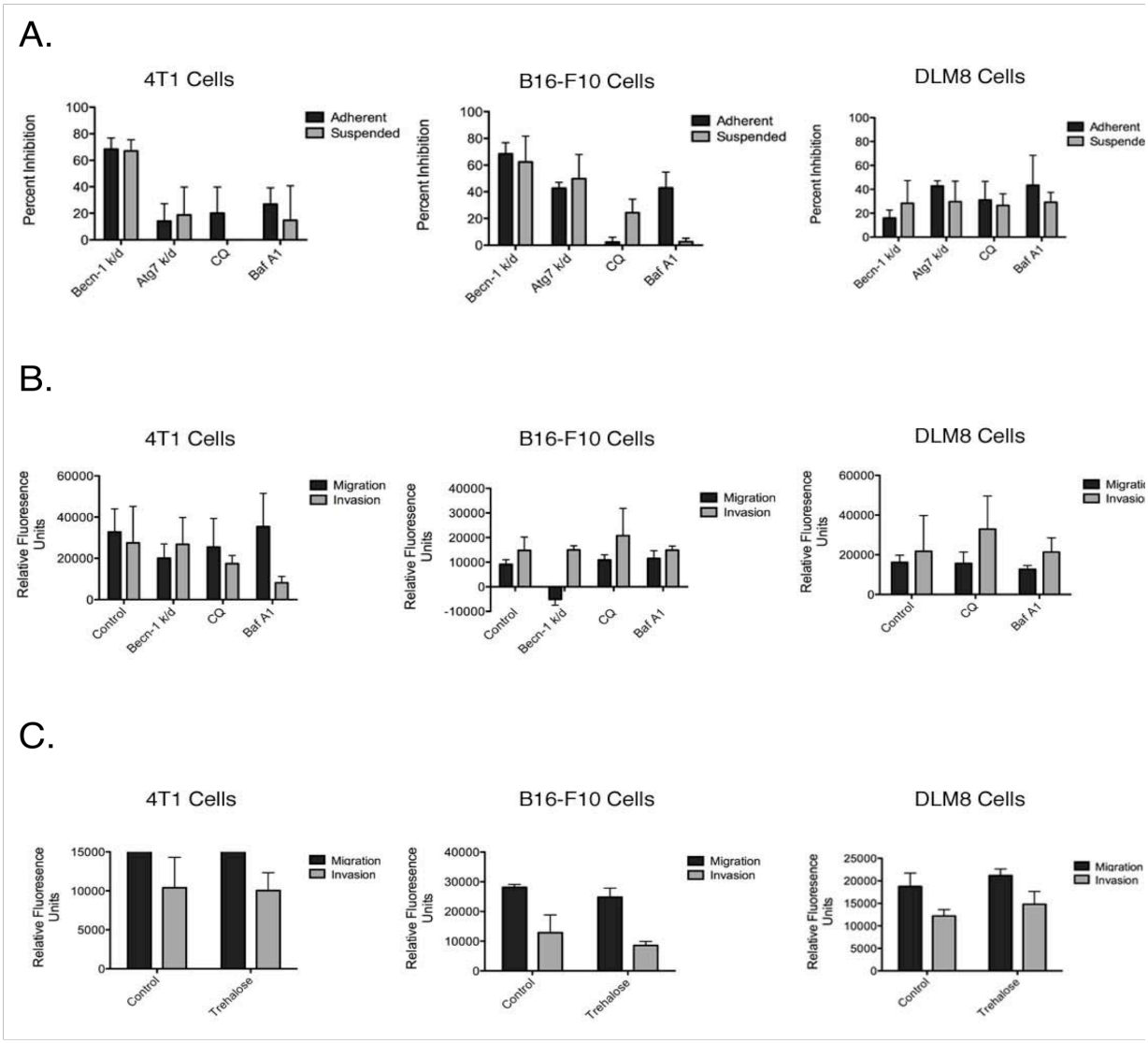

Figure 2.13. Autophagy does not affect *in vitro* metastatic characteristics (A) 4T1, B16-F10, and DLM8 cell proliferation with or without functional autophagy was assessed by Alamar Blue assay. Cells were treated for 72 h +/- 10 μM CQ or 5 nM Baf A1. Becn-1 and Atg7 knockdown cells were grown for 72h. For anchorage independent growth, cells were grown on PolyHEMA coated plates to prevent attachment. Graphs represent the mean and standard deviation of the percentage of growth inhibition compared to control cells. Autophagy inhibition induced growth inhibition was not augmented in suspended cells. **(B)** Autophagy inhibition did not affect the ability of 4T1, B16-F10, and DLM8 to invade or migrate. Graphs represent the mean and standard deviation of the relative fluorescence subtracted from the negative control. **(C)** Autophagy stimulation by 100 mM trehalose did not significantly effect migration or invasion.

Therefore, flow cytometric analysis was performed on the lungs and blood of mice treated either with trehalose, vehicle, or CQ for 15 days, which is just prior to the development of metastases. There was a significant increase in cells expressing both VEGFR1/VLA4 in trehalose treated mice compared to vehicle and CQ treated mice (lungs: p = 0.0021 and 0.0351, blood: p = 0.0424 and 0.0177) (Fig. 2.14). These cells were even further reduced in the blood of CQ treated mice, indicating that autophagy may play a role in priming the pre-metastatic niche for tumor cell invasion (p = 0.0493). These cells were even further reduced in the blood of CQ treated mice,

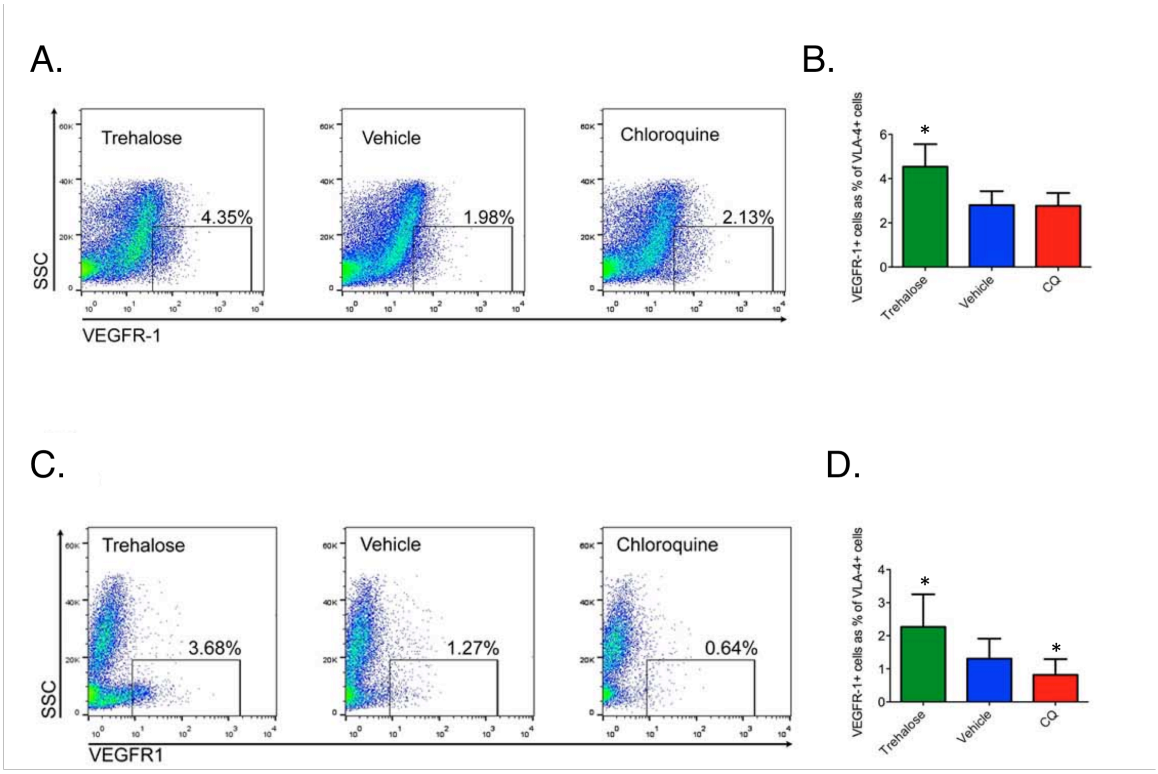

Figure 2.14. Autophagy modulation corresponds to changes in BMDC number Representative relative flow plots of of VEGFR1^{+}/VLA4^{+}/CD117^{+} cells in (A) lung and (C) blood with corresponding graphs (B) and (D). There are significantly more cells in trehalose treated mice and significantly less in the blood of CQ treated mice compared to vehicle.

indicating that autophagy may play a role in priming the pre-metastatic niche for tumor cell invasion.

Discussion

The role of autophagy in metastasis development and progression still remains unclear. Therefore, we sought to interrogate the effect of autophagy inhibition along various stages of the metastatic cascade. Additionally, we used a variety of cancer models to address whether the effects we observed were context dependent. Although CQ is the most clinically relevant and one of the most widely used autophagy inhibitors, it can affect other processes in addition to autophagy [44]. Thus, we employed another pharmacologic inhibitor, Baf A1, which is mechanistically similar to CQ, as well as generating several metastatic cell lines stably transfected with shRNA towards Becn-1 and Atg7. Becn-1 is a Class III PI3K and is involved in the early nucleation stage of the autophagosome [62]. Atg7 is part of a complex including Atg5, Atg12, and Atg16 that is also necessary for autophagosome formation [62]. These genes are not only integral to the autophagy pathway but are also involved in other processes including Becn-1 regulation of p53 and apoptosis, hence the need to include multiple means of autophagy blockade [63, 64].

After lentiviral transduction, we ensured that not only were Becn-1 or Atg7 knocked down, but autophagy was also successfully inhibited. While there is still a slight increase in LC3-II after serum withdrawal in the knockdown lines, it is not as robust as their corresponding NS controls (Fig 2.3). The lack of complete inhibition in some lines is likely due to the fact that the cells simply could not survive without some degree of autophagic turnover. Subsequent experiments were performed at low passage number as suggested by Staskiewicz *et al* [65].

Utilizing these various methods of autophagy inhibition in the different cancer models, we determined that autophagy inhibition alone diminished cell proliferation, however, not enough to alter the ability of cells to colonize the lungs in experimental 4T1 and B16-F10 metastasis models. Inhibition was tested in two settings: 1) autophagy inhibition already systemically on board in the murine host and 2) autophagy impairment in cells before entry into the lungs. In both instances, autophagy inhibition on its own was not effective at delaying metastases. These results suggest that once the tumor cells are present in the lung, autophagy is not as important for establishment.

The lack of efficacy was likely not attributable to CQ dosing. Evidence of autophagy inhibition was apparent as LC3 II increased in the liver, which is characteristically used to observe autophagy modulation *in vivo,* and redistributed into punctate formations in lung metastases after treatment *[45]*. The 60 mg/kg daily dosing regimen was also previously demonstrated to be efficacious in slowing primary tumor growth [41]. There still could be a possibility that the amount of inhibition achieved by CQ treatment was not strong enough. More potent inhibitors of autophagy with better therapeutic indexes are currently being developed and may prove to be more efficacious [66].

We next tested autophagy inhibition in surgical adjuvant and neoadjuvant models. These models allow for the more natural progression of metastases as well as provide a more clinically relevant setting. Cisplatin was also added as a treatment since it is a common therapy for all three cancer types and has been shown to enhance cell death in combination with autophagy inhibition *in vitro* [67, 68]. The combination did have an additive effect on inhibiting cell growth, but similar to the i.v. delivered metastases, there was no delay in metastatic development, by any treatment in the surgical adjuvant model. Yet, in the neoadjuvant model, CQ alone was able to

slow time to progression. This was recapitulated using the Becn-1 knockdown line. The fact that autophagy inhibition only has an effect in the neoadjuvant and not the other models suggest that autophagy's importance lies in the very early events of the metastatic cascade. Though more potent inhibitors of autophagy could show more efficacy than CQ as adjuvant therapy, the response will still likely be better before cells have had a chance to reach the metastatic site. Future studies should also examine other sites of metastasis such as bone to see if the case is similar or site specific.

The combination of cisplatin and CQ actually had a significantly antagonistic effect though it was not as pronounced with genetically inhibited autophagy. This could indicate that the loss of autophagy alters the surrounding environment. Autophagy has been shown to have many immune-related affects including antigen presentation, differentiation, and recruitment of dendritic cells to participate in immunogenic cell death. This is due to the fact that cells with functional autophagy release ATP [37, 38]. A similar effect was observed by Ko et al with the combination of autophagy inhibition and radiation. In culture and in nude mice, autophagy inhibition sensitized to radiation, but in the immune competent Balb/c model, the combination was ineffective. While cisplatin is unable to trigger immunogenic cell death since it fails to cause ER stress and the resultant surface expression of calreticulin, there still may be a shift in the populations present that creates a more permissive growth environment. Thus we used flow cytometry to determine if there was a change in infiltrating cell populations in the various treatment groups. We found that there was a significant increase in the number of neutrophils present in the CQ and combination treated mice. Autophagy appears to be required for the release of ATP. ATP facilitates the recruitment of immature myeloid cells and influences their differentiation into cytotoxic immune cells like CD 8+ T-cells and dendritic cells. In the absence

of ATP, the immature myeloid cells are more likely to differentiate into neutrophils [69]. Neutrophils may have pro-tumor effects such as promoting angiogenesis through the release of MMP-9 and VEGF, increasing invasiveness by degrading the extracellular matrix using neutrophil elastase, and immune suppression by ariginase-1 release [57]. Depletion of neutrophils is associated with increased active CD 8+ T-cells. Infiltrating neutrophil numbers are correlated with poor clinical outcome. While increased neutrophil infiltration may not be the only explanation for decreased cisplatin efficacy, it does demonstrate that autophagy is also exerting effects on the surrounding environment. By inhibiting autophagy, there may be unanticipated and even counterproductive results related to alterations within the metastatic microenvironment.

Since a survival model examining the effects of autophagy stimulation has not been tested to date, we used the disaccharide trehalose to induce autophagy in our neoadjuvant model. Though systemic autophagy inhibition appeared to abrogate cisplatin efficacy, autophagy stimulation neither hindered nor enhanced cisplatin efficacy. Where autophagy inhibition was able to slow metastasis, trehalose-induced autophagy correspondingly accelerated metastasis development. A sucrose control arm was included to confirm this was not simply a result of added sugar. Since autophagy only seemed to influence metastatic growth early, before cells have escaped the primary tumor, we examined the effect of autophagy modulation on the metastatic characteristics necessary to precipitate this event. There was no difference in growth inhibition over all, whether cells were allowed to adhere or were suspended. If autophagy inhibition were critical to anchorage independent growth, there should have been augmented growth inhibition in the suspended cells compared to the adherent ones. The suspended B16-F10 cells did demonstrated greater growth inhibition after CQ treatment; however, this was not the

case with any other method of autophagy inhibition and likely due to an autophagy-independent drug effect. This is probably a similar case where CQ efficacy decreased in 4T1 suspended cells and Baf A1 efficacy decreased in B16-F10 suspended cells. Trehalose was also unable to enhance anchorage independent growth or adherent cell proliferation. Similarly, there was still no change in the ability of cells to invade and migrate when autophagy was altered.

We next explored if autophagy was involved in alteration of the lung microenvironment. This is based on the idea of a premetastatic niche where BMDCs, particularly those expressing VEGFR1/VLA-4, infiltrate the lung and begin to change the environment. These cells activate other integrins and chemokines, such as SDF-1 that can not only recruit the tumor cells to the site of metastasis but also promote their attachment, survival, and vascularization [70]. These cells are mobilized to the lung by chemokines secreted by the tumor cells and stroma to prepare the way for the incoming tumor cells [70]. The number of cells expressing VEGFR1/VLA-4 were measured in the lungs and blood of mice after autophagy modulation but before the arrival of tumor cells. There was a significant increase in these cells in the trehalose treated mice and further reduction in the CQ treated mice, notably within circulation. Some recent studies have shown that autophagy is cytoprotective in bone marrow-derived stem cells, including endothelial progenitor cells, and that it can be activated by chemokines such as SDF-1 [71, 72]. Therefore, the increased levels of autophagy in the trehalose treated mice may give an advantage toward the survival of $VEGFR1^+$ cells, particularly since more cells were in circulation. Thus the metastatic microenvironment may not have been as growth permissive or recruitment signal not as strong. This is in line with the other mouse models showing autophagy inhibition is not as effective once cells have already reached the metastatic site. More in depth studies looking for the presence of cytokines and growth factors such as SDF-1, should be conducted to determine the extent of

microenvironment alteration. Since the impact of genetic autophagy inhibition on these cells was not tested, it will also be important for future research to determine if this effect has any involvement in the tumor cell's ability to mobilize BMDC.

Conclusions

Although autophagy has been identified as a potential mechanism of survival and resistance for tumor cells, it is still unclear exactly how cells utilize autophagy while undergoing metastatic dissemination. Understanding this role can allow us to maximize the potential of autophagy inhibition as a therapy. In this study, we pinpointed the efficacy of autophagy inhibition as likely impeding the ability of BMDCs to survive in circulation and arrive at the pre-metastatic site. Therefore, autophagy inhibition may be more effective if used to prevent the development of the pre-metastatic niche. We also found that autophagy may have a contrasting, though no less important, role once cells have been established. Functional autophagy of the microenvironment may actually keep cell growth in check as it could alter the phenotype or recruitment of immune cell populations. Consequently, caution is recommended in combining therapies, particularly if cytotoxicity can be attributed to immune related cell death. Pharmacologic autophagy inhibition may have effects outside of the tumor including changes in the surrounding microenvironment that may not be detectable in immune deficient models. Continued studies will be best served by employing multiple avenues of data collection including cell culture, xenografts, and immune competent model organisms in order to develop a more complete picture of autophagy inhibition in the context of an anti-cancer therapy.

References

1. Mizushima, N., T. Yoshimori, and B. Levine, *Methods in mammalian autophagy research.* Cell, 2010. **140**(3): p. 313-26.

2. Mortimore, G.E. and A.R. Poso, *Intracellular protein catabolism and its control during nutrient deprivation and supply.* Annu Rev Nutr, 1987. **7**: p. 539-64.

3. Kroemer, G., G. Marino, and B. Levine, *Autophagy and the integrated stress response.* Mol Cell, 2010. **40**(2): p. 280-93.

4. Choi, A.M., S.W. Ryter, and B. Levine, *Autophagy in human health and disease.* N Engl J Med, 2013. **368**(7): p. 651-62.

5. Ichimura, Y. and M. Komatsu, *Pathophysiological role of autophagy: lesson from autophagy-deficient mouse models.* Exp Anim, 2011. **60**(4): p. 329-45.

6. Marino, G., et al., *Tissue-specific autophagy alterations and increased tumorigenesis in mice deficient in Atg4C/autophagin-3.* J Biol Chem, 2007. **282**(25): p. 18573-83.

7. Qu, X., et al., *Promotion of tumorigenesis by heterozygous disruption of the beclin 1 autophagy gene.* J Clin Invest, 2003. **112**(12): p. 1809-20.

8. Yang, S., et al., *Pancreatic cancers require autophagy for tumor growth.* Genes Dev, 2011. **25**(7): p. 717-29.

9. Guo, J.Y., et al., *Activated Ras requires autophagy to maintain oxidative metabolism and tumorigenesis.* Genes Dev, 2011. **25**(5): p. 460-70.

10. Lazova, R., et al., *Punctate LC3B expression is a common feature of solid tumors and associated with proliferation, metastasis, and poor outcome.* Clin Cancer Res, 2012. **18**(2): p. 370-9.

11. Song, Y.J., et al., *Autophagy contributes to the survival of CD133+ liver cancer stem cells in the hypoxic and nutrient-deprived tumor microenvironment.* Cancer Lett, 2013. **339**(1): p. 70-81.

12. Rausch, V., et al., *Autophagy mediates survival of pancreatic tumour-initiating cells in a hypoxic microenvironment.* J Pathol, 2012. **227**(3): p. 325-35.

13. Bristol, M.L., et al., *Dual functions of autophagy in the response of breast tumor cells to radiation: cytoprotective autophagy with radiation alone and cytotoxic autophagy in radiosensitization by vitamin D 3.* Autophagy, 2012. **8**(5): p. 739-53.

14. Sasaki, K., et al., *Chloroquine potentiates the anti-cancer effect of 5-fluorouracil on colon cancer cells.* BMC Cancer, 2010. **10**: p. 370.

15. Ding, Z.B., et al., *Autophagy activation in hepatocellular carcinoma contributes to the tolerance of oxaliplatin via reactive oxygen species modulation.* Clin Cancer Res, 2011. **17**(19): p. 6229-38.

16. Gewirtz, D.A., *When cytoprotective autophagy isn't... and even when it is.* Autophagy, 2014. **10**(3).

17. Gewirtz, D.A., *Cytoprotective and nonprotective autophagy in cancer therapy.* Autophagy, 2013. **9**(9): p. 1263-5.

18. Barnard, R.A., et al., *Phase I clinical trial and pharmacodynamic evaluation of combination hydroxychloroquine and doxorubicin treatment in pet dogs treated for spontaneously occurring lymphoma.* Autophagy, 2014. **10**(8).

19. Rosenfeld, M.R., et al., *A phase I/II trial of hydroxychloroquine in conjunction with radiation therapy and concurrent and adjuvant temozolomide in patients with newly diagnosed glioblastoma multiforme.* Autophagy, 2014. **10**(8).

20. Rangwala, R., et al., *Phase I trial of hydroxychloroquine with dose-intense temozolomide in patients with advanced solid tumors and melanoma.* Autophagy, 2014. **10**(8).

21. Vogl, D.T., et al., *Combined autophagy and proteasome inhibition: A phase 1 trial of hydroxychloroquine and bortezomib in patients with relapsed/refractory myeloma.* Autophagy, 2014. **10**(8).

22. Rangwala, R., et al., *Combined MTOR and autophagy inhibition: Phase I trial of hydroxychloroquine and temsirolimus in patients with advanced solid tumors and melanoma.* Autophagy, 2014. **10**(8).

23. Mahalingam, D., et al., *Combined autophagy and HDAC inhibition: A phase I safety, tolerability, pharmacokinetic, and pharmacodynamic analysis of hydroxychloroquine in combination with the HDAC inhibitor vorinostat in patients with advanced solid tumors.* Autophagy, 2014. **10**(8).

24. Talmadge, J.E. and I.J. Fidler, *AACR centennial series: the biology of cancer metastasis: historical perspective.* Cancer Res, 2010. **70**(14): p. 5649-69.

25. Caino, M.C., et al., *Metabolic stress regulates cytoskeletal dynamics and metastasis of cancer cells.* J Clin Invest, 2013. **123**(7): p. 2907-20.

26. Tuloup-Minguez, V., et al., *Autophagy modulates cell migration and beta1 integrin membrane recycling.* Cell Cycle, 2013. **12**(20): p. 3317-28.

27. Fung, C., et al., *Induction of autophagy during extracellular matrix detachment promotes cell survival.* Mol Biol Cell, 2008. **19**(3): p. 797-806.

28. Avivar-Valderas, A., et al., *PERK integrates autophagy and oxidative stress responses to promote survival during extracellular matrix detachment.* Mol Cell Biol, 2011. **31**(17): p. 3616-29.

29. Guadamillas, M.C., A. Cerezo, and M.A. Del Pozo, *Overcoming anoikis--pathways to anchorage-independent growth in cancer.* J Cell Sci, 2011. **124**(Pt 19): p. 3189-97.

30. Macintosh, R.L., et al., *Inhibition of autophagy impairs tumor cell invasion in an organotypic model.* Cell Cycle, 2012. **11**(10): p. 2022-9.

31. Peng, Y.F., et al., *Promoting Colonization in Metastatic HCC Cells by Modulation of Autophagy.* PLoS One, 2013. **8**(9): p. e74407.

32. Peng, Y.F., et al., *Autophagy inhibition suppresses pulmonary metastasis of HCC in mice via impairing anoikis resistance and colonization of HCC cells.* Autophagy, 2013. **9**(12): p. 2056-68.

33. Bristol, M.L., et al., *Autophagy inhibition for chemosensitization and radiosensitization in cancer: do the preclinical data support this therapeutic strategy?* J Pharmacol Exp Ther, 2013. **344**(3): p. 544-52.

34. Ghadimi, M.P., et al., *Targeting the PI3K/mTOR axis, alone and in combination with autophagy blockade, for the treatment of malignant peripheral nerve sheath tumors.* Mol Cancer Ther, 2012. **11**(8): p. 1758-69.

35. Yan, J., et al., *Timing is critical for an effective anti-metastatic immunotherapy: the decisive role of IFNgamma/STAT1-mediated activation of autophagy.* PLoS One, 2011. **6**(9): p. e24705.

36. Asakura, K., et al., *The cytostatic effects of lovastatin on ACC-MESO-1 cells.* J Surg Res, 2011. **170**(2): p. e197-209.

37. Michaud, M., et al., *Autophagy-dependent anticancer immune responses induced by chemotherapeutic agents in mice.* Science, 2011. **334**(6062): p. 1573-7.

38. Ko, A., et al., *Autophagy inhibition radiosensitizes in vitro, yet reduces radioresponses in vivo due to deficient immunogenic signalling.* Cell Death Differ, 2013.

39. Pfaffl, M.W., *A new mathematical model for relative quantification in real-time RT-PCR.* Nucleic Acids Res, 2001. **29**(9): p. e45.

40. Chou, T.C. and P. Talalay, *Quantitative analysis of dose-effect relationships: the combined effects of multiple drugs or enzyme inhibitors.* Adv Enzyme Regul, 1984. **22**: p. 27-55.

41. Maycotte, P., et al., *STAT3-mediated autophagy dependence identifies subtypes of breast cancer where autophagy inhibition can be efficacious.* Cancer Res, 2014. **74**(9): p. 2579-90.

42. Solomon, V.R. and H. Lee, *Chloroquine and its analogs: a new promise of an old drug for effective and safe cancer therapies.* Eur J Pharmacol, 2009. **625**(1-3): p. 220-33.

43. Maes, H., et al., *Autophagy: shaping the tumor microenvironment and therapeutic response.* Trends Mol Med, 2013. **19**(7): p. 428-46.

44. Maycotte, P., et al., *Chloroquine sensitizes breast cancer cells to chemotherapy independent of autophagy.* Autophagy, 2012. **8**(2): p. 200-12.

45. Ni, H.M., et al., *Dissecting the dynamic turnover of GFP-LC3 in the autolysosome.* Autophagy, 2011. **7**(2): p. 188-204.

46. Liang, X.H., et al., *Beclin 1 contains a leucine-rich nuclear export signal that is required for its autophagy and tumor suppressor function.* Cancer Res, 2001. **61**(8): p. 3443-9.

47. Komatsu, M., et al., *Impairment of starvation-induced and constitutive autophagy in Atg7-deficient mice.* J Cell Biol, 2005. **169**(3): p. 425-34.

48. Mizushima, N. and T. Yoshimori, *How to interpret LC3 immunoblotting.* Autophagy, 2007. **3**(6): p. 542-5.

49. Aslakson, C.J. and F.R. Miller, *Selective events in the metastatic process defined by analysis of the sequential dissemination of subpopulations of a mouse mammary tumor.* Cancer Res, 1992. **52**(6): p. 1399-405.

50. Fidler, I.J., *Biological behavior of malignant melanoma cells correlated to their survival in vivo.* Cancer Res, 1975. **35**(1): p. 218-24.

51. Asai, T., et al., *Establishment and characterization of a murine osteosarcoma cell line (LM8) with high metastatic potential to the lung.* Int J Cancer, 1998. **76**(3): p. 418-22.

52. Ruggiero, A., et al., *Platinum compounds in children with cancer: toxicity and clinical management.* Anticancer Drugs, 2013. **24**(10): p. 1007-19.

53. Atallah, E. and L. Flaherty, *Treatment of metastatic malignant melanoma.* Curr Treat Options Oncol, 2005. **6**(3): p. 185-93.

54. Shamseddine, A.I. and F.S. Farhat, *Platinum-based compounds for the treatment of metastatic breast cancer.* Chemotherapy, 2011. **57**(6): p. 468-87.

55. Chen, P., M. Cescon, and P. Bonaldo, *Autophagy-mediated regulation of macrophages and its applications for cancer.* Autophagy, 2014. **10**(2): p. 192-200.

56. Li, Y., et al., *The vitamin E analogue alpha-TEA stimulates tumor autophagy and enhances antigen cross-presentation.* Cancer Res, 2012. **72**(14): p. 3535-45.

57. Schaeffer, V. and M. Goedert, *Stimulation of autophagy is neuroprotective in a mouse model of human tauopathy.* Autophagy, 2012. **8**(11): p. 1686-7.

58. Zhang, X., et al., *MTOR-independent, autophagic enhancer trehalose prolongs motor neuron survival and ameliorates the autophagic flux defect in a mouse model of amyotrophic lateral sclerosis.* Autophagy, 2014. **10**(4).

59. Sarkar, S., et al., *Trehalose, a novel mTOR-independent autophagy enhancer, accelerates the clearance of mutant huntingtin and alpha-synuclein.* J Biol Chem, 2007. **282**(8): p. 5641-52.

60. Kaplan, R.N., et al., *VEGFR1-positive haematopoietic bone marrow progenitors initiate the pre-metastatic niche.* Nature, 2005. **438**(7069): p. 820-7.

61. Itakura, E. and N. Mizushima, *Characterization of autophagosome formation site by a hierarchical analysis of mammalian Atg proteins.* Autophagy, 2010. **6**(6): p. 764-76.

62. Liu, J., et al., *Beclin1 controls the levels of p53 by regulating the deubiquitination activity of USP10 and USP13.* Cell, 2011. **147**(1): p. 223-34.

63. Kang, R., et al., *The Beclin 1 network regulates autophagy and apoptosis.* Cell Death Differ, 2011. **18**(4): p. 571-80.

64. Staskiewicz, L., et al., *Inhibiting autophagy by shRNA knockdown: Cautions and recommendations.* Autophagy, 2013. **9**(10).

65. Yang, Y.P., et al., *Application and interpretation of current autophagy inhibitors and activators.* Acta Pharmacol Sin, 2013. **34**(5): p. 625-35.

66. Xu, Y., et al., *Inhibition of autophagy enhances cisplatin cytotoxicity through endoplasmic reticulum stress in human cervical cancer cells.* Cancer Lett, 2012. **314**(2): p. 232-43.

67. Kaminskyy, V.O., et al., *Suppression of basal autophagy reduces lung cancer cell proliferation and enhances caspase-dependent and -independent apoptosis by stimulating ROS formation.* Autophagy, 2012. **8**(7): p. 1032-44.

68. Peinado, H., S. Lavotshkin, and D. Lyden, *The secreted factors responsible for pre-metastatic niche formation: old sayings and new thoughts.* Semin Cancer Biol, 2011. **21**(2): p. 139-46.

69. Herberg, S., et al., *Stromal cell-derived factor-1beta mediates cell survival through enhancing autophagy in bone marrow-derived mesenchymal stem cells.* PLoS One, 2013. **8**(3): p. e58207.

70. Wang, H.J., et al., *Autophagy in endothelial progenitor cells is cytoprotective in hypoxic conditions.* Am J Physiol Cell Physiol, 2013. **304**(7): p. C617-26.

Chapter Three

In silico approaches identify autophagy dependent cancer cell types and pathways

Summary

Autophagy is a highly conserved lysosomal degradation process that involves the recycling of the cell's own cytoplasmic material. Autophagy has been implicated as a mechanism of survival and resistance in cancer, but there is no definitive marker identifying autophagy dependent cancers. Recently, Stat3 activated triple negative breast cancers (TNBCs) had been found to be highly dependent on autophagy whereas other breast cancer types were not. We tested the efficacy of autophagy inhibitor chloroquine (CQ) in mouse xenograft models of TNBC, MDA-MB-231 and estrogen receptor positive breast cancer, MCF-7. CQ was able to significantly delay tumor progression in MDA-MB-231 cells. We then tested the relationship of autophagy dependence and Stat3 signaling in canine osteosarcoma cells. Unlike in breast cancer, CQ sensitivity did not correlate to Stat3 expression, but cells were still responsive to CQ treatment. To find effective therapies to combine with autophagy inhibition, we used gene expression and pathway analysis to discover pathways that had been altered after autophagy inhibition. We found a number of pathways that had been previously linked to autophagy in other cell types, including increased cholesterol synthesis. As inhibition of cholesterol

biosynthesis had not been explored in the context of canine osteosarcoma, we determined the sensitivity of the HMG-CoA reductase inhibitor, lovastin in the osteosarcoma cell lines. While single agent lovastatin was highly effective in osteosarcoma cells, the combination of CQ and lovastatin was less than additive. We confirmed that TNBCs are autophagy dependent and high levels of phospho-Stat3 may predict autophagy inhibition sensitivity, but this relationship may not apply in other cell types. We also identified pathways that may serve as synergistic targets to combine with autophagy inhibition, but will require further study.

Introduction

Autophagy is a catabolic process characterized by cellular self-digestion. The chief function of autophagy is turnover of the cytoplasm which results in the recycling and removal of damaged cellular components [1]. Autophagy is not a singular mechanism but rather multiple processes that ultimately end with lysosomal degradation of cytoplasmic material [2]. The most commonly studied and well-known form of autophagy is macroautophagy. In macroautophagy, (here after simply referred to as autophagy), cargo is trafficked via double-membraned vesicles called autophagosomes [2]. Dysregulation of this form of autophagy has been linked to a number of different disorders, including cancer [3]. Although autophagy's role in cancer development and progression is highly complex, there is a large body of evidence supporting autophagy as a tumor-protective mechanism [4]. Autophagy can sustain the high metabolic demand required for tumor growth and allow cells to withstand environmental stress such as hypoxia and nutrient depravation [5]. Inhibition of autophagy can reduce cellular proliferation and sensitize cells to

chemotherapy. However, sensitivity to autophagy inhibition or its effectiveness in combination with a specific therapy is not universal.

Oncogene driven cancers, specifically RAS and MYC, have elevated autophagic activity [6, 7]. RAS and MYC activated cancers also appear to require functional autophagy for tumorigenesis [8, 9]. Additionally, pancreatic cancers with high KRAS and MYC driven lymphoma respond to the autophagy inhibitor chloroquine (CQ) as a single agent [10, 11]. This data would seem to suggest then, that RAS and MYC activated cancers would be dependent on autophagy and ideal targets for autophagy inhibition. However, p53 mutational status may affect response. Combined loss of p53 and autophagy actually makes RAS driven cancers more tumorigenic [12]. p53 status can also influence the efficacy of the combination of autophagy inhibition and certain therapies like topotecan and 5-fluorouracil [13, 14]. Furthermore, KRAS activity, independent of p53 status, does not predict autophagy inhibition sensitivity in non-small cell lung cancer [15]. Therefore, RAS and MYC activation alone is not sufficient to identify autophagy dependent tumors. Treating cancer with autophagy inhibition indiscriminately is not without consequence. Loss of autophagy has been associated with resistance against EGFR and estrogen receptor targeted therapies [16, 17]. Autophagy also has immunomodulatory effects that may promote immune related cell death [18, 19]. More biomarkers indicative of autophagy dependence or cytoprotective induction are sorely needed.

In silico approaches have become an effective means to identify predictors of drug sensitivity or complementary pathways to target in a high-throughput manner. Two widely used mechanisms are synthetic lethal screens and micro-array based expression profiles. Synthetic lethal screens are used to identify pairs of genes or pathways required for viability [20]. Inhibiting either gene or pathway alone does not result in cell death while simultaneous loss of

function does. This screen is termed “synthetic” as it is not possible to isolate a cell with mutations in both as the cell would not be viable. Genetic inhibition is achieved using small interfering RNA (siRNA) or short hairpin RNA (shRNA). These types of RNA hybridize with complementary mRNA, targeting the mRNA for degradation and resulting in loss of protein expression. In large studies, the siRNA or shRNA can contain a barcode, which can be identified via sequencing. siRNAs or shRNAs that target essential genes will be lost as no viable cells can be harvested. The loss of siRNAs or shRNAs gives an indication as to secondary pathways a cell relies on once a former has been inhibited. The utility of the synthetic lethal approach identifies synergistic targets or pathways leading to acquired resistance.

Identifying alterations in gene expression profiles after treatment can also be used for pathway or biomarker discovery. Gene expression can be determined using microarray analysis. Pieces of DNA representing a single gene, referred to as probes, are spotted onto a chip, the microarray. RNA isolated from treated and untreated samples is fluorescently labeled and then allowed to hybridize with complementary probes. Signal strength corresponds to expression level. Differentially expressed genes between the two sample sets can then be compared. The Gene Set Enrichment Analysis (GSEA) algorithm can take the changes in gene expression and use that information to determine the overall change to a designated pathway, thus giving an indication of whether that pathway has been activated, turned off, or is unaffected after treatment. Pathways that have been upregulated could represent a cytoprotective response. Similar to pathways uncovered by synthetic lethal screens, targeting the newly identified pathway with the original therapy may lead to enhanced cell death. Microarray may be preferred over a synthetic lethal screen as large siRNA/shRNA libraries only exist for a few species whereas chips are available for a larger range of species.

Preliminary work by Dr. Paola Maycotte identified triple negative breast cancer cells (TNBCs) as autophagy addicted using an autophagy focused shRNA library. TNBCs are a subtype of breast cancer that lacks three receptors commonly activated in breast cancer, estrogen (ER), progesterone (PR) and HER2/Neu receptors [21]. TNBCs tend to have a much poorer prognosis than receptor positive breast cancers. She found that autophagy related shRNAs were generally not recovered in the TNBC cell lines, indicating dependence on autophagy, where as the hormone dependent cell lines could still survive without autophagy. She confirmed this differential sensitivity with Beclin-1 (BECN1) or Atg7 specific knockdown and CQ treatment. Signal transducer and activator of transcription 3 (Stat3) is constitutively activated in TNBC and regulates autophagy [22, 23]. She then tested the correlation of autophagy dependence and Stat3 activation, demonstrating that cells with activated Stat3 are more sensitive to autophagy inhibition *in vitro,* and is required for autophagy induction.

Under basal conditions, Stat3 resides in the cytoplasm [24]. Once activated by ctyokine or growth factor stimulation, Stat3 will be phosphorylated causing stabilization and dimerization. Activated Stat3 then translocates to the nucleus and promotes transcription of inflammatory response and cell survival genes. Stat3 has been shown to have a number of tumor promoting roles including induction of chronic inflammation, immune evasion, suppression of cell differentiation, cell cycle progression, and resistance to apoptosis [24]. Physiologic Stat3 represses autophagy, by sequestering protein kinase RNA-activated (PKR) [25]. PKR inhibits eukaryotic initiation factor 2α (eIF2α). Inhibition of eIF2α induces autophagy by promoting ATF4 expression, which regulates transcription of autophagy related genes. As oncogenic Stat3 is constitutively activated and located within the nucleus, autophagy can occur. Thus phosphorylated Stat3 may indicate active autophagy. There does appear to be autophagy related

Stat3 regulation. IFN-γ induction of Stat signaling requires functional autophagy [26]. Autophagy is also necessary for hypoxia induced phosphorylation of Stat3 [27]. Inhibition of autophagy and Stat3 signaling by RAGE ablation decreases tumorigenesis in pancreatic cancer [28]. Therefore, cancers with high Stat3 activity may also be dependent on autophagy.

A subset of canine osteosarcomas also have constitutively active Stat3. Canine osteosarcoma is the most common primary tumor of the skeleton in dogs [29]. The disease is highly metastatic, with 90% of patients presenting with micrometastasis at time of diagnosis. Survival rate is still very poor. Similarly in humans, 80% of patients are thought to have micrometastases at diagnosis, with only 20% of those with metastasis surviving beyond 5 years. Mutations common to both human and canine osteosarcoma include c-Myc amplification, Akt activation, and overexpression of Met. Thus findings in canine osteosarcoma are also relevant to human osteosarcoma. Recently, Cheryl London's group demonstrated that Stat3 is constitutively activated in both human and canine osteosarcoma [30], and yjay Stat3 inhibition could reduce cell growth. Thus, if the correlation of Stat3 activation and autophagy dependence exists in canine osteosarcoma as well, then autophagy inhibition may prove to be a novel approach to osteosarcoma treatment.

We therefore, tested the relationship between Stat3 activity and sensitivity to autophagy inhibition in two different tumor types, human breast cancer and canine osteosarcoma. Although these tumor types may be highly sensitive to autophagy inhibition, autophagy inhibition will not be clinically used as a monotherapy. Thus, synergistic drug combinations need to be identified as well. Changes in gene expression after autophagy inhibition could reveal pathways that, when simultaneously blocked, lead to increased cytotoxicity. Thus, we also used microarrary analysis to determine gene expression profiles of the two cancer types to determine pathways altered

upon autophagy inhibition. The results revealed a number of previously reported responses in other cancer types, but also upregulation of cholesterol synthesis. As inhibition of cholesterol production is a novel approach to osteosarcoma treatment, we tested the combination of statin inhibitor, lovastatin, and CQ in canine osteosarcoma cell lines.

Materials and Methods

Cell Lines and Cell Culture

The canine osteosarcoma cell lines Abrams, D17, Gracie, McKinley, Moresco, and Osa8 were validated as canine in origin and unique in April 2014 and used within 6 months after thawing. Cells were maintained in DMEM (Cellgro, Herndon, VA). Human breast cancer cell lines MDA-MB-231, MCF-7, MDA-MB-468, BT549, HCC1937, and T47D were received from Dr. Andrew Thorburn at University of Colorado School of Medicine, Aurora, CO. MDA-MB-231, MCF-7, MDA-MB-468, HCC1937, and T47D lines were validated October 2011 and BT549 May 2012. MDA-MB-231 and MDA-MB-468 were maintained in DMEM/F12 media (Cellgro, Herndon, VA), HCC1937, T47D, and BT549 in RPMI (Cellgro, Herndon, VA), and MCF-7 in MEM (Cellgro, Herndon, VA). T47D, BT549, and MCF-7 media was supplemented with insulin at 0.2 U/mL, 0.02 U/mL, and 0.6 U/mL (Life Technologies, Carlsbad, CA). All media was also supplemented with 10% fetal bovine serum (FBS) (Cellgro, Herndon, VA) and 5% penicillin+streptomycin (Hyclone Laboratories Inc, Logan, UT). Cells were incubated at 37°C and 5% CO_2.

Animal Studies

All animal studies were performed in accordance with the Colorado State University Animal Care and Use Committee. Female nude nu/nu mice were purchased from the National Cancer Institute (Frederick, MD) and challenged with 5 x 10^6 MDAMB231 cells. Female nude nu/nu mice were first ovari-ectomized and received a subcutaneous, 60 day release, 0.25-mg estradiol implant (Innovative Research). Mice were then challenged, 7 days later, with 5 x 10^6 MCF7 cells. Cells (100 uL) in 50% serum-free media and 50% Matrigel (BD Biosciences) were injected into the fourth mammary fat pad. Upon reaching a tumor volume of 100 mm^3, mice received either 60 mg/kg chloroquine diphosphate salt (CQ) or 0.9% saline given by intraperitoneal injection, once daily for the duration of the study. The study was followed until tumors reached four times their initial volume (TV*4, [31]

Proliferation Assays

Cells were seeded into a 96 well tissue culture plate in quadruplicates. A concentration of 2,000 cells per well was used for the osteosarcoma lines. Cells were allowed to attach for 24h then treated with CQ (Sigma, St. Louis, MO), Stattic (Sigma, St. Louis, MO), Lovastatin InSolution, (Merck Millipore, Damstadt Germany) or vehicle for 72 h at indicated concentrations. Proliferation was visualized by Alamar Blue (10% of 200 μg/mL rezazurin salt in PBS) and incubated for 2 h. Plates were read at 530/590 nm excitation/emission in a Synergy HT plate reader (BioTEK, Winooski, VT). All experiments were repeated in triplicate.

Measure of Synergy

The IC_{50} (Dm) value was determined as described in Chou and Talalay [32]. Drug combinations were then tested at 4x-0.25x the IC_{50} values The Bliss model of independence was used to determine if the combination was antagonistic, additive, or syngergistic, as detailed in (Bliss, 1939). Briefly, the additive effect for a drug is E_{xy} as predicted by the individual effect (fraction of affected cells) of each drug E_x and E_y. Thus E_{xy} is defined as $E_{xy} = (E_x + E_y) – (E_xE_y)$ for $0 < E < 1$. The ratio of the actual observed effect compared to the predicted effect was calculated. This value was used to determine combination efficacy, with < 0.8 as antagonistic, 0.8 – 1.2 as additive, and > 1.2 as synergistic.

Western Blot Analysis

Cells were lysed with a lysis buffer (0.01% Triton X-100, 150 mM NaCl, 10 mM Tris pH 7.5, 0.2 mM Na-Orthovanadate, 34.8 μg/mL PMSF, and 1x Protease Inhibitor Cocktail, [Roche, Indianapolis, IN]). The lysate was centrifuged at 14,000 rpm for 5 min at 4°C and supernatant collected. Protein was quantitated using a bicinchoninic acid (BCA) protein assay (Pierce, Rockford, IL). 40 μg of protein was used in SDS-PAGE and transferred onto PVDF membranes (Millipore, Billerica, MA). Blots were blocked in 5% BSA in Tris-buffered saline-Tween 20 for one hour at room temperature. Blots were probed with anti-LC3 (NB100-2220 Novus Biologicals, Littleton, CO) at 1:1000, anti-Stat3 (124H6, Cell Signaling Technologies, Danvers, MA) at 1:1000, anti-phospho-Stat3 (TYR 705) (D3A7, Cell Signaling Technologies, Danvers, MA) at 1:500, anti-Survivin (Novus Biologicals, Littleton, CO) at 1:1000, anti-actin at 1:5000 (A5441 Sigma, St. Louis, MO), or anti-tubulin at 1:5000 (T-5168 Sigma, St. Louis, MO) antibodies and incubated overnight at 4°C. Blots were incubated for one hour at room

temperature with either anti-rabbit (31460, Pierce, Rockford, IL) or anti-mouse (31430 Pierce, Rockford, IL) secondary antibodies conjugated to HRP at 1:5000. Blots were developed using West Dura (Pierce, Rockford, IL) and imaged in a ChemiDoc XRS^{+} (Bio Rad, Hercules, CA) using Image Labs version 3.0 software for analysis. Densitometry was measured using ImageJ64 and target protein was normalized to actin or tubulin.

Measuring Stat3 Activity

Stat3 activity was measured using a Stat3-luciferase reporter (Clontech kit 631915) transfected into canine osteosarcoma cell lines per manufacturer's instructions. Briefly, competent DH5a *E. coli* cells were transformed with pStat3-TA-luc or pTA-luc (control) vector and cultured. Plasmids were isolated using Midi-prep Kit (Qiagen, Venlo, Limburg). Osteosarcoma cells were plated in triplicate at 20,000 cells per well in a 96 well plate. Reaction mix of 100 ng of DNA and Mirus Transfection reagent (1:3 DNA) (MirusBio), diluted in OptiMEM media (Life Technologies, Carlsbad, CA) was used to transfect cells. Cells were incubated overnight. The following day, cells were then treated with 1 uM Stattic or 10 uM CQ for 24 h. Cells were then lysed and luciferase expression measured using the Dual-glo luciferase assay (Promega) and read in Syngergy HT plate reader (BioTEK, Winooski, VT). Stat3 activity was expressed as mean percentage of luciferase signal above control.

Microarray Analysis

Cells were treated with 20 uM hydroxycholorquine (HCQ) for 24 h. RNA was harvested using RNeasy kit (Qiagen, Venlo, Limburg). RNA was then sent to the University of Colorado's Functional Genomics Core for processing and microarray analysis. Chips used were Affymetrix Canine 2.0 and Human UG133 Plus (Affymetrix). Gene expression, normalized using RMA, was

uploaded to Pathway Studio. Expression data was mapped using Gene Symbol. Altered pathways were discovered using GSEA as performed by Pathway Studio (Elseiver) on all of Pathway Studio's collection of pathways.

Results

Autophagy dependent triple negative breast cancer cells with activated Stat3 respond to chloroquine in vivo

Dr. Maycotte identified TNBC cells expressing high levels of phospho-Stat3 as particularly dependent on autophagy compared to ER+ cells, which do not express active Stat3. To determine if this differential sensitivity existed *in vivo*, orthotopic mouse xenograft studies were performed with an autophagy dependent, MDA-MB-231, and autophagy independent, MCF-7, cell line. Mice were treated with 60 mg/kg daily i.p. CQ once tumors reached 100 mm^3. Mice were followed until tumors reached 4 times their starting volume (TV*4). CQ was able to significantly delay the time to reach TV*4 in MDA-MB-231 cells ($p= 0.0218$), but not in MCF-7 ($p = 0.4426$) (Fig. 3.1). This suggests then that not all cell lines will respond to autophagy inhibition, but *in vitro* identification of autophagy dependent cells may predict *in vivo* sensitivity.

A subset of canine osteosarcoma has constitutive Stat3 activity

Dr Maycotte also demonstrated a correlation between constitutively activated Stat3 and autophagy dependence. The TNBC cells expressed phospho-Stat3 under basal conditions whereas other breast cancer types did not. She also showed that autophagy could regulate Stat3.

Autophagy inhibition decreased phospho-Stat3 and sensitivity to a Stat3 inhibitor, Stattic. Osteosarcoma has also been reported to have constitutively active Stat3 and Stat3 inhibitors can

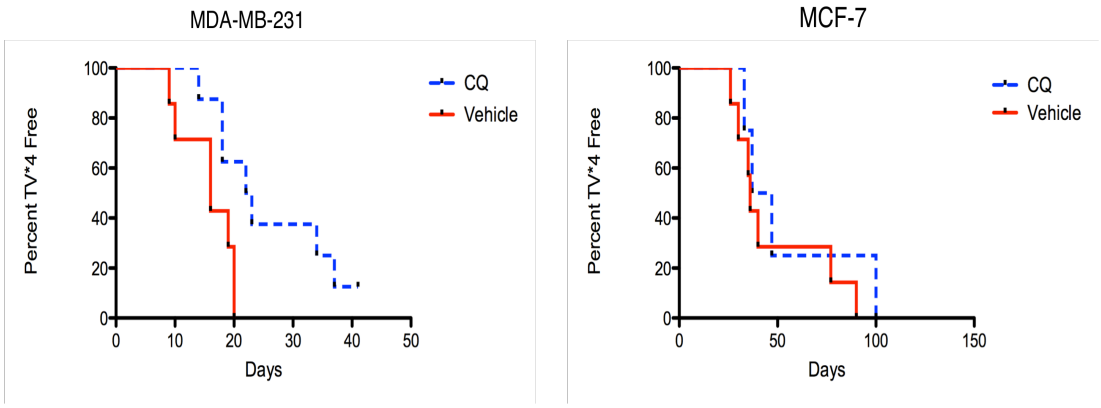

Figure 3.1 CQ slows tumor growth in TNBC. Female nu/nu mice were injected with 5 x10^6 MDAMB231 or MCF7 cells into the fourth mammary fat pad. Upon reaching a tumor volume of 100 mm^3, mice were treated with chloroquine (60 mg/kg/d) or 0.9% saline, intraperitoneally. Data are presented as time to reach four times initial volume (TV4). Logrank (Mantel–Cox) analysis of the curves shows significant difference for the MDAMB231 tumors (p = 0.0218) and no significant

reduce cellular proliferation. Therefore, we measured phospho-Stat3 expression in our canine osteosarcoma cell lines, Abrams, D17, Gracie, MacKinley, Moresco, and Osa8. Abrams, D17,

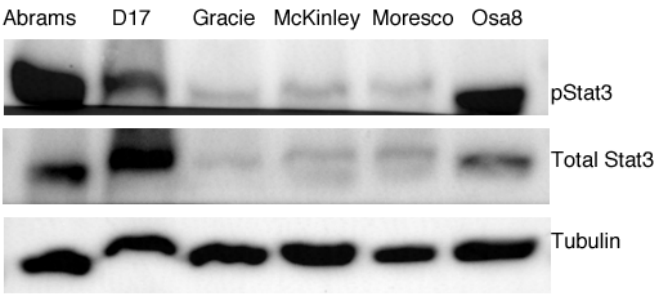

Figure 3.2 Stat3 expression in canine osteosarcoma cell lines. Western blot analysis of basal Stat3 expression shows that Abrams, D17, and Osa8 have activated Stat3 evidenced by phospho-Stat3 expression.

and Osa8 lines had high levels of phospho-Stat3 while Gracie, MacKinley, and Moresco did not (Fig 3.2).

To measure Stat3 activity, cells were transfected with a luciferase reporter under the control of a Stat3 promoter. Luciferase expression was higher in the D17 and Osa8 lines compared to the Moresco and MacKinley lines and adding a Stat3 inhibitor, Stattic, was able to correspondingly reduce expression, except in the Moresco cell line (Fig 3.3). Interestingly, CQ could also decrease expression in the Stat3 activated lines D17 and Osa8.

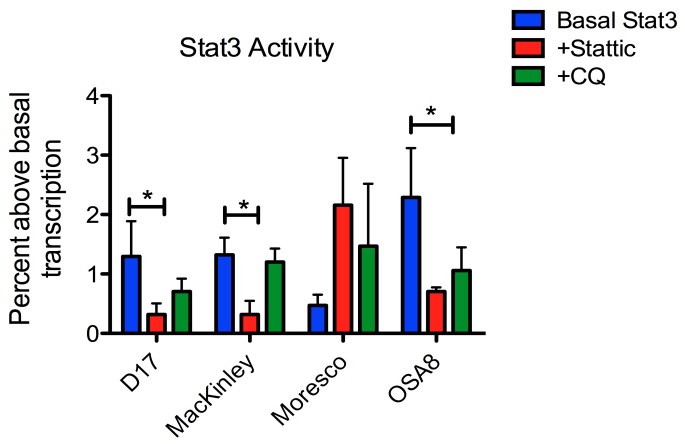

Figure 3.3 Stat3 activity in canine osteosarcoma cell lines. Cells were transfected with a Stat3 or a control, basal transcription luciferase reporter in triplicate and then treated with either 1 uM Stattic or 10 uM CQ for 24h. Luciferase expression was used as a measure for Stat3 activity. Data is expressed as percent above the average luciferase expression for basal transcription. Error bars represent standard deviation. Cell lines that had phospho-Stat3 expression also had greater Stat3 activity. Stat3 inhibitor, Stattic ccould reduce Stat3 activity for most cell lines. CQ also reduced Stat3 acitvity in Stat3 activated lines.

Stat3 activity does not correlate to sensitivity in canine osteosarcoma

As phospho-Stat3 expression predicted autophagy sensitivity in breast cancer cells, we determined the IC_{50} for CQ in the canine osteosarcoma lines. Cell lines with constitutively activated Stat3 were equally sensitive to CQ than those that did not have active Stat3 (Fig 3.4).

The CQ IC_{50} was higher than the confirmed autophagy dependent MDA-MB-231 cells, but lower than the autophagy independent MCF-7s. This may suggest that the canine osteosarcoma cells are only moderately dependent on autophagy.

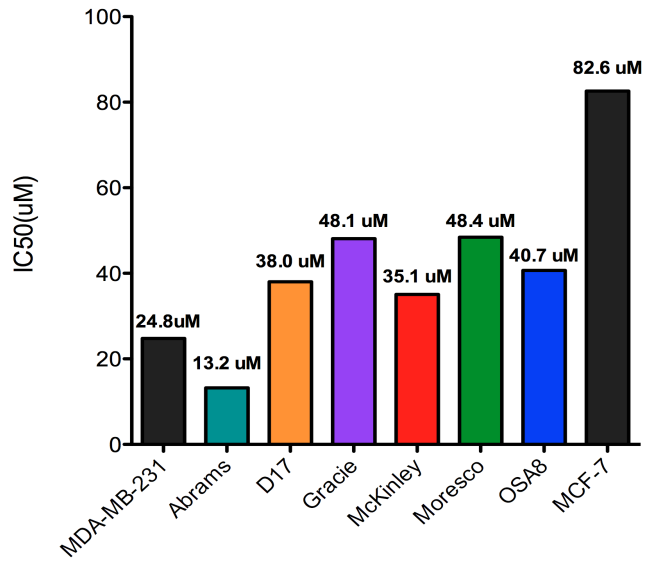

Figure 3.4 Stat3 activation does not predict CQ sensitivity. The IC_{50} was calculated using the Chou and Talalay method for the six osteosarcoma, autophagy dependent TNBC MDA-MB-231, and autophagy independent ER+ MCF7 cell lines. Stat3 activated osteosarcoma lines were no more sensitive to CQ than non-activated lines. The IC_{50}s of the osteosarcoma fell in between the autophagy

Surprisingly, Stat3 activity did not predict sensitivity to Stattic either (Fig 3.5). The MDA-MB-231 cells were also more sensitive to Stattic than the osteosarcoma cells. Though the addition of CQ did not reduce Stattic efficacy, the combination was less than additive (Fig 3.6). Even though some osteosarcoma lines have activated Stat3, they may not be particularly dependent on Stat3 signaling and therefore not especially dependent on autophagy either.

Pathway analysis reveals pathways altered upon HCQ treatment

Although no differential sensitivity to autophagy inhibition existed between the canine osteosarcoma lines, all six cell lines still responded to CQ treatment. Osteosarcoma still carries a poor prognosis and more treatment options are needed. Therefore, we may be able to identify

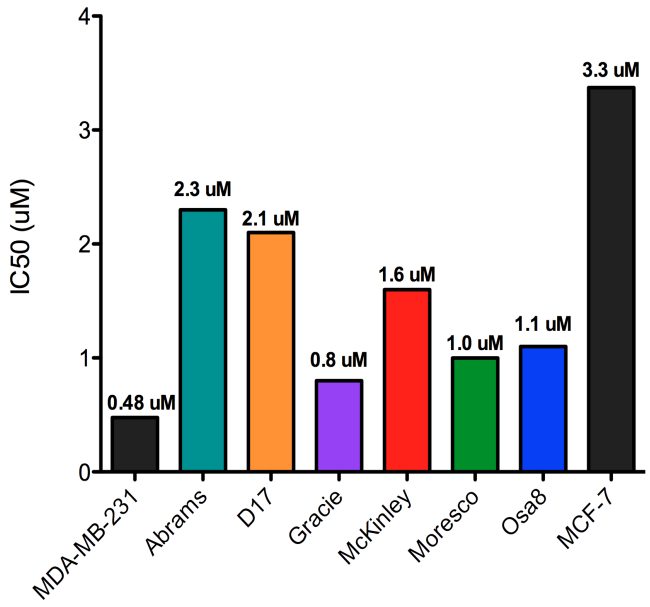

Figure 3.5 Stat3 inhibitor, Stattic, sensitivity. The IC_{50} was calculated using the Chou and Talalay method for the six osteosarcoma, autophagy dependent TNBC MDA-MB-231, and autophagy independent ER+ MCF7 cell lines. No differential sensitivity was observed between Stat3 activated and non-activated osteosarcoma cell lines, unlike in human breast cancer lines.

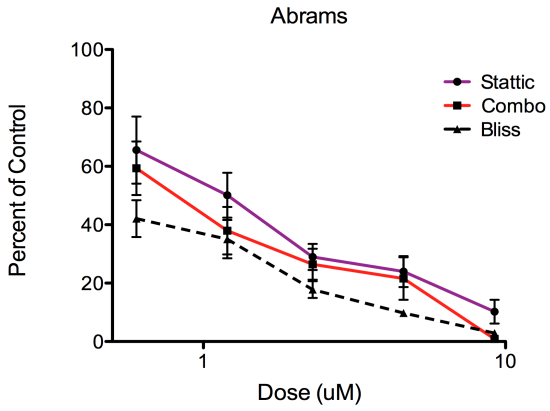

Figure 3.6 Combination of CQ and Stattic is not additive. Representative dose curves of Stattic and the combination with CQ. Dotted line represents theoretical Bliss curve for additivity. Experiments were repeated in triplicate. Dose is represented in log scale. Error bars represent standard deviation.

particularly efficacious drug combinations with autophagy inhibition. In addition, though TNBC appear very sensitive to autophagy inhibition, combination therapy will also be necessary. Thus we used microarray analysis followed by GSEA performed by Pathway Studio to discover pathways that have been upregulated after autophagy inhibition. The six canine osteosarcoma cell lines and six human breast cancer lines (MDA-MB-231, MDA-MB-468, MCF-7, BT549, T47D, and HCC1937) were treated for 24h with 20 uM hydroxycholoroqine (HCQ), a derivative of CQ that is currently being used in clinical trials. RNA was harvested and used for microarray analysis. Pathway studio returned a number of different pathways, most of which had been shown to be connected to autophagy or CQ treatment in other cell types. The most relevant ones are summarized in Tables 3.1 and 3.2.

Table 3.1 Pathways upregulated in canine osteosarcoma after autophagy inhibition

Pathway	Citation	Median Change	p-value
Biosynthesis of Cholesterol	Yang 2010 [36], Araki 2012 [37], Misirkic 2012 [38], Thurnher 2012 [39]	1.47	3.01 E-8
Notch	Maes 2014 [44], Perez 2014 [45]	1.01	3.64 E-4
Histone Acetylation	Gammoh 2012 [54], Fullgrabe 2013 [55], Mahalingam 2014 [56]	1.04	1.2 E-3
Hedgehog	Balic, 2014 [57], Wang 2014 [58]	1.02	9.9 E-3
DNA Repair	Botrungo 2012 [59], Fang 2014 [60], Chen 2015 [61]	1.05	2.6 E-2

Table 3.2 Pathways upregulated in human breast cancer after autophagy inhibition

Pathway	Citation	Median Change	p-value
AP-1/ CREB Signaling	Carloni 2010 [33] Seok 2014 [34], Yogev 2010 [35]	1.02-1.06	3.22 E-5 - 9.2 E-4
Biosynthesis of Cholesterol	Yang 2010 [36], Araki 2012 [37], Misirkic 2012 [38], Thurnher 2012 [39]	1.2	1.14 E-4
ER Stress	Gills 2007 [40], Thomas, 2012 [41] Dey 2013 [7]	1.1	1.41 E-11
Insulin Action	Grokvic 2013 [42], Geng 2014 [43]	1.05	2.01 E-16
Notch	Maes 2014 [44], Perez 2014 [45]	1.03	1.89 E-5
Protein Degradation	Milani 2009 [46], Zhu 2010, Kao 2014 [47], Vogl 2014 [48]	1.05	5.48 E-6
Response to Oxidative Stress	Kang 2011 [49], Hah 2012 [50], Dutta 2013 [51], Hollomon 2013 [52], Li 2014 [53]	1.07	6.22 E-6

One pathway that has only been recently connected to cancer and autophagy inhibition was cholesterol synthesis. Statin inhibitors have been shown to have some efficacy in a number of different cancer types, are widely available, and have few side effects [62, 63]. Therefore we tested the combination of CQ and lovastatin. We found that, as a single agent, the osteosarcoma cells were sensitive to lovastatin (Fig 3.7). However, the addition of CQ appeared to abrogate lovastatin efficacy, as there was no enhanced cell death (Fig 3.8). Although pathway analysis indicated increased cholesterol synthesis was increased after autophagy inhibition, and cells did respond to a statin inhibitor, the combination was not successful.

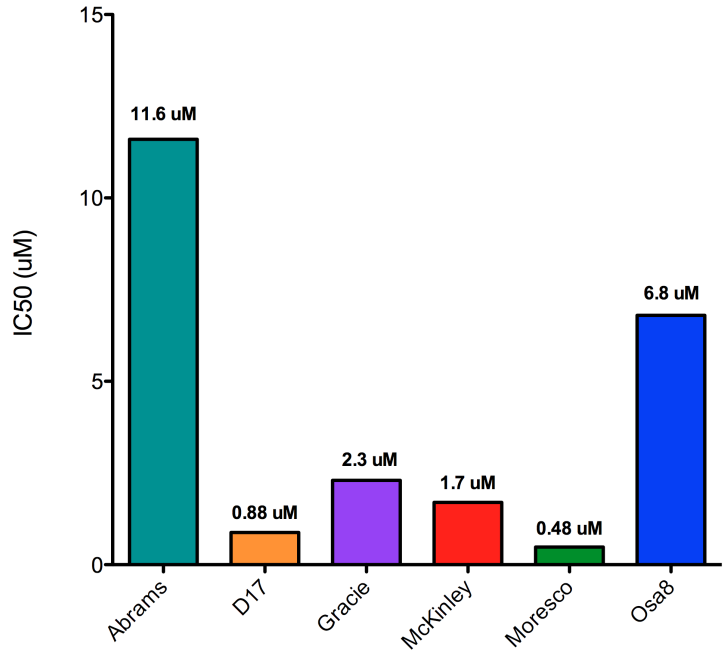

Figure 3.7 Osteosarcoma sensitivity to lovastatin. Cholesterol biosynthesis was upregulated after autophagy inhibition. Therefore, the IC_{50} for single agent statin inhibitor, lovastatin was determined in the osteosarcoma cells using the Chou and Talalay method.

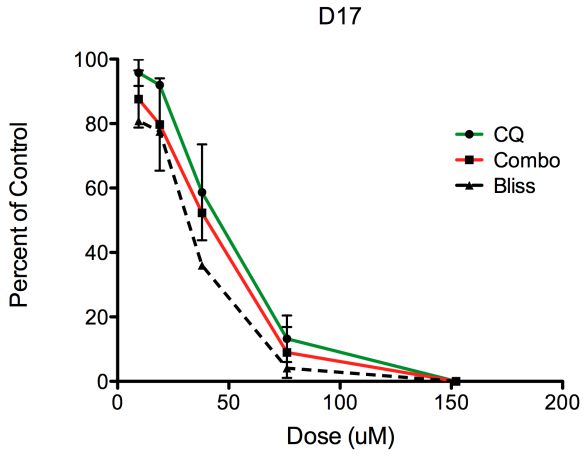

Figure 3.8 The combination CQ and lovastatin is not effective. Representative dose curves of CQ and the combination with lovastatin. Dotted line represents theoretical Bliss curve for additivity. Experiments were repeated in triplicate. Error bars represent standard deviation.

Discussion

Autophagy has been recognized as a mechanism for tumor survival and therapy resistance. However, not all types of cancer may respond or all therapies work effectively with autophagy inhibition. Therefore, more biomarkers are needed to identify autophagy dependent tumor types as well as potential therapies that can work synergistically in combination with autophagy inhibition. Dr. Maycotte had recently demonstrated that TNBCs were highly sensitive to autophagy inhibition whereas other types of breast cancer were not. Therefore we tested the *in vivo* efficacy of CQ in xenograft models of TNBC, MDA-MB-231 cells and ER+ breast cancer, MCF-7 cells. As in culture, the different tumor types maintained their differential sensitivity. CQ was able to delay tumor progression only in the TNBC. Taken with Dr. Maycotte's *in vitro* data, this study demonstrates that autophagy inhibition will not be a particularly effective therapy for all breast cancers. However, autophagy dependent or "addicted" cell types may be discovered through the method used by Dr. Maycotte, an autophagy focused shRNA screen. Additionally, cells found to be dependent on autophagy in culture may be predictive of sensitivity *in vivo.* This work also has implications for TNBC therapy as this subtype of breast cancer carries the worst prognosis and there are no targeted therapies currently available. Autophagy inhibition could function as a chemosensitizer and enhance efficacy in this therapy-resistant tumor type.

The highly autophagy dependent TNBC were also found to have constitutive activation of Stat3 where the autophagy independent cells did not. Stat3 was able to regulate autophagy induction specifically in the TNBC. Canine osteosarcoma is another tumor type that can have constitutive Stat3 activation and has poor survival. Thus we determined if there was a correlation between autophagy inhibition sensitivity and phospho-Stat3 expression in canine osteosarcoma as there was in human breast cancer. Alhough all of the osteosarcoma cells did respond to CQ

treatment, Stat3 activity was not predictive of CQ sensitivity. All of the six cell lines tested had roughly the same IC_{50}. The same was true, however, with Stat3 inhibitor Stattic. This suggests that the osteosarcoma cells may not actually be dependent on Stat3 and therefore only moderately dependent on autophagy as the IC_{50} values fall between the highly dependent MDA-MB-231 and independent MCF-7. One explanation for why all six osteosarcoma cell lines responded to Stattic inhibition similarly is cross-specificity with Stat1 [64]. Some Stat3 inhibitors like Stattic target the Src homology 2 (SH2) domain, which interacts with the phosphotyrosine motifs regulating receptor binding and dimerization. SH2 domains are found on all Stat family members. Stattic and other SH2 domain based competitive inhibitors appear equally effective at blocking Stat1. Therefore the observed growth inhibition could also be due to Stat1 inhibition. Despite this, if cells were truly dependent on Stat3, there should be differential sensitivity as observed in the breast cancer cells. Therefore, Stat3 phosphorylation alone may not be sufficient to predict autophagy dependence in all tumor types. Although Stat3 dependence may still indicate a dependence on autophagy as well, Stat3 activity alone does not seem to predict Stat3 reliance and this relationship will still require empirical determination.

Even autophagy dependent tumors will still progress, as the MDA-MB-231 tumors eventually did. Thus, combination therapy will still be required. Although the osteosarcoma cells were not as sensitive to autophagy inhibition as the TNBC cells, they still responded to treatment and there exists very little therapy options. Therefore, we tried to identify pathways that had been upregulated after HCQ treatment in order to find targets that could lead to synergistic drug combinations in human breast cancer and canine osteosarcoma. Using pathway analysis, we found similar responses despite being two different tumor types and species. Of note, DNA repair, DNA acetylation, proteasome degradation, ER stress, and cholesterol synthesis were

upregulated. All of these pathways have been connected with autophagy inhibition and cancer previously, however, cholesterol inhibition as an anti-cancer therapy has been a more recent development. Additionally, it has not been tested in canine osteosarcoma. Therefore, we first tested the statin inhibitor, lovastatin, in combination with CQ. Osteosarcoma cells were sensitive to lovastatin. Yet, the combination was less than additive. It appeared that by inhibiting autophagy, lovastatin no longer had any effect. It has been reported that autophagy is induced upon cholesterol inhibition, but the results are conflicting whether autophagy is cytoprotective or cytotoxic [36-39]. In some instances, autophagy inhibition potentiates statin inhibitor efficacy, but in others, functional autophagy is required for cell death. In the case of osteosarcoma cells, autophagy appears to have the latter function. As to why autophagy inhibition increased the cholesterol synthesis pathway, autophagy has been shown to regulate lipid homeostasis, and the inhibition of autophagy can lead to accumulation of cholesterol in lipid droplets and lysosomes and prevent its breakdown [65]. The sequestration of cholesterol may create a false sense of lipid depravation stimulating cholesterol synthesis [66].

As the lovastatin combination studies demonstrate, the microarray and pathway analysis approach requires careful pathway selection and some trial and error. While synthetic lethal screens may yield more definitive pathway connections, there shRNA libraries do not exist for the canine. Therefore, microarray is the only high throughput option. Additionally, as autophagy inhibition on its own is lethal in TNBC cells, the synthetic lethal screen would not work. The pathway analysis did return a number of other pathways that have been shown to be good targets to block in combination with autophagy inhibition in other cell types. For example, proteasome degradation was increased after HCQ treatment. TNBC cells also appear to be dependent on proteasome degradation [67]. Autophagy has been shown to protect breast cancer cells against

proteasome inhibitor bortezomib and the combination of HCQ and bortezomib is currently being investigated in clinical trials for the treatment of multiple myeloma [46, 48]. Additionally, autophagy inhibition can also work synergistically with histone deacetylase inhibitors (HDACs) like voronistat and this combination is also being explored in clinical trials [54, 56]. HDAC inhibitors were found to elicit some growth inhibition in canine osteosarcoma cells and can safely be administered to dogs [68]. Therefore, targeting these other pathways may prove successful.

Conclusions

We confirmed that TNBC cells are sensitive to autophagy inhibition by CQ *in vivo*. These cells are also dependent on Stat3 signaling and have high expression of phospho-Stat3. For TNBC, phospho-Stat3 expression could be a used as a predictive marker for autophagy dependence. However, this may not apply to all cancer types as Stat3 activated canine osteosarcoma cells were only moderately responsive to CQ. We also identified pathways that, while not exactly novel, have not been tested in combination with autophagy inhibition and TNBC or canine osteosarcoma at this time. We did test the combination of statin inhibitor, lovastatin, and CQ in the osteosarcoma cells, yet found it to be unsuccessful. However, lovastatin on its own was highly effective against canine osteosarcoma cells and may be worth pursuing in future studies. In summary, autophagy inhibition will be most useful in only specific types of cancer and thorough study is needed before combining it with other therapies.

References

1. Klionsky, D.J., et al., *A comprehensive glossary of autophagy-related molecules and processes (2nd edition).* Autophagy, 2011. **7**(11): p. 1273-94.

2. Cuervo, A.M., *Autophagy: many paths to the same end.* Mol Cell Biochem, 2004. **263**(1-2): p. 55-72.

3. Murrow, L. and J. Debnath, *Autophagy as a stress-response and quality-control mechanism: implications for cell injury and human disease.* Annu Rev Pathol, 2013. **8**: p. 105-37.

4. Thorburn, A., D.H. Thamm, and D.L. Gustafson, *Autophagy and cancer therapy.* Mol Pharmacol, 2014. **85**(6): p. 830-8.

5. Kroemer, G., G. Marino, and B. Levine, *Autophagy and the integrated stress response.* Mol Cell, 2010. **40**(2): p. 280-93.

6. White, E., *Exploiting the bad eating habits of Ras-driven cancers.* Genes Dev, 2013. **27**(19): p. 2065-71.

7. Dey, S., F. Tameire, and C. Koumenis, *PERK-ing up autophagy during MYC-induced tumorigenesis.* Autophagy, 2013. **9**(4): p. 612-4.

8. Hart, L.S., et al., *ER stress-mediated autophagy promotes Myc-dependent transformation and tumor growth.* J Clin Invest, 2012. **122**(12): p. 4621-34.

9. Guo, J.Y., et al., *Activated Ras requires autophagy to maintain oxidative metabolism and tumorigenesis.* Genes Dev, 2011. **25**(5): p. 460-70.

10. Yang, S., et al., *Pancreatic cancers require autophagy for tumor growth.* Genes Dev, 2011. **25**(7): p. 717-29.

11. Amaravadi, R.K., et al., *Autophagy inhibition enhances therapy-induced apoptosis in a Myc-induced model of lymphoma.* J Clin Invest, 2007. **117**(2): p. 326-36.

12. Rosenfeldt, M.T., et al., *p53 status determines the role of autophagy in pancreatic tumour development.* Nature, 2013. **504**(7479): p. 296-300.

13. Li, D.D., et al., *The inhibition of autophagy sensitises colon cancer cells with wild-type p53 but not mutant p53 to topotecan treatment.* PLoS One, 2012. **7**(9): p. e45058.

14. Yang, B., et al., *Wild-type p53 protein potentiates cytotoxicity of therapeutic agents in human colon cancer cells.* Clin Cancer Res, 1996. **2**(10): p. 1649-57.

15. Morgan, M.J., et al., *Regulation of autophagy and chloroquine sensitivity by oncogenic RAS in vitro is context-dependent.* Autophagy, 2014. **10**(10): p. 1814-26.

16. Wei, Y., et al., *EGFR-mediated Beclin 1 phosphorylation in autophagy suppression, tumor progression, and tumor chemoresistance.* Cell, 2013. **154**(6): p. 1269-84.

17. Gonzalez-Malerva, L., et al., *High-throughput ectopic expression screen for tamoxifen resistance identifies an atypical kinase that blocks autophagy.* Proc Natl Acad Sci U S A, 2011. **108**(5): p. 2058-63.

18. Ko, A., et al., *Autophagy inhibition radiosensitizes in vitro, yet reduces radioresponses in vivo due to deficient immunogenic signalling.* Cell Death Differ, 2014. **21**(1): p. 92-9.

19. Michaud, M., et al., *Autophagy-dependent anticancer immune responses induced by chemotherapeutic agents in mice.* Science, 2011. **334**(6062): p. 1573-7.

20. Chan, D.A. and A.J. Giaccia, *Harnessing synthetic lethal interactions in anticancer drug discovery.* Nat Rev Drug Discov, 2011. **10**(5): p. 351-64.

21. Macintosh, R.L., et al., *Inhibition of autophagy impairs tumor cell invasion in an organotypic model.* Cell Cycle, 2012. **11**(10): p. 2022-9.

22. Garcia, R., et al., *Constitutive activation of Stat3 by the Src and JAK tyrosine kinases participates in growth regulation of human breast carcinoma cells.* Oncogene, 2001. **20**(20): p. 2499-513.

23. Pietrocola, F., et al., *Regulation of autophagy by stress-responsive transcription factors.* Semin Cancer Biol, 2013. **23**(5): p. 310-22.

24. Yu, H., et al., *Revisiting STAT3 signalling in cancer: new and unexpected biological functions.* Nat Rev Cancer, 2014. **14**(11): p. 736-46.

25. Shen, S., et al., *Cytoplasmic STAT3 represses autophagy by inhibiting PKR activity.* Mol Cell, 2012. **48**(5): p. 667-80.

26. Chang, Y.P., et al., *Autophagy facilitates IFN-gamma-induced Jak2-STAT1 activation and cellular inflammation.* J Biol Chem, 2010. **285**(37): p. 28715-22.

27. Noman, M.Z., et al., *Blocking hypoxia-induced autophagy in tumors restores cytotoxic T-cell activity and promotes regression.* Cancer Res, 2011. **71**(18): p. 5976-86.

28. Kang, R., et al., *The expression of the receptor for advanced glycation endproducts (RAGE) is permissive for early pancreatic neoplasia.* Proc Natl Acad Sci U S A, 2012. **109**(18): p. 7031-6.

29. Mueller, F., B. Fuchs, and B. Kaser-Hotz, *Comparative biology of human and canine osteosarcoma.* Anticancer Res, 2007. **27**(1a): p. 155-64.

30. Fossey, S.L., et al., *Characterization of STAT3 activation and expression in canine and human osteosarcoma.* BMC Cancer, 2009. **9**: p. 81.

31. Teicher, B., in *Tumor models in cancer research*, B. Teicher, Editor. 2002, Humana Press: Totowa, NJ. p. 593-616.

32. Chou, T.C. and P. Talalay, *Quantitative analysis of dose-effect relationships: the combined effects of multiple drugs or enzyme inhibitors.* Adv Enzyme Regul, 1984. **22**: p. 27-55.

33. Carloni, S., et al., *Activation of autophagy and Akt/CREB signaling play an equivalent role in the neuroprotective effect of rapamycin in neonatal hypoxia-ischemia.* Autophagy, 2010. **6**(3): p. 366-77.

34. Seok, S., et al., *Transcriptional regulation of autophagy by an FXR-CREB axis.* Nature, 2014. **516**(7529): p. 108-11.

35. Yogev, O., et al., *Jun proteins are starvation-regulated inhibitors of autophagy.* Cancer Res, 2010. **70**(6): p. 2318-27.

36. Yang, P.M., et al., *Inhibition of autophagy enhances anticancer effects of atorvastatin in digestive malignancies.* Cancer Res, 2010. **70**(19): p. 7699-709.

37. Araki, M., M. Maeda, and K. Motojima, *Hydrophobic statins induce autophagy and cell death in human rhabdomyosarcoma cells by depleting geranylgeranyl diphosphate.* Eur J Pharmacol, 2012. **674**(2-3): p. 95-103.

38. Misirkic, M., et al., *Inhibition of AMPK-dependent autophagy enhances in vitro antiglioma effect of simvastatin.* Pharmacol Res, 2012. **65**(1): p. 111-9.

39. Thurnher, M., O. Nussbaumer, and G. Gruenbacher, *Novel aspects of mevalonate pathway inhibitors as antitumor agents.* Clin Cancer Res, 2012. **18**(13): p. 3524-31.

40. Gills, J.J., et al., *Nelfinavir, A lead HIV protease inhibitor, is a broad-spectrum, anticancer agent that induces endoplasmic reticulum stress, autophagy, and apoptosis in vitro and in vivo.* Clin Cancer Res, 2007. **13**(17): p. 5183-94.

41. Thomas, S., et al., *Preferential killing of triple-negative breast cancer cells in vitro and in vivo when pharmacological aggravators of endoplasmic reticulum stress are combined with autophagy inhibitors.* Cancer Lett, 2012. **325**(1): p. 63-71.

42. Grkovic, S., et al., *IGFBP-3 binds GRP78, stimulates autophagy and promotes the survival of breast cancer cells exposed to adverse microenvironments.* Oncogene, 2013. **32**(19): p. 2412-20.

43. Geng, Y., et al., *Insulin receptor substrate 1/2 (IRS1/2) regulates Wnt/beta-catenin signaling through blocking autophagic degradation of dishevelled2.* J Biol Chem, 2014. **289**(16): p. 11230-41.

44. Maes, H., et al., *Tumor vessel normalization by chloroquine independent of autophagy.* Cancer Cell, 2014. **26**(2): p. 190-206.

45. Perez, E., et al., *Autophagy regulates tissue overgrowth in a context-dependent manner.* Oncogene, 2014. **0**.

46. Milani, M., et al., *The role of ATF4 stabilization and autophagy in resistance of breast cancer cells treated with Bortezomib.* Cancer Res, 2009. **69**(10): p. 4415-23.

47. Kao, C., et al., *Bortezomib enhances cancer cell death by blocking the autophagic flux through stimulating ERK phosphorylation.* Cell Death Dis, 2014. **5**: p. e1510.

48. Vogl, D.T., et al., *Combined autophagy and proteasome inhibition: a phase 1 trial of hydroxychloroquine and bortezomib in patients with relapsed/refractory myeloma.* Autophagy, 2014. **10**(8): p. 1380-90.

49. Kang, R., et al., *HMGB1 as an autophagy sensor in oxidative stress.* Autophagy, 2011. **7**(8): p. 904-6.

50. Hah, Y.S., et al., *Cathepsin D inhibits oxidative stress-induced cell death via activation of autophagy in cancer cells.* Cancer Lett, 2012. **323**(2): p. 208-14.

51. Dutta, D., et al., *Upregulated autophagy protects cardiomyocytes from oxidative stress-induced toxicity.* Autophagy, 2013. **9**(3): p. 328-44.

52. Hollomon, M.G., et al., *Knockdown of autophagy-related protein 5, ATG5, decreases oxidative stress and has an opposing effect on camptothecin-induced cytotoxicity in osteosarcoma cells.* BMC Cancer, 2013. **13**: p. 500.

53. Li, J., et al., *Synthetic lethality of combined glutaminase and Hsp90 inhibition in mTORC1-driven tumor cells.* Proc Natl Acad Sci U S A, 2014.

54. Gammoh, N., P.A. Marks, and X. Jiang, *Curbing autophagy and histone deacetylases to kill cancer cells.* Autophagy, 2012. **8**(10): p. 1521-2.

55. Fullgrabe, J., D.J. Klionsky, and B. Joseph, *Histone post-translational modifications regulate autophagy flux and outcome.* Autophagy, 2013. **9**(10): p. 1621-3.

56. Mahalingam, D., et al., *Combined autophagy and HDAC inhibition: a phase I safety, tolerability, pharmacokinetic, and pharmacodynamic analysis of hydroxychloroquine in combination with the HDAC inhibitor vorinostat in patients with advanced solid tumors.* Autophagy, 2014. **10**(8): p. 1403-14.

57. Balic, A., et al., *Chloroquine targets pancreatic cancer stem cells via inhibition of CXCR4 and hedgehog signaling.* Mol Cancer Ther, 2014. **13**(7): p. 1758-71.

58. Wang, J., et al., *Inhibition of autophagy potentiates the efficacy of Gli inhibitor GANT-61 in MYCN-amplified neuroblastoma cells.* BMC Cancer, 2014. **14**: p. 768.

59. Botrugno, O.A., et al., *Molecular pathways: old drugs define new pathways: non-histone acetylation at the crossroads of the DNA damage response and autophagy.* Clin Cancer Res, 2012. **18**(9): p. 2436-42.

60. Fang, E.F., et al., *Defective mitophagy in XPA via PARP-1 hyperactivation and NAD(+)/SIRT1 reduction.* Cell, 2014. **157**(4): p. 882-96.

61. Chen, S., et al., *RAD6 Promotes Homologous Recombination Repair by Activating the Autophagy-Mediated Degradation of Heterochromatin Protein HP1.* Mol Cell Biol, 2015. **35**(2): p. 406-16.

62. Jiang, P., et al., *In vitro and in vivo anticancer effects of mevalonate pathway modulation on human cancer cells.* Br J Cancer, 2014. **111**(8): p. 1562-71.

63. Wong, W.W., et al., *Cerivastatin triggers tumor-specific apoptosis with higher efficacy than lovastatin.* Clin Cancer Res, 2001. **7**(7): p. 2067-75.

64. Szelag, M., et al., *In silico simulations of STAT1 and STAT3 inhibitors predict SH2 domain cross-binding specificity.* Eur J Pharmacol, 2013. **720**(1-3): p. 38-48.

65. Singh, R., et al., *Autophagy regulates lipid metabolism.* Nature, 2009. **458**(7242): p. 1131-5.

66. Ordonez, M.P., *Defective mitophagy in human Niemann-Pick Type C1 neurons is due to abnormal autophagy activation.* Autophagy, 2012. **8**(7): p. 1157-8.

67. Petrocca, F., et al., *A genome-wide siRNA screen identifies proteasome addiction as a vulnerability of basal-like triple-negative breast cancer cells.* Cancer Cell, 2013. **24**(2): p. 182-96.

68. Wittenburg, L.A., D.L. Gustafson, and D.H. Thamm, *Phase I pharmacokinetic and pharmacodynamic evaluation of combined valproic acid/doxorubicin treatment in dogs with spontaneous cancer.* Clin Cancer Res, 2010. **16**(19): p. 4832-42.

Chapter Four

Phase I clinical trial and pharmacodynamic evaluation of combination hydroxychloroquine and doxorubicin treatment in pet dogs treated for spontaneously occurring lymphoma

Summary

Autophagy is a lysosomal degradation process that may act as a mechanism of survival in a variety of cancers. While pharmacologic inhibition of autophagy with hydroxychloroquine (HCQ) is currently being explored in human clinical trials, it has never been evaluated in canine cancers. Non-Hodgkin's lymphoma (NHL) is one of the most prevalent tumor types in dogs and has similar pathogenesis and response to treatment as human NHL. Clinical trials in canine patients are conducted in the same way as in human patients, thus, to determine a maximum dose of HCQ that can be combined with a standard chemotherapy, a Phase I, single arm, dose escalation trial was conducted in dogs with spontaneous NHL presenting as patients to an academic, tertiary-care veterinary teaching hospital. HCQ was administered daily by mouth throughout the trial, beginning 72 hours prior to doxorubicin (DOX), which was given intravenously on a 21-day cycle. Peripheral blood mononuclear cells and biopsies were collected before and 3 days after HCQ treatment and assessed for autophagy inhibition and HCQ concentration. A total of 30 patients were enrolled in the trial. HCQ alone was well tolerated

with only mild lethargy and gastrointestinal-related adverse events. The overall response rate (ORR) for dogs with lymphoma was 100%, stable disease or better, with median progression free interval (PFI) of 5 months. Pharmacokinetic analysis revealed a 100 fold increase in HCQ in tumors compared to plasma. There was a trend that supported therapy-induced increase in LC3 II and p62 after treatment. The superior ORR and comparable PFI to single agent DOX provide strong support for further evaluation via randomized, placebo-controlled trials in canine and human NHL.

Introduction

(Macro) Autophagy is a lysosomal degradation process which allows for the recycling of cytosolic proteins and organelles [1]. Autophagy is therefore often upregulated in response to stress, acting as a quality control mechanism as well as replenishing amino acid, lipid, and nucleic acid pools [2-5]. These roles for autophagy are thought to enhance survival and therapy resistance in a variety of cancers [6, 7]. A number of pre-clinical cancer therapy mouse xenograft models have been used to demonstrate the enhanced efficacy of cancer therapies when combined with the autophagy inhibitors chloroquine (CQ) or hydroxychloroquine (HCQ) [8-10]. Thus, autophagy appears to be an attractive pathway to target. However, autophagy has been shown to have a protective role in a variety of organs including the gut, kidneys, and liver and combining HCQ with other drugs may exacerbate the toxicities of chemotherapy especially in these tissues [11-13]. Induction of autophagy may also enhance the cytotoxicity of certain drugs [14-16]. Therefore establishing the safe and tolerable dose of HCQ in combination with standard

of care drugs for canine cancers is an important first step in demonstrating the potential benefit of autophagy inhibition for these diseases.

Currently, the only autophagy inhibitor being used clinically is hydroxychloroquine (HCQ), a 4-aminoquinolone drug historically used in treatment of malaria and autoimmune diseases such as systemic lupus erythematosis and rheumatoid arthritis. HCQ pharmacokinetics are characterized by an extremely prolonged terminal half-life (up to 40 days) and a very large volume of distribution, in part due to the partitioning of the drug into red blood cells and strong binding to heme proteins [17, 18]. In humans, HCQ is rapidly and almost completely absorbed following an oral dose with approximately 50% being bound to plasma proteins; three HCQ metabolites have been identified, including desethylchloroquine, desethylhydroxychloroquine (DHCQ), and bidesethylchloroquine [18, 19]. However, little is known about HCQ pharmacokinetics in dogs. HCQ has been used in canine discoid and cutaneous lupus erythematosus, similar to humans, at doses of 5-10 mg/kg/day with some evidence of clinical efficacy, suggesting adequate blood and tissue concentrations for that specific indication [20, 21]. An early laboratory study evaluating chloroquine and HCQ administration in dogs demonstrated that doses up to 32 mg/kg/day for 13 weeks were well tolerated, with no significant alterations of liver function or hematology[22]. When compared to chloroquine administration, equivalent doses of HCQ were better tolerated and provided higher blood and tissue concentrations. However, the study did not evaluate pharmacokinetic parameters of HCQ in dogs following repeat administration. Additionally, the use of HCQ in treatment of canine cancer has yet to be studied.

The translational utility of the canine cancer model is based in the greater similarity to humans in terms of carcinogenesis and tumor biology. Dogs are relatively outbred,

immunocompetent animals that share environments with humans, and experience spontaneously developing tumors with spontaneous metastasis and therapy resistance, representing a spectrum of tumor histotypes similar to humans. The relatively large size of canine tumors closely approximates human solid tumors in regard to biologic factors such as clonal variation and hypoxia, and this relatively large size allows for multiple sampling of tumor tissues over time for pharmacodynamic assessments [23, 24]. In addition, when compared to humans, disease progression in dogs is accelerated which allows for more rapid assessment of therapeutic endpoints than might be possible in similar human trials [23, 24]. Pet dogs with spontaneous cancer have been utilized for the clinical evaluation of multiple novel cytotoxic, targeted and immunomodulatory therapies. These studies have then been used to inform the design of further human clinical trials as well as determining treatment protocols in veterinary medicine [25-32].

Therefore canine clinical trials are designed like and have the same objectives (e.g. a Phase I trial is intended to determine doses and assess pharmacokinetics) as human clinical trials but with the possibility of more rapid and complete assessments than is often possible in humans.

Canine non-Hodgkin's lymphoma (NHL) is a useful naturally occurring model of NHL in humans owing to significant similarities in pathogenesis, histology/biology, and response to treatment. Correlations between genetic factors and the development or progression of NHL have been identified in both canine and human NHL. In dogs, the main aneuploidies observed in NHL include gains of chromosomes 13 and 31 which are analogous to the partial gains of human chromosomes 4 and 8 and a gain of chromosome 21 [33]. Subchromosomal regions of CFA 13/HSA8 and CFA31/HSA21 harbor genes important in tumorigenesis such as *c-myc*, frequently involved in human B-cell lymphomas through aberrant fusion with immunoglobin genes [34]. Canine and human peripheral T-cell lymphomas also demonstrate some conservation of copy

number aberrations with both having deletions in chromosomal regions leading to loss of CDKN2A/B and p16/RB pathway activity [35, 36]. In addition to chromosomal aberrations, epigenetic changes such as methylation of CpG islands and promoter hypermethylation of orthologous tumor-suppressor genes has been identified in human and canine NHL [37, 38]. In dogs, NHL is one of the most prevalent tumor types, making up 7-24% of all cancers and 83% of hematopoietic cancers [39]. The incidence of canine NHL (15-30/100,000) is very similar to that seen in human NHL (15.5-29.9/100,000) [23]. Based on the REAL/WHO or National Cancer Institute Working Formulation schema, canine NHL represents a relatively homogenous population with respect to histologic type with 85% classified as medium to high grade B-cell non-Hodgkin's lymphoma and the majority being diffuse large B-cell lymphoma (DLBCL) [40]. At presentation, most dogs with NHL are asymptomatic and have generalized, non-painful enlargement of peripheral lymph nodes. As in humans, canine NHL is initially highly responsive to multi-agent, CHOP-based chemotherapy which is likely to yield complete responses in approximately 90% of dogs [39]. However, the duration of first remission is short and 85% of cases will relapse within 6-11 months [39]. Owing to toxicity and cost of multiagent chemotherapy, single agent doxorubicin (DOX) is a frequently used alternative that produces a substantially lower response rate of 63-85% and a median progression free survival of approximately 5 months [41-43].

Although there have been reports of enhancement of anti-tumor activity with combinations of cytotoxic drugs and autophagy inhibition *in vitro* and with *in vivo* mouse models, there are no reports on the clinical utility of autophagy inhibition using HCQ in canine cancer patients. Here we report the results of a Phase I/II clinical trial of oral HCQ given continuously, starting 72 hours prior to a standard dose of DOX. This trial was conducted in

client-owned (pet) dogs with spontaneous neoplasia presenting as patients to an academic, tertiary-care veterinary teaching hospital. As would be the case in early-phase human clinical trials, primary endpoints included maximum tolerated dose, dose-limiting toxicities, and pharmacokinetic/pharmacodynamic relationships. Preliminary evidence of antitumor activity was also assessed.

MATERIALS AND METHODS

Cell Lines and Cell Culture

Canine lymphoma cell lines OSW and 1771 were maintained in RPMI (Cellgro, Herndon, VA). Media was supplemented with 10% fetal bovine serum (FBS) (Cellgro, Herndon, VA) and 5% penicillin+streptomycin (Hyclone Laboratories Inc, Logan, UT). Cells were incubated at 37°C and 5% CO_2.

Proliferation Assays

Cells were seeded into a 96 well tissue culture plate in quadruplicate. A concentration of 5,000 cells per well was used for the OSW and 1771 lymphoma lines. Cells were treated with Chloroquine diphosphate (CQ) (Sigma, St. Louis, MO), doxorubicin (Pfizer, New York, NY; NDC 0069-3034-20), or vehicle for 72 h at indicated concentrations. Proliferation was visualized by Alamar Blue (10% at 200 μg/mL rezazurin salt in PBS) and incubated for 2 h. Plates were read at 530/590 nm excitation/emission in a Syngergy HT plate reader (BioTEK, Winooski, VT). All experiments were repeated in triplicate.

Measure of Synergy

The IC_{50} (Dm) value was determined as described in Chou and Talalay [44]. Drug combinations were then tested at 4x-0.25x the IC_{50} values. The Bliss model of independence and was used to determine if the combination was antagonistic, additive, or syngeristic. The additive effect for a drug is E_{xy} as predicted by the individual effect (fraction of affected cells) of each drug E_x and E_y. Thus E_{xy} is defined as $E_{xy} = (E_x + E_y) – (E_xE_y)$ for $0 < E < 1$. The ratio of the actual observed effect compared to the predicted effect was calculated. This value was used to determine combination efficacy, with < 0.8 as antagonistic, $0.8 – 1.2$ as additive, and > 1.2 as synergistic.

Patient recruitment

All dogs in this study were client-owned, pet dogs presenting to the Colorado State University Flint Animal Cancer Center. Study participation was offered in cases where standard therapy had been declined by the dog's owner or such therapy had previously failed, or in cases of advanced disease where no meaningful standard therapy exists. Protocol approval was obtained from the Institutional Animal Care and Use Committee and the Colorado State University Veterinary Teaching Hospital Clinical Review Board. All dogs were treated in accordance with the NIH Guidelines for Care and Use of Laboratory Animals. Signed informed consent and consent to necropsy were obtained from all owners prior to enrollment in the study. This study was initially open to dogs with histologically or cytologically confirmed neoplasia of any histotype for which single agent DOX would be an acceptable therapy. Dogs with regional or distant metastasis or locally advanced disease were included if a survival time of > 6 weeks was anticipated. Dogs were required to be free of other severe complicating concurrent disease

conditions, and were required to have adequate clinical indices to safely undergo chemotherapy and, in some cases, sedation for tumor biopsy acquisition (specifically, total bilirubin not exceeding 1.5x normal; creatinine no exceeding 2x normal; at least 2,500 neutrophils/μL, 75,000 platelets/μL, and a hematocrit of at least 28%). A Veterinary Comparative Oncology Group (VCOG) performance status of 0 or 1 was required for study inclusion [0, normal activity; 1, restricted activity (decreased from predisease status); 2, compromised (ambulatory only for vital activities, consistently defecates and urinates in acceptable areas); 3, disabled (requires force feeding, is unable to confine urination and defecation to acceptable areas); 4, dead]. Prior chemotherapy and radiation therapy were allowed with a 3 and 6-week washout period, respectively. If prednisolone was utilized as an antineoplastic agent a 72-hour washout was required and no concurrent antineoplastic therapy was allowed. For dogs previously administered DOX, prior cumulative exposure could not exceed 90 mg/m^2.

Pretreatment procedures and evaluations

A complete blood count (CBC), serum biochemistry profile, and urinalysis were done prior to enrollment. Staging and immunophenotyping were performed as appropriate for the specific tumor type. Heparinized whole blood (10-12 mL) was collected for separation of peripheral blood mononuclear cells (PMBC), and a 14-gauge needle core biopsy was obtained from accessible tumors using local anesthesia or brief sedation, as necessary.

Treatments

All dogs were given oral HCQ sulfate tablets (Ranbaxy Pharmaceuticals Inc) once daily, beginning 72 hours prior to DOX administration and continuing through the remainder of the study. An initial dose of 5 mg/kg was chosen as the starting point and doses were escalated

according to a standard 3 x 3 dose-escalation protocol whereby three dogs were enrolled in each dose cohort and the cohort expanded to six if dose limiting toxicity (Grade 3 or higher) was encountered in one of the first three dogs. Dogs were scheduled to receive a standard dose of DOX (30 mg/m^2 intravenously, or 1 mg/kg if < 15 kg) as initial treatment on day 4 and continued on a 21-day cycle for a maximum of 5 treatments or disease progression. As with single agent DOX, dose reductions of 20% were instituted for subsequent treatments if Grade 3 or 4 toxicities were observed after the first dose.

Monitoring procedures and evaluations

Adverse events were recorded on days 4, 11, and at each subsequent visit. All treatment related adverse events were graded based upon the guidelines set forth in the Veterinary Comparative Oncology Group-Common Terminology Criteria for adverse events v1.0 [45]. A CBC and blood chemistry were obtained 72 hours after initiation of HCQ therapy. Serum, plasma, and heparinized whole blood were collected prior to DOX administration on day 4 for determination of trough HCQ/DHCQ levels and evaluation of HCQ pharmacodynamics in blood. For six dogs in the highest HCQ dose cohort (12.5 mg/m^2), plasma was obtained at 5, 45, and 60 minutes for evaluation of DOX exposure utilizing a previously published limited-sampling model [46]. Tumor biopsies were obtained following the initial 72 hour therapy with HCQ for determination of HCQ/DHCQ levels and pharmacodynamics. A CBC and blood chemistry were obtained 7 and 21 days following DOX administration. Owners were asked to fill out Quality of Life/Pain questionnaires prior to the study, after the initial 72 hours of HCQ therapy, and again at each subsequent visit. The HCQ/DOX combination was continued on an every-3-week basis until disease progression, maximal cumulative DOX dosage (> 150 mg/m^2) or owner request. Tumor responses were evaluated using RECIST criteria [47] on measured lymph nodes.

PBMC Isolation

Twenty milliliters of whole blood was collected from dogs and divided. Peripheral blood mononuclear cells (PBMC) were isolated using lymphocyte separation media (Cellgro, 25-072-CV). Briefly, one volume of phosphate-buffered saline containing 5 mmol/L EDTA was added to heparinized blood samples, which were then underlaid with 2 mL of lymphocyte separation media. The samples were centrifuged at 400 x g for 20 minutes and the lymphocyte layer was aspirated and washed three times in one volume of PBS/EDTA. Isolated PBMCs were stored at -80°C until processing for flow cytometry, or electron microscopy (EM) analysis.

Flow Cytometry

After PBMCs were isolated, cells were immediately resuspended in 200 μL of FACs buffer (2% FBS and 0.05% sodium azide in phosphate buffered saline). Cells were centrifuged at 1800 rpm for 2 minutes and then fixed and permeabilized for 18 hours at 4°C in diluted Fix/Perm buffer (eBiosciences, 00-5123-43 and 00-5223-56). Cells were washed once in diluted Perm Buffer (eBiosciences 00-8333-56) and then stained with anti-LC3 (Novus Biologicals NB100-2220) at 1:40 for 30 min at room temperature. Two wash steps were done in Perm Buffer and cells were stained with anti-rabbit secondary conjugated to FITC (Bethyl Laboratories A120-101F) at 1:40 for 30 min at room temperature then washed twice with FACs buffer. Cells were then analyzed by flow cytometry using a Cyan (DakoCytomation, Carpintera, CA) cytometer with Summit version 4.3.02 and FlowJo version 7 analysis software. The mean fluorescence intensity (MFI) between pre- and post-treatment with HCQ was used to compare samples for evidence of autophagy inhibition.

Electron Microscopy

PBMC samples were fixed in Karnovsky's fixative (3% glutaraldehyde, 2% formaldehyde, 0.1M sodium phosphate buffer, pH 7.4, Electron Microscopy Sciences, 15720) and stored at 4°C until processing. Following fixation, samples were washed 3 x 10 min with buffer, and post-fixed for one hour with 1% osmium tetroxide in 0.1 M sodium phosphatebuffer. After osmication, samples were again washed three times with buffer, dehydrated through a graded ethanol series (10 min each in 50%, 70%, 80%, and 90% ethanol, 2 x 10 min in 100% ethanol), transferred to propylene oxide (10 min in 1:1 ethanol:propylene oxide, 2 x 10 min in 100% propylene oxide), and infiltrated with Eponate 12 resin (medium hardness fornulation). Resin-embedded samples were polymerized for 24 h at 65^{o}C. Ultrathin sections 60-90 nm in thickness were cut from the embedded samples using a Diatome diamond knife and a Reichert Ultracut E ultramicrotome, mounted on formvar-coated slot grids, and post-stained with uranyl acetate and lead citrate. Sections were examined and photographed at 12,000X using a JEOL JEM-2000EX II electron microscope operated at 100 kV. Negatives were scanned at 1200 ppi using an Epson Perfection flatbed scanner.

Western Blot Analysis

For protein extraction from tumors, snap-frozen biopsies were placed in 500 μL of lysis buffer (0.01% Triton X-100, 150 mM NaCl, 10 mM Tris pH 7.5, 0.2 mM Na-Orthovanadate, 34.8 μg/mL PMSF, and 1x Protease Inhibitor Cocktail [Roche, 11836153001]). Samples were then homogenized for 20 seconds on ice and sonicated on ice for three, 3 second pulses. Samples were centrifuged at 14,000 rpm for 5 min at 4°C and supernatant collected.

Protein concentration was determined using a bicinchoninic acid (BCA) protein assay (Thermo Scientific, 23225). Thirty μg of protein was used in SDS-PAGE and transferred onto PVDF membranes (Millipore IPVH0010). Blots were blocked in 2.5% non-fat dry milk in Tris-buffered saline/Tween 20 for one hour at room temperature. Blots were probed with anti-LC3 (Novus Biologicals NB100-2220), at 1:1000, anti-p62 (Abnova H0008878-M01), at 1:1000, or anti-actin (Sigma A5441), at 1:5000, antibodies were incubated overnight at 4°C. After three washes in TBST, membranes were incubated for one hour at room temperature with either anti-rabbit (Pierce 31460) or anti-mouse (Pierce 31430) secondary antibodies conjugated to HRP. Immunoreactive proteins were detected using West Dura (Thermo Scientific 37071) and imaged in a ChemiDoc XRS$^+$ (Bio Rad, Hercules, CA) using Image Labs version 3.0 software. Densitometry analysis was performed using Image J software available online from the NIH (http://rsb.info.nih.gov/ij/index.html). LC3 I or II and p62 were normalized to actin loading controls. Fold change of LC3 II expression is expressed as the percentage of normalized LC3 II after HCQ treatment in relation to normalized LC3 II expression before HCQ administration.

Hydroxychloroquine analysis in plasma and tumor tissue by liquid chromatography/tandem mass spectrometry.

Hydroxychloroquine and the main metabolite DHCQ were measured in dog plasma and tissue biopsies using a liquid chromatography/tandem mass spectrometry assay using chloroquine as an internal standard. Positive ion electrospray ionization mass spectra were obtained with a MDS Sciex 3200 Q-TRAP triple quadrupole mass spectrometer (Applied Biosystems, Inc., Foster City, CA) with a turbo ionspray source interfaced to Shimadzu LC-20AD Series Binary Pump HPLC system. Samples were chromatographed with a Sunfire 2.5 μm, C8, 4.6 x 50 mm column. A liquid chromatography gradient was employed with mobile

phase A consisting of 20 mM ammonium acetate containing 0.5% acetic acid and mobile phase B consisting of acetonitrile containing 0.5% acetic acid at 800 µL/min. Chromatographic separation was achieved by holding mobile phase B steady at 2% from 0 to 0.25 minutes, increasing linearly to 95% at 3 minutes, holding mobile phase B steady at 95% from 3.0 to 3.5 minutes, decreasing linearly to 2% at 3.75 minutes, followed by re-equilibration at 2% B until 4.5 minutes. The sample injection volume was 10 µL and the analysis run time was 4.5 minutes. The mass spectrometer settings were optimized as follows: turbo ionspray temperature, 550°C; ion spray voltage, 1500 V; source gas 1, 60 units; source gas 2, 50 units; curtain gas, 45; collision gas, medium. Compound parameters for HCQ were optimized as follows: declustering potential, 47.9 V; entrance potential, 4.30 V; collision cell entrance potential, 14.0 V; collision energy, 29.7 V; collision cell exit potential 3.9 V. Sample concentrations of HCQ and metabolite were quantified by internal standard reference method in the multiple reaction monitoring mode with ion transitions *m/z* 336.2→247.1 amu for HCQ, *m/z* 308.2→179.0 and 308.2→130.1 amu (summed) for N-desethylHCQ, and *m/z* 320.3→247.1 amu for the internal standard, CQ. Scan times were 200 ms, and Q1 and Q3 were both operated in unit resolution mode.

Analytical standards (1 ng – 1,000 ng/mL), quality control (5, 50 and 500 ng/mL), and unknown plasma samples were prepared via a liquid-liquid extraction method whereby 180 µL of unknown or fortified plasma samples were added to 1.5 mL polypropylene tubes containing 50 ng of internal standard (CQ) followed by 500 µL of ethyl acetate. Samples were then vortex mixed for 8 minutes and centrifuged at 14,000 rpm for 8 minutes. The organic phase was transferred to fresh Eppendorf tubes and evaporated to dryness. Samples and standards were then reconstituted in 200 µL of a 1:1 methanol/20 mM ammonium acetate mixture at pH 4.0 and transferred to autosampler vials containing glass inserts. For analysis in tissue, biopsy samples

were homogenized in Milli-Q H_20 at a concentration of 100 mg/mL and 180 µL of homogenate was prepared as described above. The lower limit of quantitation (LOQ) for HCQ was 5 ng/mL and the LOQ for the DHCQ, was 10 ng/mL. The standard curves were linear across the range of concentrations utilized. Accuracy of the standard curve and the quality control samples was within 15% at all concentrations and precision was within 15% of the coefficient of variation.

Doxorubicin/doxorubicinol/aglycone analysis in plasma by liquid chromatography/tandem mass spectrometry

Doxorubicin and its metabolites, doxorubicinol and doxorubicin aglycone, were measured in canine plasma using a liquid chromatography/tandem mass spectrometry assay. Negative ion electrospray ionization mass spectra were obtained with the instrumentation described above. Samples were chromatographed on a Waters Sunfire 5 µm, C8 column (4.6 x 50 mm) with a Phenomenex C18 filter frit guard cartridge. A liquid chromatography gradient was employed with mobile phase A consisting of 10 mM ammonium acetate containing 0.1% formic acid and mobile phase B consisting of methanol at 1,200 µL/min. Chromatographic separation was achieved by holding mobile phase B steady at 25% from 0 to 1.0 minutes, increasing linearly to 98% at 2 minutes, holding mobile phase B steady at 98% from 2.0 to 3.0 minutes, decreasing linearly to 25% at 4.0 minutes, followed by re-equilibration at 25% B until 4.5 minutes. The sample injection volume was 60 µL and the analysis run time was 4.5 minutes. The mass spectrometer settings were optimized as follows: turbo ionspray temperature, 575°C; ion spray voltage, -4500 V; source gas 1, 60 units; source gas 2, 60 units; curtain gas, 10; collision gas, low. Compound parameters for DOX were optimized as follows: declustering potential, -41.7 V; entrance potential, -6.3 V; collision cell entrance potential, -15.9 V; collision energy, -22.5 V; collision cell exit potential -3.9 V. Sample concentrations of DOX and

metabolite were quantified by internal standard reference method in the multiple reaction monitoring mode with ion transitions *m/z* 542.3→395.4 amu for DOX, *m/z* 544.3→397.4 and 544.3→309.5 amu (summed) for doxorubicinol, and *m/z* 526.2→379.3 amu for the internal standard, daunorubicin. Scan times were 200 ms, and Q1 and Q3 were both operated in unit resolution mode. Analytical standards (1 – 1,000 ng/mL), quality control (5, 100 and 500 ng/mL), and unknown plasma samples were prepared via a liquid-liquid extraction method whereby 100 µL of unknown or fortified plasma samples were added to 1.5 mL polypropylene tubes containing 100 ng/mL of internal standard (daunorubicin) followed by 1,000 µL of ethyl acetate. Samples were then vortex mixed for 10 minutes and centrifuged at 13,300 rpm for 10 minutes. The organic phase (950 µL) was transferred to fresh Eppendorf tubes and evaporated to dryness. Samples and standards were then reconstituted in 100 µL of 1:1 methanol/10 mM ammonium acetate with 0.1% formic acid and transferred to autosampler vials containing polypropylene inserts.

Prediction of doxorubicin exposure by limited sampling

Six dogs in the 12.5 mg/kg dose cohort had plasma samples collected at 5, 45 and 60 minutes following the first dose of DOX. Plasma DOX concentrations at these time points were used to predict the overall DOX exposure (AUC) using a limited sampling method that was previously validated and published by the authors [46]. In this model, overall DOX exposure was predicted using the equation:

$$AUC = 46.9 + 0.63 \cdot C_{5min} + 1.96 \cdot C_{45min} + 6.63 \cdot C_{60min}$$

where $C_{5min,\ 45min,\ 60min}$ refer to plasma DOX concentrations at those time points. These AUC values were dose-normalized and compared to historical control data generated in our laboratory

for dogs receiving DOX alone to evaluate for potential interactions between HCQ and doxorubicin that might result in alterations in overall exposure [48].

Statistical analysis

All statistical analysis was performed in Prism version 5.0 (GraphPad Software). A paired, 1-tailed t-test was used to compare average MFI, autophagosome number, LC3 II expression and p62 expression pre- and post-HCQ administration. An unpaired, two-tailed t-test was used to compare DOX exposure between study subjects and historical controls. Pearson correlation was performed to determine correlations between pharmacokinetic and pharmacodynamic endpoints. A p-value of less than 0.05 was considered significant.

RESULTS

CQ and DOX efficacy in canine lymphoma cell lines

The combination of CQ and DOX was tested in canine lymphoma cell lines OSW and 1771. According to the Bliss model of independence, this combination was considered additive and CQ was able to sensitize cells to DOX (Fig 4.1).

Dose-escalation trial

A 3x3 dose escalation trial design was used to govern dose escalation toward a maximum oral dose (MTD) of HCQ (5- mg/kg that could be tolerated when administered concurrently with standard dosages of DOX (30 mg/m^2 given once every 3 weeks) in dogs with any spontaneously occurring tumor. In all, 30 dogs met the inclusion criteria and were enrolled in the study

beginning in February 2011 and running through September 2013. All dogs underwent pretreatment evaluation and blood chemistry and CBC, and pretreatment biopsies were obtained from accessible tumors.

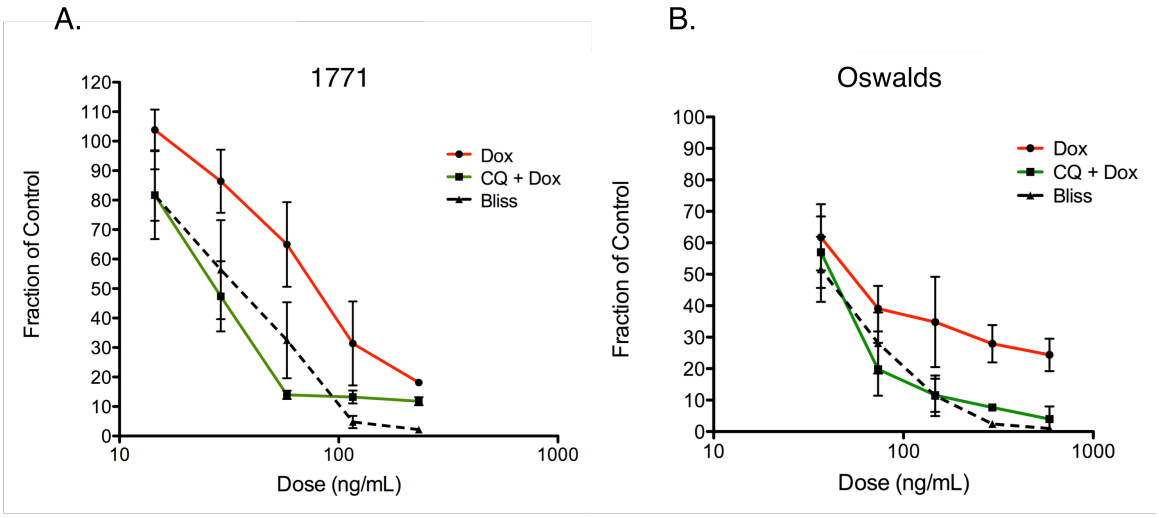

Figure 4.1 CQ sensitizes canine lymphoma cells to DOX. Dose curves of DOX and the combination with CQ in **(A)** 1771 and **(B)** OSW. Dotted line represents theoretical Bliss curve for additivity. Experiments were repeated in triplicate. Error bars represent standard deviation.

Patient parameters such as age, sex, weight, breed and tumor type were recorded for each patient (Table 4.1). In all, 27 of 30 (90%) dogs presented with multicentric lymphoma; 24 (88.9%) and 3 (11.1%) were identified as B-and T-cell lymphoma, respectively. At enrollment, 2 of 30 dogs (6.7%) had documented pulmonary metastasis (one fibrosarcoma and one osteosarcoma) and 2 of 30 had received prior chemotherapy. One dog with lymphoma had been previously enrolled in, and failed, a separate clinical trial.

Oral HCQ was well tolerated in dogs with no Grade 3 or 4 toxicities attributable to the HCQ in any of the dose cohorts in the three days prior to DOX administration.

Table 4.1 Patient characteristics

Characteristic	Patients (n=30) No. (%)
Sex	
Male	20 (66.6)
Female	10 (33.3)
Age, years	
Median	7
Range	4-14
Weight, kg	
Median	29.8
Range	8.5-66.5
Breed	
Purebred	18 (59.3)
Mixed	12 (40.7)
Tumor histology	
Lymphoma	27 (88.9)
B-cell	24
T-cell	3
Fibrosarcoma	1 (3.7)
Soft tissue sarcoma	1 (3.7)
Osteosarcoma	1 (3.7)
HCQ dose cohort (mg/kg/day)	
5 mg/kg	6 (20)
7.5 mg/kg	6 (20)
10 mg/kg	3 (10)
12.5 mg/kg	15 (50)
Completed trial	17 (56.7)

Adverse effects of the HCQ were generally mild and self-limiting and mostly grade 1 or 2 lethargy and/or gastrointestinal upset (Table 4.2). A total of 112 treatment cycles were administered with an average of 3.7 per patient (range, 1-5). In all, 9 of 30 dogs (30%) required dose reductions in DOX following the first treatment cycle because of Grade 3 or 4 toxicities

attributable to DOX. The first HCQ dose cohort (5 mg/kg) was expanded to six dogs because of a Grade 4 neutropenia in the first cycle in one dog. Upon subsequent genetic testing this dog was found to be a heterozygous ABCB1-1Δ mutant, a mutation leading to reduced expression and function of the drug transporter P-glycoprotein which predisposes to increased toxicity of substrate drugs, including DOX [49]. No other Grade 3 or 4 toxicities were encountered in the cohort. One dog in the 7.5 mg/kg HCQ cohort developed Grade 4 neutropenia following the first cycle of DOX resulting in expansion of that cohort to 6 patients; this patient was found to be homozygous for the ABCB1-1Δ mutation leading to a complete lack of P-glycoprotein expression. Of the first three dogs enrolled in the 12.5 mg/kg HCQ cohort, 2 treatment related deaths occurred following the first cycle of DOX and were related to severe neutropenia, gastrointestinal signs (vomiting and diarrhea) and sepsis; one dog developed Grade 5 disseminated intravascular coagulation. As the oral HCQ at 12.5 mg/kg was well tolerated and the toxicities were associated with DOX administration, this cohort was expanded with an initial reduction in DOX dose to 25 mg/m^2. Therefore, 12.5 mg/kg HCQ and 25 mg/m^2 DOX was determined to be the MTD of the combination. This combination was well tolerated, as 12 dogs were enrolled with only one Grade 4 neutropenia and all other toxicities being Grade 1 or 2 gastrointestinal effects (Table 4.2).

Responses were evaluated by Response Evaluation Criteria in Solid Tumors [47] and for the 27 dogs with lymphoma, best responses included 22 of 27 (81.5%) complete response, 3 of 27 (11.1%) partial response and 2 of 27 (7.4%) stable disease (Table 4.3). A total of 17 dogs (56.7%) completed five cycles of DOX. Of the 13 dogs that did not complete 5 cycles, seven (53.8%) were due to progressive disease; two of these dogs had an initial complete response

prior to being removed because of progressive disease. In two cases, dogs were removed from the trial by owner choice due to perceived reduction in quality of life.

Table 4.2 Hydroxychloroquine and doxorubicin adverse events by HCQ dose cohort.

	5 mg/kg (n=6)	**7.5 mg/kg (n=6)**	**10 mg/kg (n=3)**	**12.5 mg/kg (n=3)**	**12.5 mg/kg[†] (n=12)**
HCQ Toxicities[‡]					
Grade 1/2 toxicities	3 events/ *3 dogs*		2 events/ *1 dog*	3 events/ *3 dogs*	5 events/ *5 dogs*
Lethargy	1 (16.7)		1 (33.3)	1 (33.3)	1 (8.33)
Gastrointestinal[§]	2 (33.3)		1 (33.3)	2 (33.3)	4 (25.0)
DOX Toxicities					
Grade 1/2 toxicities	10 events/ *5 dogs*	4 events/ *3 dogs*	3 events/ *2 dogs*	1 event/ *1 dog*	11 events/ *8 dogs*
Lethargy	1 (16.6)				1 (8.33)
Gastrointestinal[§]	5 (83.3)	3 (50.0)	2 (66.7)	1 (33.3)	7 (50.0)
Neutropenia	4 (66.7)		1 (33.3)		3 (16.7)
Thrombocytopenia		1 (16.7)			
Grade 3/4 toxicities	1 event/ *1 dog*	6 events/ *3 dogs*		2 events/ *2 dogs*	5 events/ *2 dogs*
Lethargy		1 (16.7)			1 (8.33)
Gastrointestinal		2 (33.3)			2 (16.7)
Neutropenia	1 (16.6)	3 (50.0)		2 (66.7)	1 (8.33)
Thrombocytopenia					1 (8.33)
Grade 5 Sepsis				2 (66.7)	
DOX dose reduction	3 (50.0)	3 (50.0)			3 (16.7)

[†]Initial reduction in DOX dose from 30 mg/m^2 to 25 mg/m^2. [‡]HCQ toxicities were determined as only those occurring during the 72-hour administration period prior to the initial dose of DOX. [§]Gastrointestinal toxicities included vomiting, diarrhea, and/or inappetance. Numbers in parenthesis indicate the percentage of dogs in the cohort experiencing toxicity.

Table 4.3 Treatment efficacy of hydroxychloroquine and doxorubicin in dogs with multicentric lymphoma.

	12.5 mg/kg HCQ (n=15)
Best Response	
Complete Response	11 (73.3)
Partial Response	3 (20.0)
Stable Disease	1 (6.7)
Progressive Disease	
Overall Response Rate	93.3
Progression Free Interval (months)	4.9

Numbers in parentheses indicate percent of dogs in the cohort with the response.

The overall median progression free interval was 5.0 months, which is similar to single agent DOX when given at 30 mg/m^2 (Fig 4.2) [41, 42].

Pharmacokinetics

For determination of plasma trough HCQ and N-desethylHCQ levels in the highest dose cohort (12.5 mg/kg), plasma was collected 72 hours prior to initiation of therapy and prior to the first dose of DOX. Eleven of the dogs in this cohort had samples available for evaluation. Substantial inter-individual variation was noted in these plasma samples and concentrations (mean ± SD) of HCQ and its metabolite were 105.1 ± 73.1 ng/mL and 16.6 ± 5.4 ng/mL, respectively.

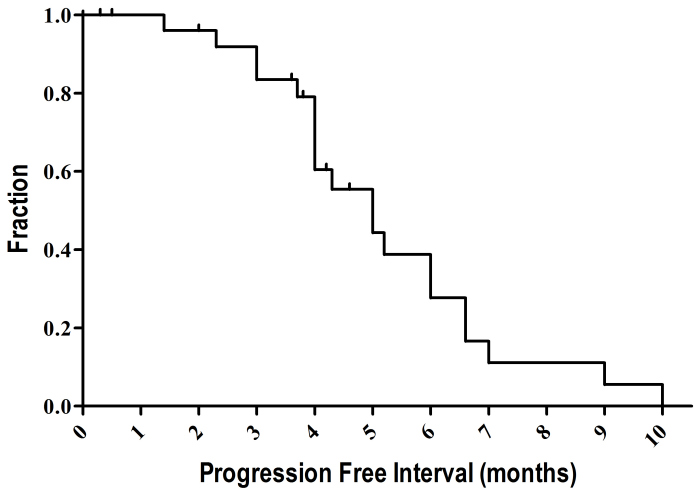

Figure 4.2 Progression Free Interval. Progression free interval was determined for the 27 lymphoma patients receiving the HCQ and DOX combination. Median time to progression was 4.9 months.

In six of these dogs, plasma was also collected for determination of DOX exposure via a validated limited-sampling method. Predicted plasma DOX exposure ($AUC_{0\text{-}6h}$) in these dogs (mean ± SD) was 615.8 ± 208.6 ng/mL. Comparison of the DOX exposure in dogs in this study receiving HCQ followed by DOX at 25 mg/m^2 with historical controls receiving single agent DOX at 30 mg/m^2 demonstrated an approximate 25% reduction in AUC (Table 4.4); however, the dose-normalized exposure (AUC divided by dose) was not significantly different from that observed in dogs receiving single-agent therapy [48, 50]. This suggests no pharmacokinetic interaction between HCQ and DOX that would result in altered plasma DOX exposure.

Tumor tissue concentrations of HCQ and its metabolite were also determined in the eleven dogs in which plasma concentrations were available. Results indicate a significant accumulation of HCQ and the metabolite in tumor tissues, with an approximate 100-fold increase

Table 4.4 Comparison of predicted and dose-normalized doxorubicin exposure between dogs administered hydroxychloroquine at 12.5 mg/kg daily and historical controls receiving single agent doxorubicin

Parameter	Current Study (n=12) Mean ± SD	Historical Controls (n=27) Mean ± SD
DOX_{5min} (ng/mL)	492.2 ± 250.1	411.97 ± 166.3
DOX_{45min} (ng/mL)	35.8 ± 7.5	69.2 ± 24.4
$DOX_{60\ min}$ (ng/mL)	28.45 ± 8.5	57.9 ± 12.1
Pred $AUC_{0\text{-}6h}$ (ng*mL/hr)	615.8 ± 208.6	825.6 ± 176.9‡
Dose-normalized exposure (ng*mL/hr)/(mg/m^2)	24.6 ± 8.3	27.5 ± 5.9

‡ Significant difference in $AUC_{0\text{-}6h}$ between study subjects receiving 25 mg/m^2 doxorubicin and historical controls receiving doxorubicin alone at 30 mg/m^2; two-tailed T-test, P = 0.016. Difference in dose-normalized exposure is not significant between study subjects and historical controls.

in tumor compared to plasma (Fig. 4.3a). Although tumor tissue concentrations were consistently higher, there was no significant correlation between the plasma and tumor concentration for individual dogs (Pearson correlation = 0.143, P = 0.695, Fig. 4.3b).

Pharmacodynamic response in peripheral blood and tumor tissue

The pharmacodynamic response to HCQ was evaluated in peripheral blood mononuclear cells (PBMCs) through flow cytometric evaluation of changes in LC3 for 6 dogs treated at 12.5 mg/kg po qd HCQ/25 mg/m2 DOX. All 6 dogs had a complete response and minimal toxicity (Table

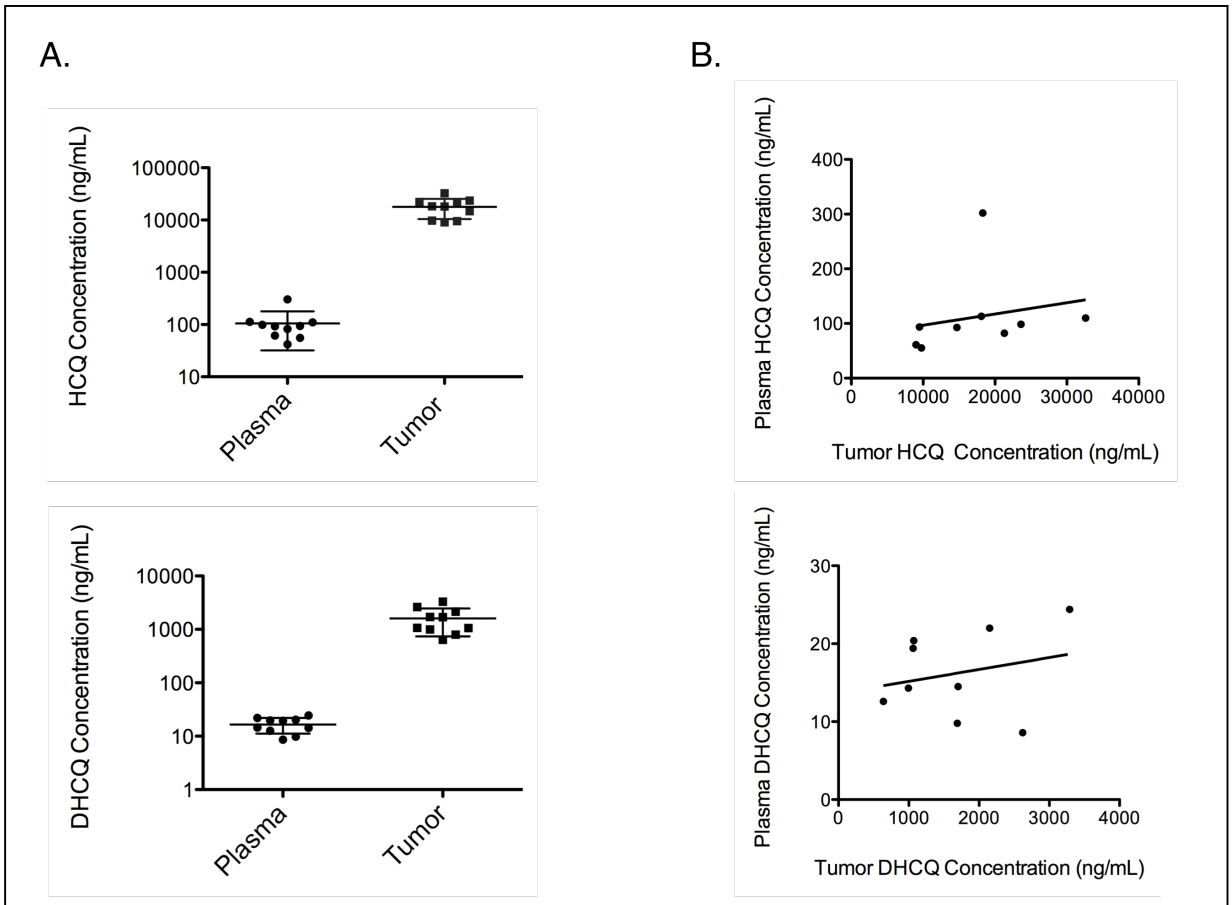

Figure 4.3 Concentration of HCQ and DHCQ in plasma and tumor. (A) Concentrations of hydroxychloroquine (HCQ) and the metabolite N-desethylhydroxychloroquin (DHCQ) in dogs administered 12.5 mg/kg HCQ daily were significantly higher in tumor tissues compared to plasma [HCQ ($P < .0001$) and DHCQ ($P = .0003$)]. **(B)** There was no significant correlation between plasma and tumor HCQ or DHCQ concentrations (Pearson correlation = 0.143 and 0.238, P = 0.695 and 0.537).

4.2 and 4.3). Comparison of pre- and post-treatment MFI for LC3 by flow cytometry in PBMC revealed a significant increase of nearly 2-fold ($p = .033$) (Fig. 4.4). Additionally, we employed the gold standard, electron microscopy (EM), to visualize the formation and accumulation of autophagosomes, which is indicative of a blockade in the autophagic pathway by a drug such as HCQ, which inhibits the lysosome and thus prevents fusion with autophagosomes, leading to

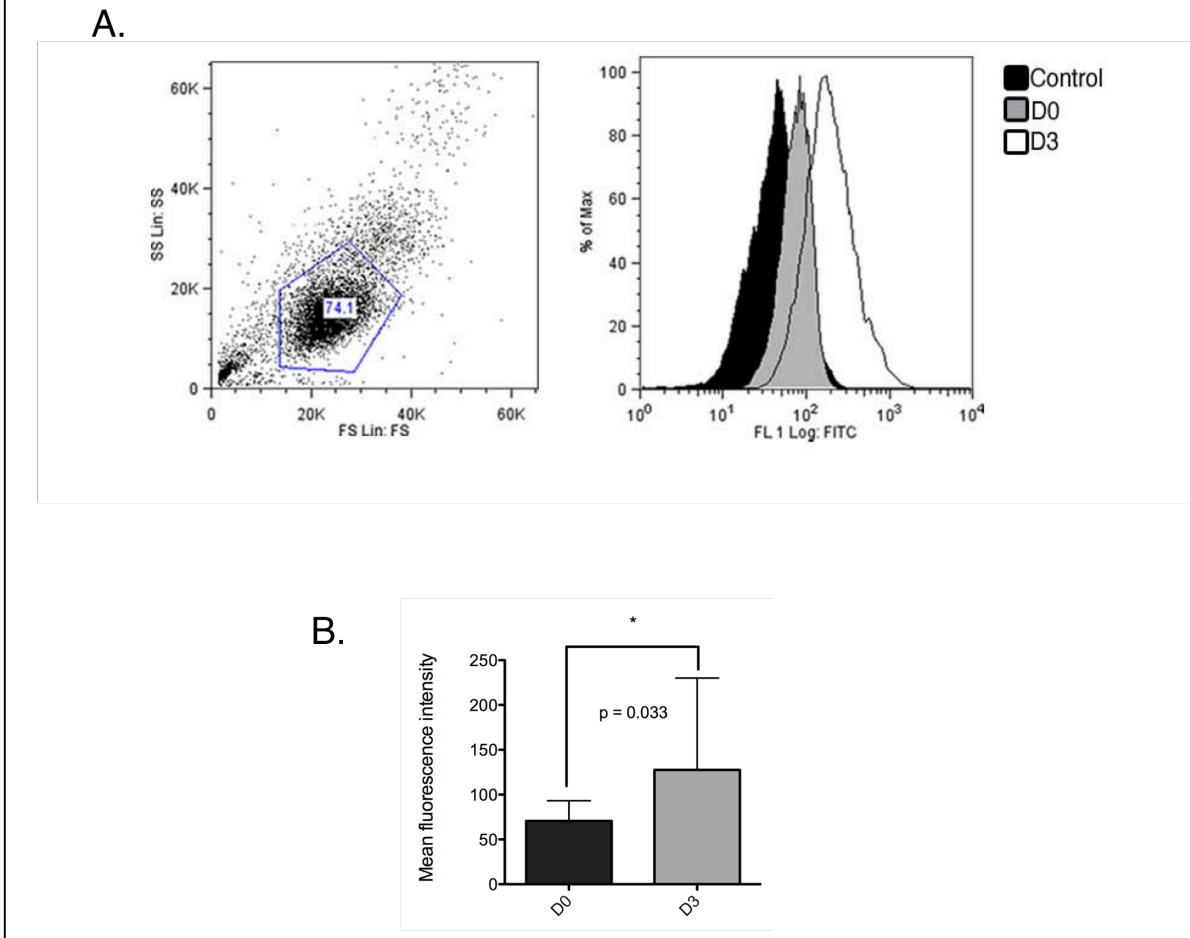

Figure 4.4 Assessment of LC3 expression by flow cytometry. PBMCs were isolated from whole blood before and 3 days post HCQ administration. **(A)** The representative plot shows gating of cells and histograms demonstrate the increase of LC3 positive cells after HCQ administration **(B)**. Overall there was a significant increase in the mean fluorescence intensity post HCQ.

increased accumulation of autophagosomes (Fig 4.5) [51]. Though there was an overall increase in autophagosome number after HCQ administration, it was not significant.

In tumor tissues, the pharmacodynamic response was evaluated by western analysis for changes in LC3 and p62. All biopsies were from involved lymph nodes in patients with NHL in the 12.5 mg/kg dose cohort. Although not significant, there was a trend toward

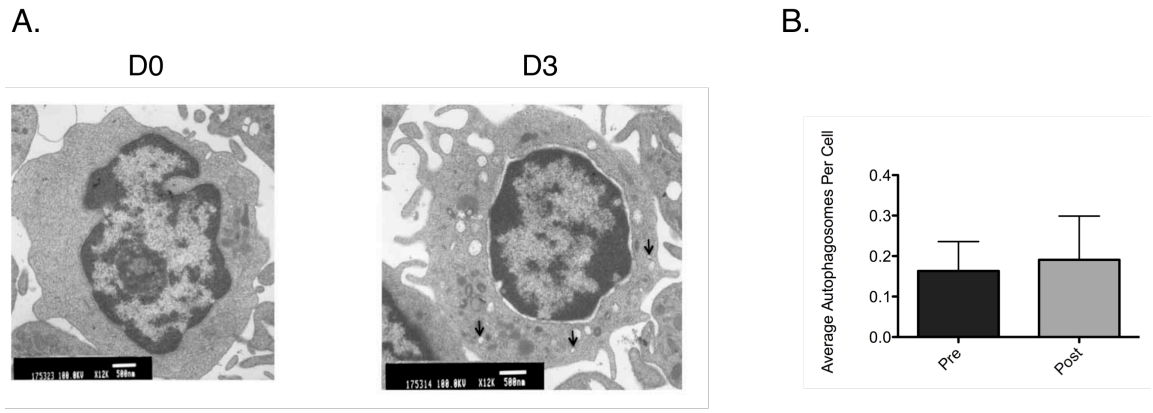

Figure 4.5 Visualization of autophagic vesicles. Representative EM images of PBMCs taken pre and post HCQ administration. There is an increase in autophagic vesicles after HCQ treatment, indicated by arrows. Overall there was an increase in vesicles after treatment, though not significantly.

increases in LC3 II and p62 expression in biopsy samples as well as tissue aspirates following HCQ administration (Fig 4.6). Taken together, these data indicate that a variety of pharmacodynamic assays, that are feasible in the clinical setting, show strong evidence of autophagy inhibition in PBMCs and also in tumor tissue. It should however be noted that in the tumor tissue these responses were less robust than in the blood.

Fold change in LC3 II expression, as determined by western blot, in PBMCs did not correlate with change in tumor tissue (Fig 4.7a). If LC3 II increased in PBMCs, this did not necessarily mean that LC3 II had also increased in tumors. There was a trend between HCQ concentration and LC3 expression, although not significant (4.7b). The patients with the two highest concentrations of HCQ, 23,600 ng/mL and 32,000 ng/mL, also had the most substantial amount of LC3 II expression. Thus, there was not a linear dose relationship, but rather implies a threshold level of HCQ required to block autophagy.

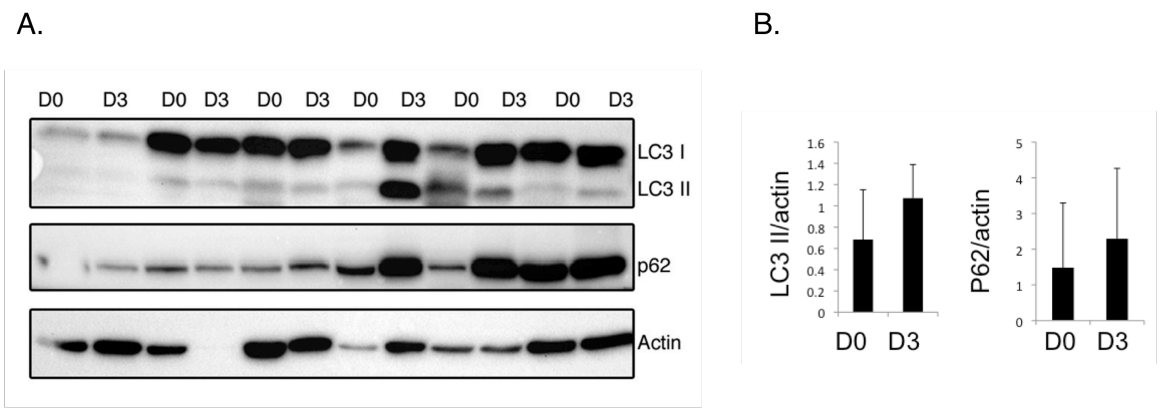

Figure 4.6 Assessment of LC3 expression by western blot in tumor tissue. (A) Tumor biopsies were taken from the prominent lymph node before and 3 days post HCQ administration. Western blot analysis was performed on biopsies to determine expression of LC3 I/II and p62. **(B)** Although not significant, both increased overall after treatment.

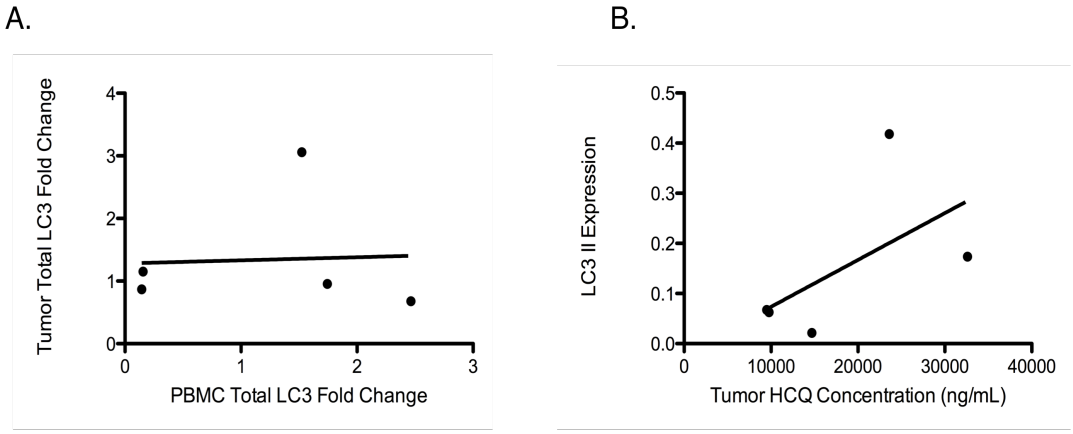

Figure 4.7 Assessment of pharmacodyanmic response. (A) There was no correlation between fold change in total LC3 expression, as determined by western blot, PBMCs and tumor, indicating that response in the blood may not be reflective of response in the tumor. **(B)** There was a trend in LC3 II expression and HCQ concentration in the tumor, but dose response was not necessarily linear. It appears a threshold of HCQ may be required to inhibit autophagy.

DISCUSSION

Autophagy inhibition is thought to be a mechanism of survival and drug resistance for many types of cancers. Thus combining the autophagy inhibitor HCQ with cytotoxic chemotherapy may enhance efficacy. Here we report the results of a phase I/II clinical trial evaluating the use of combined HCQ and DOX in dogs with spontaneously occurring cancer, aimed at defining a safe and potentially biologically effective dose of HCQ. The rationale for the dosing scheme of 72-hour pre-treatment prior to the first dose of DOX followed by continuous daily dosing with HCQ was based on the reported long half-life and time to reach steady state in humans, and the lack of any corresponding pharmacokinetic data in dogs [19-21]. Four dose cohorts, ranging from 5 mg/kg/day up to 12.5 mg/kg/day, were evaluated. This study identified maximum tolerated doses of HCQ in combination with DOX of 12.5 mg/kg/day, and 25 mg/m^2, respectively. Consistent with previous reports of the clinical use of HCQ in dogs, toxicities attributable to HCQ alone were generally mild with the most commonly reported adverse events being grade 1 lethargy and gastrointestinal disturbance [20, 21]. Dose limiting toxicities following DOX administration were observed in one dog in each of the 5 mg/kg and 7.5 mg/kg dose cohorts; however, the finding that both of these dogs were MDR1-1Δ mutants would support the argument that these toxicities were not due to the combination of HCQ and DOX but an intrinsic sensitivity to DOX because of reduced or absent function of the P-glycoprotein efflux pump. Our finding of 12.5 mg/kg/day as the MTD of HCQ is based on the necessity to reduce the DOX dose by approximately 20% (30 mg/m^2 to 25 mg/m^2) in order to avoid the grade 5 adverse events that occurred at the standard DOX dose. Twelve dogs with lymphoma were subsequently enrolled in the 12.5 mg/kg/day HCQ and 25 mg/m^2 DOX cohort with two requiring an additional 20% dose reduction in DOX due to grade 4 neutropenia. Importantly, 9 of these

dogs achieved a complete remission and 8 of these dogs completed the trial, which would indicate that the reduced DOX dose did not result in a reduction in initial response. We did observe a substantial overall response rate in dogs with lymphoma (100%). These results are encouraging given that reported response rates with DOX alone for treatment-naive lymphoma in dogs range from 60-85% [41, 42]. The median progression free interval in dogs with lymphoma in this study was 5.0 months, which is comparable to single agent DOX at 30 mg/m^2 [41, 42]. A larger study group with longer follow up would be required to determine if the combined HCQ and lower DOX (25 mg/m^2) dose is superior, or at least as effective, as single agent DOX administered at the standard 30 mg/m^2 dose.

We were able to evaluate plasma exposure (area under the concentration-time curve) of DOX in six dogs within the highest HCQ dose cohort. Samples from this cohort were chosen as it was assumed that if changes in DOX PK were to be seen it would most likely occur with the highest HCQ dose. This was evaluated with the use of a validated limited-sampling model to predict overall exposure to DOX. We were able to demonstrate that overall plasma DOX exposure (dose-normalized area under the plasma concentration-time curve) was not significantly different in our group from dogs receiving DOX alone [48, 50].

In our study we were able to detect pharmacodynamic activity in PBMC and in tumor tissue following 72 hours of oral HCQ administration, although the extent of autophagy inhibition, at least as determined by analysis of LC3, was less robust and at a lower level of statistical significance in tumor tissue compared with blood. Importantly, we found significant accumulation of HCQ in tumor tissue relative to plasma. A substantial fraction of HCQ partitions to red blood cells, and it is possible that whole blood levels would correlate with concentrations in homogenized tumor especially since the tumor samples also include some blood cells in them

and do not reflect only tumor cells; however, this seems unlikely as 4-aminoquinolone binding to red blood cells has been reported to be linear with concentration and RBC density [52]. This infers a constant relationship between total concentration and the fraction bound to RBCs, and while whole blood levels are certain to be higher than plasma, the same relationship to tumor concentrations would hold true. It is important to note that this study also evaluated plasma HCQ concentrations after 72 hours of therapy and, based on the reported long half-life in humans (see Rosenfeld et al, Vogl et al., Rangwala), it is possible samples were taken before dogs achieved steady-state concentrations [53-56]. Variability and delays in achieving steady state concentrations have been reported to contribute to the variability in tissue PD response in humans [17]. However, it does appear that plasma HCQ concentration in PMBCs is not an adequate surrogate for concentrations within the tumor and, similarly, evidence of autophagy inhibition in PBMCs is not necessarily sufficient to infer that autophagy was effectively inhibited in the tumor. These data suggest that although HCQ is capable of inhibiting autophagy in tumors of cancer patients, autophagy inhibitors with better pharmacokinetics and tumor bioavailability would be useful. Additionally our results suggest that one should be cautious in inferring from surrogate markers in the blood that sufficient tumor drug levels for effective autophagy inhibition have been achieved and emphasize the value in future clinical trials of attempting to make such measurements in tumor tissue.

Conclusions

In conclusion, this is the first study to evaluate the safety and potential clinical utility of autophagy inhibition using HCQ combined with cytotoxic chemotherapy in dogs with

spontaneous cancer. We used continuous oral administration of HCQ combined with DOX on a 21-day cycle and showed that HCQ at doses up to 12.5 mg/kg/day are well tolerated but necessitate a reduction in the standard dose of DOX used in order to avoid unacceptable toxicity. Importantly, this reduction in DOX still provided a superior ORR and comparable PFI to dogs receiving single-agent, standard dose DOX. We were able to show target modulation in both PBMC and tumor tissue. The superior overall response rate and comparable progression free interval in our study provide strong support for further evaluation of this combination in randomized, placebo-controlled studies in canine lymphoma, and the strength of the canine model of NHL supports initiation of similar clinical trials in human lymphoma patients.

.

References

1. Mizushima, N., T. Yoshimori, and B. Levine, *Methods in mammalian autophagy research.* Cell, 2010. **140**(3): p. 313-26.

2. Ichimura, Y. and M. Komatsu, *Pathophysiological role of autophagy: lesson from autophagy-deficient mouse models.* Exp Anim, 2011. **60**(4): p. 329-45.

3. Suraweera, A., et al., *Failure of amino acid homeostasis causes cell death following proteasome inhibition.* Mol Cell, 2012. **48**(2): p. 242-53.

4. Kaushik, S., et al., *Autophagy in hypothalamic AgRP neurons regulates food intake and energy balance.* Cell Metab, 2011. **14**(2): p. 173-83.

5. Fujiwara, Y., et al., *Direct uptake and degradation of DNA by lysosomes.* Autophagy, 2013. **9**(8): p. 1167-71.

6. Loos, B., et al., *The variability of autophagy and cell death susceptibility: Unanswered questions.* Autophagy, 2013. **9**(9).

7. Jin, S. and E. White, *Role of autophagy in cancer: management of metabolic stress.* Autophagy, 2007. **3**(1): p. 28-31.

8. Amaravadi, R.K., et al., *Autophagy inhibition enhances therapy-induced apoptosis in a Myc-induced model of lymphoma.* J Clin Invest, 2007. **117**(2): p. 326-36.

9. Selvakumaran, M., et al., *Autophagy inhibition sensitizes colon cancer cells to antiangiogenic and cytotoxic therapy.* Clin Cancer Res, 2013. **19**(11): p. 2995-3007.

10. Ding, Z.B., et al., *Autophagy activation in hepatocellular carcinoma contributes to the tolerance of oxaliplatin via reactive oxygen species modulation.* Clin Cancer Res, 2011. **17**(19): p. 6229-38.

11. Kimura, T., et al., *Chloroquine in cancer therapy: a double-edged sword of autophagy.* Cancer Res, 2013. **73**(1): p. 3-7.

12. Ni, H.M., et al., *Activation of autophagy protects against acetaminophen-induced hepatotoxicity.* Hepatology, 2012. **55**(1): p. 222-32.

13. Cabrera, S., et al., *ATG4B/autophagin-1 regulates intestinal homeostasis and protects mice from experimental colitis.* Autophagy, 2013. **9**(8): p. 1188-200.

14. Levine, B. and J. Yuan, *Autophagy in cell death: an innocent convict?* J Clin Invest, 2005. **115**(10): p. 2679-88.

15. Kanzawa, T., et al., *Role of autophagy in temozolomide-induced cytotoxicity for malignant glioma cells.* Cell Death Differ, 2004. **11**(4): p. 448-57.

16. Bristol, M.L., et al., *Autophagy inhibition for chemosensitization and radiosensitization in cancer: do the preclinical data support this therapeutic strategy?* J Pharmacol Exp Ther, 2013. **344**(3): p. 544-52.

17. Lim, H.S., et al., *Pharmacokinetics of hydroxychloroquine and its clinical implications in chemoprophylaxis against malaria caused by Plasmodium vivax.* Antimicrob Agents Chemother, 2009. **53**(4): p. 1468-75.

18. Carmichael, S.J., B. Charles, and S.E. Tett, *Population pharmacokinetics of hydroxychloroquine in patients with rheumatoid arthritis.* Ther Drug Monit, 2003. **25**(6): p. 671-81.

19. Tett, S.E., *Clinical pharmacokinetics of slow-acting antirheumatic drugs.* Clin Pharmacokinet, 1993. **25**(5): p. 392-407.

20. Oberkirchner, U., K.E. Linder, and T. Olivry, *Successful treatment of a novel generalized variant of canine discoid lupus erythematosus with oral hydroxychloroquine.* Vet Dermatol, 2012. **23**(1): p. 65-70, e15-6.

21. Mauldin, E.A., et al., *Exfoliative cutaneous lupus erythematosus in German shorthaired pointer dogs: disease development, progression and evaluation of three immunomodulatory drugs (ciclosporin, hydroxychloroquine, and adalimumab) in a controlled environment.* Vet Dermatol, 2010. **21**(4): p. 373-82.

22. McChesney EW, M.A., *Laboratory Studies of the 4-aminoquinoline antimalarials: I. Some biochemical characteristics of chloroquine, hydroxychloroquine, and SN-7718* Antibiotics and Chemotherapy. , 1961. **11**(12): p. 800-810.

23. Hansen, K. and C. Khanna, *Spontaneous and genetically engineered animal models; use in preclinical cancer drug development.* Eur J Cancer, 2004. **40**(6): p. 858-80.

24. Kimmelman, J. and J. Nalbantoglu, *Faithful companions: a proposal for neurooncology trials in pet dogs.* Cancer Res, 2007. **67**(10): p. 4541-4.

25. Vail, D.M., et al., *Efficacy of pyridoxine to ameliorate the cutaneous toxicity associated with doxorubicin containing pegylated (Stealth) liposomes: a randomized, double-blind clinical trial using a canine model.* Clin Cancer Res, 1998. **4**(6): p. 1567-71.

26. Thamm, D.H., et al., *Systemic administration of an attenuated, tumor-targeting Salmonella typhimurium to dogs with spontaneous neoplasia: phase I evaluation.* Clin Cancer Res, 2005. **11**(13): p. 4827-34.

27. Paoloni MC, T.A., Mazcko C, Hanna E, Kachala S, LeBlanc A, Newman S, Vail DM, Henry C, Thamm DH, Sorenmo K, Haitjou A, Pasqualini R, Arap W, Khanna C, Libutti SK. , *Launching a novel preclinical infrastructure: Comparative Oncology Trials Consortium directed therapeutic targeting of TNF-a to cancer vasculature.* PLoS ONE, 2009. **4**(3): p. e4972.

28. Vail, D.M., et al., *Assessment of GS-9219 in a pet dog model of non-Hodgkin's lymphoma.* Clin Cancer Res, 2009. **15**(10): p. 3503-10.

29. Thamm, D.H., et al., *Preclinical investigation of PEGylated tumor necrosis factor alpha in dogs with spontaneous tumors: phase I evaluation.* Clin Cancer Res, 2010. **16**(5): p. 1498-508.

30. Wittenburg, L.A., D.L. Gustafson, and D.H. Thamm, *Phase I pharmacokinetic and pharmacodynamic evaluation of combined valproic acid/doxorubicin treatment in dogs with spontaneous cancer.* Clin Cancer Res, 2010. **16**(19): p. 4832-42.

31. Honigberg, L.A., et al., *The Bruton tyrosine kinase inhibitor PCI-32765 blocks B-cell activation and is efficacious in models of autoimmune disease and B-cell malignancy.* Proc Natl Acad Sci U S A, 2010. **107**(29): p. 13075-80.

32. London, C.A., et al., *Phase I dose-escalating study of SU11654, a small molecule receptor tyrosine kinase inhibitor, in dogs with spontaneous malignancies.* Clin Cancer Res, 2003. **9**(7): p. 2755-68.

33. Thomas, R., et al., *Refining tumor-associated aneuploidy through 'genomic recoding' of recurrent DNA copy number aberrations in 150 canine non-Hodgkin lymphomas.* Leuk Lymphoma, 2011. **52**(7): p. 1321-35.

34. Hartmann, E.M., G. Ott, and A. Rosenwald, *Molecular biology and genetics of lymphomas.* Hematol Oncol Clin North Am, 2008. **22**(5): p. 807-23, vii.

35. Fosmire, S.P., et al., *Inactivation of the p16 cyclin-dependent kinase inhibitor in high-grade canine non-Hodgkin's T-cell lymphoma.* Vet Pathol, 2007. **44**(4): p. 467-78.

36. Zettl, A., et al., *Genomic profiling of peripheral T-cell lymphoma, unspecified, and anaplastic large T-cell lymphoma delineates novel recurrent chromosomal alterations.* Am J Pathol, 2004. **164**(5): p. 1837-48.

37. Shaknovich, R. and A. Melnick, *Epigenetics and B-cell lymphoma.* Curr Opin Hematol, 2011. **18**(4): p. 293-9.

38. Bryan, J.N., et al., *Hypermethylation of the DLC1 CpG island does not alter gene expression in canine lymphoma.* BMC Genet, 2009. **10**: p. 73.

39. Vail, D.M., and Young, K M, *Canine lymphoma and lymphoid leukemia*, in *Withrow and MacEwen's Small Animal Clinical Oncology*, S.J. Withrow, and Vail D M, Editor. 2007, WB Saunders: St. Louis. p. 699-712.

40. Jacobs R M, M.J.B., Valli V E, *Tumors of the hemolymphatic system*, in *Tumors in Domestic Animals*, M. D, Editor. 2002, Iowa State Press: Ames, IA. p. 119-198.

41. Lori, J.C., T.J. Stein, and D.H. Thamm, *Doxorubicin and cyclophosphamide for the treatment of canine lymphoma: a randomized, placebo-controlled study.* Vet Comp Oncol, 2010. **8**(3): p. 188-95.

42. Postorino NC, S.J., Withrow SJ, *Single agent therapy with Adriamycin for canine lymphosarcoma.* J Am Anim Hosp Assoc, 1989. **24**: p. 221-225.

43. Valerius, K.D., et al., *Doxorubicin alone or in combination with asparaginase, followed by cyclophosphamide, vincristine, and prednisone for treatment of multicentric lymphoma in dogs: 121 cases (1987-1995).* J Am Vet Med Assoc, 1997. **210**(4): p. 512-6.

44. Chou, T.C. and P. Talalay, *Quantitative analysis of dose-effect relationships: the combined effects of multiple drugs or enzyme inhibitors.* Adv Enzyme Regul, 1984. **22**: p. 27-55.

45. *Veterinary Co-operative Oncology Group - Common Terminology Criteria for Adverse Events (VCOG-CTCAE) following chemotherapy or biological antineoplastic therapy in dogs and cats v1.0.* Vet Comp Oncol, 2004. **2**(4): p. 195-213.

46. Wittenburg, L.A., D.H. Thamm, and D.L. Gustafson, *Development of a limited-sampling model for prediction of doxorubicin exposure in dogs.* Vet Comp Oncol, 2012.

47. Eisenhauer, E.A., et al., *New response evaluation criteria in solid tumours: revised RECIST guideline (version 1.1).* Eur J Cancer, 2009. **45**(2): p. 228-47.

48. Selting, K.A., et al., *Evaluation of the effects of dietary n-3 fatty acid supplementation on the pharmacokinetics of doxorubicin in dogs with lymphoma.* Am J Vet Res, 2006. **67**(1): p. 145-51.

49. Mealey, K.L., *Therapeutic implications of the MDR-1 gene.* J Vet Pharmacol Ther, 2004. **27**(5): p. 257-64.

50. Gustafson, D.L., et al., *Doxorubicin pharmacokinetics: Macromolecule binding, metabolism, and excretion in the context of a physiologic model.* J Pharm Sci, 2002. **91**(6): p. 1488-501.

51. Klionsky, D.J., et al., *Guidelines for the use and interpretation of assays for monitoring autophagy.* Autophagy, 2012. **8**(4): p. 445-544.

52. Omodeo-Sale, F., et al., *Novel antimalarial aminoquinolines: heme binding and effects on normal or Plasmodium falciparum-parasitized human erythrocytes.* Antimicrob Agents Chemother, 2009. **53**(10): p. 4339-44.

53. Rosenfeld, M.R., et al., *A phase I/II trial of hydroxychloroquine in conjunction with radiation therapy and concurrent and adjuvant temozolomide in patients with newly diagnosed glioblastoma multiforme.* Autophagy, 2014. **10**(8): p. 1359-68.

54. Vogl, D.T., et al., *Combined autophagy and proteasome inhibition: a phase 1 trial of hydroxychloroquine and bortezomib in patients with relapsed/refractory myeloma.* Autophagy, 2014. **10**(8): p. 1380-90.

55. Rangwala, R., et al., *Phase I trial of hydroxychloroquine with dose-intense temozolomide in patients with advanced solid tumors and melanoma.* Autophagy, 2014. **10**(8): p. 1369-79.

56. Rangwala, R., et al., *Combined MTOR and autophagy inhibition: phase I trial of hydroxychloroquine and temsirolimus in patients with advanced solid tumors and melanoma.* Autophagy, 2014. **10**(8): p. 1391-402.

Chapter Five

Conclusion

General Conclusions

Autophagy may have a complex role in cancer, but it seems evident that autophagy can promote survival and resistance in certain types of cancer. Consequently, inhibiting autophagy has become an attractive anti-cancer therapy. Yet there still remain a number of unanswered questions that need to be resolved if autophagy inhibition is to be an effective strategy. One such question is the role of autophagy in metastasis. This is an important issue to address as the majority of patients will succumb to recurrence or therapy resistant metastases. Although a number of studies have demonstrated autophagy's effects on metastatic characteristics like invasion, migration, anoikis resistance, and epithelial to mesenchymal transition, in culture, few have tested autophagy modulation in an *in vivo,* metastatic setting. Even less have used immune competent animal models. In Chapter Two, we utilized multiple different mouse models to assess the effect of autophagy modulation on metastatic progression. We found that inhibiting autophagy did not alter the ability of cells to colonize or survive within the lung; rather, it seemed to delay arrival of cells if treatment was delivered before dissemination. This effect was not due to any loss of metastatic capability, but may have been due to changes in the pre-metastatic niche. We found that there were significantly more bone marrow derived cells (BMDCs) in the lung and blood when autophagy was stimulated by trehalose. Correspondingly,

there were significantly less in the blood of CQ treated mice. BMDCs have been well described as the mediators of the pre-metastatic niche, thus autophagy appears to influence the development of the niche [1]. Therefore, the application of autophagy inhibition will likely be most effective before metastatic occurrence. Autophagy inhibition's clinical usefulness may be somewhat limited then; however, it may be used as a neoadjuvant therapy or if patients have macrometastases that can be surgically removed and autophagy inhibition used to prevent any further metastatic spread.

The ability of autophagy inhibition to delay metastases was modest, only a few days, thus, it will not serve as a single agent. We also tested the combination of a relevant chemotherapy, cisplatin, and autophagy inhibition. Although this combination was additive in culture, it proved to be antagonistic in the mice. As functional autophagy is required for immune-related, or immunogenic cell death, we tried to assess relevant immune cell populations [2]. We did find that neutrophils were significantly increased in CQ and combination treated mice. Neutrophils can have an immunosuppressive role, and this may be one explanation for why the combination was worse that cisplatin alone. While neutrophils may not be the only or even direct consequence of reduced cisplatin efficacy, it does demonstrate that changes are occurring within the metastatic microenvironment. This study brings to light the fact that pharmacologic inhibition will impact more than just tumor cells and may have a counterproductive result due to an altered microenvironment. Some chemotherapy drugs may be more sensitive to this effect than others and thorough study is needed before combining with autophagy inhibitors.

As autophagy is a well conserved stress response to a number of different environmental stresses, it was initially thought to be a very general tumor adaptation and inhibiting autophagy could be applied to a very broad range of tumor types. It is now clear that only some tumor types

are dependent on autophagy, but there is no consistently good marker to identify which tumors these are. In Chapter Three, we tested the efficacy of autophagy inhibition using CQ on breast cancer cells deemed to be autophagy dependent or independent by Dr. Paola Maycotte. We found that her *in vitro* assessment of autophagy dependence was also valid in the mouse xenograft model. The autophagy dependent cell lines were the triple negative subtype of breast cancer (TNBC) and had Stat3 activation. As canine osteosarcoma can also have constitutive activation of Stat3, we determined the sensitivity of six osteosarcoma lines to CQ. Unlike in breast cancer, Stat3 activation did not correlate with CQ sensitivity. Therefore, phospho-Stat3 may be a particularly useful marker to predict autophagy dependence in TNBC, but not necessarily so for other cancer types. Autophagy inhibition will work best in autophagy dependent cell types, and TNBC, which is typically therapy resistant, may be particularly responsive.

Though TNBC cells were sensitive to CQ, they eventually did progress. Therefore, we also tried to identify pathways to target that could enhance cell death when combined with autophagy inhibition. We used microarray and pathway analysis to determine pathways that had been upregulated after treatment. We also included the canine osteosarcoma samples as they still showed response to CQ and few therapies exist to treat the disease. Despite being two different tumor types and coming from two different species, similar pathways were activated upon autophagy inhibition. Notably, proteasome degradation, histone acetylation, DNA repair, ER stress, and cholesterol synthesis were all upregulated. Most of these pathways have been shown to be regulated by autophagy in other tumor types, but few studies have been conducted in relation to autophagy inhibition and TNBC or osteosarcoma. Particularly interesting was cholesterol synthesis, as inhibition of cholesterol has only recently been discovered as an anti-

cancer therapy. We tested the combination of statin inhibitor, lovastatin and CQ in canine osteosarcoma cells. Though lovastatin alone was effective, the combination was not even additive. Some studies have shown that autophagy is required for statin inhibitor efficacy, but this is inhibitor and cell type dependent. In the case of canine osteosarcoma, it appears autophagy may be necessary. Even though this particular combination was not successful, there are still a number of other pathways that can be tested and may prove to be more effective combinations.

For the time being, the only autophagy inhibitor available clinically is CQ or its derivative hydroxycholorquine (HCQ). Measuring autophagy has proved to be very difficult in patients as autophagy is a dynamic process and requires serial sampling to observe changes in flux. Multiple sampling in canine patients is more amenable than in human patients and the physiologic data is highly relevant. Canine lymphoma is one of the most prevalent canine tumor types and the majority of patients will often relapse. As there is a great need for more treatment options and autophagy inhibition has never been tested in the context of canine cancer, in Chapter Four we conduct a Phase I clinical trial to determine a maximum tolerated dose of HCQ and doxorubicin (DOX) and assess autophagy inhibition. We found the maximum tolerated dose to be 12.5 mg/kg HCQ and 25 mg/m^2, a 20% reduction, of DOX. The reduction was necessitated by Grade 5 sepsis observed at 12.5 mg/kg HCQ and 30 mg/m^2 DOX.

HCQ accumulated within the tumor, and the concentration was generally three-fold that of plasma. There was no correlation between plasma and tumor concentrations. Autophagy inhibition, determined by increase in LC3 II expression and autophagosome accumulation, could be achieved in some patients, but not all. We found that western blot and flow cytometry could be useful analytical methods to determine autophagy inhibition and could hopefully begin to replace the more costly, time consuming, and technical autophagosome analysis by electron

microscopy. Similar to drug levels, we did not see a correlation of LC3 II increase between plasma and tumor. Thus, blood measurements will not serve as a good surrogate for tumor measurement. We did see a trend in HCQ concentration and LC3 II expression, with the highest expressers having the highest HCQ concentration. The relationship did not appear truly linear, but rather a threshold of HCQ was required to achieve autophagy inhibition.

We were able to collect some follow up data. The median progression free interval was 4.7 months, which is comparable to historical single agent Dox. Our overall response rate was 100% with best response being complete remission. This response rate is better than historical Dox which is typically only 60-80%. These results suggest further clinical trials would be worth pursuing. Though, not all patients showed indications of autophagy inhibition, all of them responded to therapy, which may suggest that the results are independent of autophagy or more sensitive assays to detect autophagy are required.

In summation the overall results from this project support autophagy inhibition as an effective anti-cancer therapy and warrants its continued study, but only in specific instances. Autophagy inhibition will be most useful in autophagy dependent cancers. In collaboration with Dr. Maycotte, we identify Stat3 activated TNBC as one such cancer type, but Stat3 activation may not be a suitable determinant for other cancers. We also show that autophagy inhibition may work best as a neoadjuvant therapy, but will require combination therapy to be truly effective. We provide potential pathways that may serve as synergistic targets in human breast cancer and canine osteosarcoma, Autophagy inhibition can be achieved in patients, however it is not consistent and more potent inhibitors with a better therapeutic index are needed. Autophagy inhibition did show hints of efficacy in combination with a standard of care therapy in a clinical trial demonstrating its potential as an anti-cancer therapy.

Future Directions and Studies

Many of the conclusions drawn from this project will require further validation and bring to light new challenges and questions. In Chapter 2, we showed that autophagy inhibition was not effective at lowering metastatic burden. While treatment will still be most effective at the pre-metastatic stage, more potent autophagy inhibitors could have some success in later metastatic disease. As discussed previously, CQ and HCQ are not the most potent inhibitors. There are new autophagy inhibitors being developed such as Lys05 [3]. Repeating these studies with newer and better autophagy inhibitors may show that autophagy inhibition will have some efficacy at later stages. Additionally, as autophagy is more effectively inhibited, the BMDC and other microenvironment responses may be more robust.

We also found that autophagy modulation also affected the number of BMDCs present at the eventual site of metastasis and in circulation. While BMDCs have been well described as establishing the metastatic niche, it would be interesting to observe direct changes within the microenvironment such as recruitment of endothelial progenitor cells, release of SDF-1 and MMP9, and extracellular matrix composition. It will also be important to define how autophagy impacts BMDC number. Autophagy could either effect the recruitment of BMDCs by altering signaling molecules like cytokines or act as a cytoprotective mechanism within the BMDCs themselves. There is some evidence for both mechanisms as autophagy controls the release of a number of different extracellular signaling molecules like ATP, HMGB1, IL-1β, and IFN-γ [4]. Autophagy may also be involved in the regulation of exosome cargo loading and release [5]. Thus, different cytokines could be measured in the serum of treated mice and determine if they have an effect on BMDC release. Autophagy has also been shown to enhance the survival of bone marrow derived mesenchymal stem cells. Autophagy may then be required for BMDC

survival in circulation. BMDCs can be isolated from the marrow using magnetic beads and will grow for a period of time in culture [6]. Assessments of migration, survival in suspension or other stressor after autophagy modulation could be made in isolated cells. Determining the underlying mechanism could aid in identifying therapies that would work in concert with autophagy inhibition to prevent release of BMDCs and reduce metastatic spread.

Autophagy inhibition was found to be antagonistic with cisplatin and this could be due to autophagy's immunomodulatory functions. There are a number of other therapies that are reported to initiate immunogenic cell death, such as DOX [7]. Therefore, studies could be repeated with therapies purported to induce immunogenic cell death and determine if antagonism is also observed in combination with autophagy inhibition. Studies could also be repeated in immuno-deficient mice to see if this effect is abrogated once the context of the immune system is removed. Establishing this connection would aid in ruling out certain therapies to combine with autophagy as the result may be counterproductive.

In Chapter Three we confirmed Dr. Maycotte's finding that Stat3 activated TNBC cell lines are dependent on autophagy *in vivo*. For further validation of this relationship, CQ efficacy could be tested in patient-derived xenograft models of TNBC as well as autophagy independent tumor types like ER+ breast cancers. Stat3 expression could also be assessed in these tumors. Using patient derived xenografts will be better predictors of CQ's efficacy in the clinic as these models maintain tissue architecture, express appropriate markers, and are heterogeneous. Cell lines will lose expression of some markers and become more homogenous over time.

Although no differential sensitivity to CQ was observed in canine osteosarcoma lines under basal conditions, the Stat3 activated cell lines may be more dependent under metabolic or

hypoxic stress. Stat3 signaling can become activated under these conditions and has been shown to protect the cell [8]. Some of the osteosarcomas may have acquired an activating Stat3 mutation or constitutive signaling as a means to overcome environmental stress, and under basal conditions, Stat3 is not required for cell survival. Thus, if cells are cultured in low glucose, amino acids, or oxygen, Stat3 dependence and therefore autophagy dependence may be more apparent in these growth conditions. Autophagy's role in tumor survival and metastatic capabilities have sometimes only been realized when cells are stressed [9-11]. These results do have some relevance as tumor cells are not always in optimal conditions *in vivo*. Even if we were to see more dependence on autophagy in Stat3 activated osteosarcoma compared to the Stat3 low lines under metabolic stress, these cells would still not be as sensitive as the TNBC as these cells required Stat3 and autophagy under basal conditions.

Using pathway analysis, ER stress, proteasome degradation, histone acetylation, and DNA repair were upregulated after treatment with HCQ. Drugs targeting these pathways such as nelfinavir, bortezomib, vorinostat, and PARP inhibitors could be tested in combination with HCQ or CQ in the breast cancer and osteosarcoma lines. If the combinations do produce enhanced cytotoxicity, then further xenograft studies and even patient derived xenografts testing the *in vivo* efficacy of the combination could be performed. There also exist syngeneic, orthotopic mouse models of osteosarcoma, so these combinations could also be tested in an immune competent mouse model [12, 13]. Although lovastatin and CQ did not prove to be an effective combination, it may still be worthwhile pursuing statin inhibitors in canine osteosarcoma treatment.

In Chapter Four we demonstrated that HCQ was well tolerated in dogs, could achieve autophagy inhibition in some patients, and the combination of HCQ and DOX was superior to

historical studies employing DOX alone. These results support a Phase III trial in canine lymphoma or potentially expanding to other tumor types. As new and more potent autophagy inhibitors become available, these could also be tested in canine trials. As it was not entirely clear if success was due to autophagy inhibition or HCQ independent effects, better autophagy inhibitors could provide a more definitive answer.

The assays we used to determine autophagy inhibition, western blot and flow cytometry, were able to measure changes in LC3 expression, but they may not be sensitive enough to detect subtle changes and could be one explanation as to why LC3 II expression did not have a linear relationship to HCQ concentration. Also, we were only able to take samples at 3 days post HCQ, which may not be enough time for HCQ to inhibit autophagy. In addition, measurements with flow cytometry are not able to discern LC3 I expression from LC3 II. A saponin extraction step could be included to enrich for membrane bound LC3, depleting the cell of cytosolic LC3. Enriching for membrane bound LC3 would be more specific to LC3 II and more pronounced changes could be observed, as mostly LC3 II would be measured. Optimizing this protocol using cell lines, mouse PBMCs and tumors first could prove to be a better method of measuring LC3 *in vivo*. Using this method of measurement, pharmacokinetic studies with HCQ can also be conducted to determine a more precise relationship between concentration and LC3 II expression and find the optimal time for taking LC3 measurements. If a sensitive and reliable flow cytometry protocol can be established, this would prove to be a very useful clinical tool in determining autophagy inhibition as electron microscopy and western blot analysis are very technical and not rapid assessments.

In conclusion, autophagy inhibition warrants continued study as an anti-cancer therapy. Overall, future studies should take into account the role of the immune system and changes to the

tumor microenvironment. These studies should also focus on identifying autophagy dependent tumors and finding effective combination therapies in ones that are using more clinically relevant models, if possible, such as patient derived xenografts and spontaneous canine cancer. With these approaches, autophagy inhibition may develop into a successful anti-cancer therapy.

References

1. Kaplan, R.N., et al., *VEGFR1-positive haematopoietic bone marrow progenitors initiate the pre-metastatic niche.* Nature, 2005. **438**(7069): p. 820-7.

2. Michaud, M., et al., *Autophagy-dependent anticancer immune responses induced by chemotherapeutic agents in mice.* Science, 2011. **334**(6062): p. 1573-7.

3. Amaravadi, R.K. and J.D. Winkler, *Lys05: a new lysosomal autophagy inhibitor.* Autophagy, 2012. **8**(9): p. 1383-4.

4. Deretic, V., T. Saitoh, and S. Akira, *Autophagy in infection, inflammation and immunity.* Nat Rev Immunol, 2013. **13**(10): p. 722-37.

5. Baixauli, F., C. Lopez-Otin, and M. Mittelbrunn, *Exosomes and autophagy: coordinated mechanisms for the maintenance of cellular fitness.* Front Immunol, 2014. **5**: p. 403.

6. Herberg, S., et al., *Stromal cell-derived factor-1beta mediates cell survival through enhancing autophagy in bone marrow-derived mesenchymal stem cells.* PLoS One, 2013. **8**(3): p. e58207.

7. Ma, Y., et al., *ATP-dependent recruitment, survival and differentiation of dendritic cell precursors in the tumor bed after anticancer chemotherapy.* Oncoimmunology, 2013. **2**(6): p. e24568.

8. Pawlus, M.R., L. Wang, and C.J. Hu, *STAT3 and HIF1alpha cooperatively activate HIF1 target genes in MDA-MB-231 and RCC4 cells.* Oncogene, 2014. **33**(13): p. 1670-9.

9. Degenhardt, K., et al., *Autophagy promotes tumor cell survival and restricts necrosis, inflammation, and tumorigenesis.* Cancer Cell, 2006. **10**(1): p. 51-64.

10. Caino, M.C., et al., *Metabolic stress regulates cytoskeletal dynamics and metastasis of cancer cells.* J Clin Invest, 2013. **123**(7): p. 2907-20.

11. Noman, M.Z., et al., *Blocking hypoxia-induced autophagy in tumors restores cytotoxic T-cell activity and promotes regression.* Cancer Res, 2011. **71**(18): p. 5976-86.

12. Sottnik, J.L., et al., *An orthotopic, postsurgical model of luciferase transfected murine osteosarcoma with spontaneous metastasis.* Clin Exp Metastasis, 2010. **27**(3): p. 151-60.

13. Khanna, C., et al., *An orthotopic model of murine osteosarcoma with clonally related variants differing in pulmonary metastatic potential.* Clin Exp Metastasis, 2000. **18**(3): p. 261-71.